Project Identification No.: DE-FC07-01ID14193

Project Title: Fundamental Studies Of Structural Factors Affecting The Formability Of Continuous Cast Aluminum Alloys

Reporting Period: Aug. 1, 2001 – Jul. 31, 2002

Principal Investigator: Prof. James G. Morris,
Center for Aluminum Technology,
College of Engineering,
175 Anderson Hall,
University of Kentucky,
Lexington, KY 40506-0046

Part I

The Evolution of Microstructure and Texture in D.C. Cast and C.C. AA 5052 Aluminum Alloy During Cold Rolling & Annealing

Annual Report

(AUg.1, 2001-Jul. 31, 2002)

Jiantao Liu, Ph.D. Candidate

1. Purpose of Research

Cold rolling and annealing are the principle processing steps utilized in order to change the microstructure and texture of aluminum alloy sheet and therefore the sheet properties such as formability and mechanical anisotropy, etc. It has been found that the formability of direct chill (DC) material is superior to continuous cast (CC) material. In many respects, the mechanical anisotropy of DC cast material is easier to be controlled than that of CC material. It is therefore of great importance to determine the microstructure and texture evolution of CC material during cold rolling and annealing processes.

In an effort to understand the above mentioned differences in formability between AA 5052 CC and DC materials, the first year's work has concentrated on the microstructure and texture evolution of both materials during cold rolling and annealing processes. Intensive comparisons have been made between these two materials allowing the differences to be highlighted. In the first step, the microstructure and texture evolution during cold rolling process have been studied in order to evaluate the role that cold rolling plays on the further annealing process. In the second step, the microstructure and texture evolutions during annealing have been systematically studied. Specifically, the effects of cold rolling reduction, annealing temperature, and annealing time on microstructure and texture evolution of AA 5052 CC and DC materials have been investigated.

2. Experimental Procedure and Evaluation Techniques

2.1 Material Processing

The starting materials were industrially produced AA 5052 CC and DC hot bands. The chemical composition of the experimental materials is given in Table 1.

Plates of 3.67×101.6×127.0 mm^3 (0.145×4×5 $in.^3$) were cut from DC hot band and 4.06×101.6×127.0 mm^3 (0.160×4×5 $in.^3$) from CC hot band. The cut plates were then annealed at 550 °C (1022 °F) for 2 hours followed by cold rolling in order to generate a completely recrystallized (RX) microstructure before cold rolling. The annealed plates were homogeneously cold rolled to different reductions from 10% through 90%. In following annealing process, samples of 80% cold rolling are annealed at 400 °C (752 °F) for various time t_A. Samples of 80% cold rolling are also annealed at 300 °C (572 °F), 400 °C (752 °F) and 500 °C (932 °F) for the same time of 1000s. Samples with cold rolling reductions of 70%, 80% and 90% are annealed at 400 °C for 1000s.

2.2 Microstructure observation

Samples for microstructure observation were cut from plates in the normal direction (ND) and rolling direction (RD) cross-section, cold mounted and mechanically polished per standard metallographic processes. Prior to anodizing using Barker's reagent (5 vol. pct HBF_4 in Methanol) the samples were electropolished using 1.5 vol. pct HNO_3–5.0 vol. pct $HClO_4$ acids in Methanol to remove the deformation layer. The microstructures were observed under polarized light using an Olympus inverted metallurgical microscope.

2.3 Texture Measurements and Analyses

Samples for texture measurements were sectioned in the rolling plane (RD and the transverse direction (TD) cross-section) at the mid-thickness position. The surface for measurement was carefully polished to minimize surface stress.

Texture measurements were carried out on a Rigaku D/MAX X-ray goniometer using Cu K_a radiation by means of the Schulz reflection method. Four incomplete pole figures {111}, {200}, {220}, and {311} up to tilting angle 75° ($a_{\max} = 75^o$) were measured. All incomplete pole figure data were corrected for defocusing error and background intensity.

Three-dimensional orientation distribution functions (ODF's) $f(g)$ were calculated. g, orientations, are described by three Euler angles j_1, F, j_2, which transform the crystallographic orientation into the sample coordinate system specified by the rolling direction (RD), the transverse direction (TD), and the normal direction (ND). The ODF's are represented in three-dimensional Euler space in the range of $0^o \le j_1, F, j_2 \le 90^o$ by way of iso-intensity contour lines in different sections with j_2 constant. Each texture component is fitted by using a number of Gauss-type scattering functions for quantitative analysis, which also corrects for so-called "ghost errors". Therefore, the volume fraction M_i of each texture component i is calculated by determining the central orientations g_i, the orientation intensity f_i, and the scattering width y_i.

2.4 Microtexture Measurements

Samples for microtexture measurements were sectioned in the rolling plane at the mid-thickness position of the plate. The surface for measurement was mechanically polished followed by electropolishing using the same solution used for microstructure observation to remove the deformation layer.

In this study, EBSD work was carried out using a Hitachi 3200N SEM interfaced to a Unix workstation with orientation image microscopy (OIM) software from TexSEM Laboratories, Inc. (Draper, UT) installed. The sample was mounted on a pre-tilted sample holder with tilt angle of 72° for better pattern quality. The rolling plane was measured. The acceleration voltage and working distance were maintained at 20 keV and 20 mm, respectively. Image scan was adopted and each image contains at least 10,000 pixels (orientations). In order to ensure the reliability of the data, each data set was subject to a cleanup step using an algorithm that checks to determine if the orientation is different from its immediate neighbors. All nearest neighbor pixels must differ in orientation more than a tolerance angle that is set to 5°. Less than 5% of the data was changed in this cleanup operation.

2.5 Characterization of (Sub)Grain Boundaries

(Sub)Grain boundaries, especially coincidence site lattice (CSL) types, can be characterized and quantified from misorientation information obtained by running a EBSD scan. The misorientation is correlated because the calculation of misorientation is based on the neighbor grains. The (sub)grain boundary can be classified by different neighbor misorientations: low-angle boundaries (LABs, $q < 5^o$), moderately misorientated boundaries (MMBs, $5^o \le q < 15^o$) and high-angle boundaries (HABs, $15^o \le q$). Owing to the spatial resolution of the EBSD system, misorientations of less than 1.5° were not identified. CSL boundaries are defined following Brandon's criterion. All misorientation and CSL distributions are presented in the manner of histogram plot forms.

3. Results and Discussion

3.1 Microstructures and Textures During Cold Rolling

3.1.1 Microstructures and Textures of Hot Bands

Fig.1 shows the grain structures of hot bands (as received). It is seen that the grains are elongated along the RD for both DC and CC materials, which characterize typical deformation grain structures. There exists some recrystallized grains in the DC hot band (Fig. 1(b)). After annealing at 550 °C for 2 hours, the hot bands are completely recrystallized with an equiaxed grain structure (Fig. 2). The average grain size is somewhat finer in the CC hot band (Fig. 2(a)) as compared to the DC hot band (Fig. 2(b)).

In the CC hot band (as received), the particles form a banded structure along the RD (Fig. 3(a)), which is partially dissolved after annealing (Fig. 4(a)). On the contrary, particles in DC hot bands are distributed uniformly in the as received hot band (Fig. 3(b)) and become larger in size and smaller in number after annealing (Fig. 4(b)). It appears that particles in the DC material are distributed more uniformly than in the CC material and the distribution is independent of annealing.

3.1.2 Textures of Hot bands

Complete ODF's are given in Fig. 5(a) for the as received CC hot band and Fig. 5(b) for the as received DC hot band. The texture of the CC hot band shows a typical rolling texture with a well developed b fiber starting from the Copper orientation {112}<111> through the S orientation {123}<634> and ending at the Brass orientation {011}<211>. The maximum orientation intensity is found at the Brass orientation. The texture of the DC hot band displays a combination of a rolling texture and a recrystallization texture (Fig. 5(b)) with a Cube orientation {001}<100> which is also confirmed by microstructure observation (cf. Fig. 1(b)). The maximum orientation intensity is located close to the S orientation on the b fiber. The intensities of the Copper and Brass orientations are very close. After recrystallization, the texture of the DC hot band contains a strong Cube orientation with an intensity up to 48 while the texture of the CC hot band transforms to a weaker Cube orientation accompanied by Cube_{ND} fiber and fiber stemming from a rotated Goss orientation to the Brass orientation (Fig. 6(a) and (b)).

3.1.3 Texture Evolution during Cold Rolling

3.1.3.1 Texture Evolution of CC Material

Volume fractions of Gauss-type texture components are calculated and listed in Table 2. Volume fractions are also plotted for the CC material as a function of the degree of (thickness) rolling reduction in Fig. 7(a). As anticipated, the volume fraction of the Cube orientation decreases with an increase of rolling reduction. After 10% cold rolling, the volume fraction of both the Goss orientation and the {100} fibers increase about 5%, which indicate that grains with a Cube orientation rotate away from the exact Cube orientation along the Cube_{RD} fiber toward the Goss orientation. With an increase in cold rolling reduction up to 50%, orientations continuously evolve along the Cube_{RD} fiber to the Goss orientation at which orientations flow along the a fiber which is a tube with the skeleton (maximum intensity) line located at $0^o \le j_1 \le 30^o$, $\Phi = 45^o, j_2 = 0^o$ (Fig. 8(a)). This tube, including the Goss orientation {011}<100> and the Brass orientation {011}<211>, becomes well formed beyond 60% cold rolling. The position of the peak orientation intensity gradually shifts to the Brass orientation at $j_1 = 30^o$,

$\Phi = 45^o, j_2 = 0^o$ as cold rolling reduction increases. Another tube called the b fiber, running from the Brass orientation to the Copper orientation {112}<111> at $j_1 = 90^o$, $\Phi = 30^o, j_2 = 45^o$, is also well formed after 60% cold rolling. This skeleton includes the S orientation {123<634> at $j_1 = 60^o$, $\Phi = 30^o, j_2 = 65^o$. Fig. 9(a) shows orientation intensity distributions along the b fiber for different cold rolling reductions and Fig. 9(b) shows the position of these skeleton lines. Obviously, the intensities are not uniformly distributed along the b fiber. The intensity of the texture components near the Copper to S orientations along the b fiber is slightly larger than that near the Brass orientation. This trend becomes more pronounced at larger cold rolling reductions.

3.1.3.2 Texture Evolution of DC Material

Fig. 7(b) shows the volume fraction of various texture components of DC material during cold rolling. All data are given in Table 3. Compared with the CC hot band, the DC hot band contains a larger Cube texture component with a volume fraction up to 35% after annealing. The volume fraction of {100} fibers increases by ~27% after 10% cold rolling. In addition, the volume fraction of the Cube texture component decreases about 10%. Therefore, randomly orientated grains also contribute to the increase of the amount of the {100} fibers. It should be pointed out that some Cube oriented grains are retained even after 90% cold rolling. No apparent deformation texture components along the a and the b fibers develop until the cold rolling reduction reaches 70%. It is also interesting to note that the amount of the {100} fibers drops rapidly beyond 70% cold rolling. The development of the a fiber with increase in cold rolling reduction can be seen in Fig. 8(b) where the apparent peak intensities can be found only after 70% cold rolling. The development of the b fiber can be traced in Fig. 10. The b fiber becomes well developed beyond 70% cold rolling reduction with the highest intensities near the S orientation (Fig. 10(a)). Compared with the positions of the b fiber in CC material, DC material develops a sharper b fiber during cold rolling.

3.1.4 Microtextures of Annealed Hot Bands

Fig. 11 presents the inverse pole figure (IPF) maps with respect to ND. Each grain is painted with color based on its crystal orientation. The grain size of recrystallized CC hot band (Fig. 11(a)) is larger than that of recrystallized DC hot band (Fig. 11(b)). Cube clusters, neighbor grains with their <001> crystal directions parallel to the ND, are dominant in the DC hot band. This indicates the existence of a large amount of Cube clusters in the DC hot band. Cube clusters, however, are found to a less degree in CC hot band than in DC hot band. White segments in Figure 11 indicate annealing twin boundaries (Σ3, Σ9, Σ27a & b) in both hot bands. Quantitative analyses show that the fractions of annealing twin boundaries are 9.8% and 7.1% for recrystallized CC and DC hot bands, respectively.

3.1.5 (Sub)Grain Boundary Evolution during Cold Rolling

Misorientation distributions of recrystallized CC and DC hot bands are shown in Fig. 12(a) and 12(b), respectively. Two peaks are noteworthy for both CC and DC materials: the first is located at 40° to 45° and the second at 55° to 62.8°. The first peak can be ascribed to randomly orientated Cube grains. Smaller grain boundary populations with misorientations between 40° and 45° in DC material can be explained by more Cube grain clusters (<001>//ND). The second peak corresponds to the Σ3 (annealing twin) boundaries. Compared with grain boundary distributions in CC material, the grain boundary distributions in DC material appear random. It can also be seen that the fractions of low-angle boundaries (LABs, $q < 5^o$) and moderately misorientated boundaries (MMBs, $5^o \le q < 15^o$) are smaller in CC material than that in DC material. This can be verified in Fig. 13 that shows the fraction of Σ1 boundaries (LABs/MMBs) is about 5% in CC material (Fig. 13(a)) while it reaches about 12.5% in DC material (Fig. 13(b)).

Fig. 14 shows coincident site lattice (CSL) grain boundary distributions in CC and DC materials after 10% (Fig. 14(a) & 14(b)), 20% (Fig. 14(c) & 14(d)) and 30% (Fig. 14(e)

& 14(f)) cold rolling reductions. In CC material, the fraction of Σ1 boundaries keeps increasing with increase in cold rolling reduction (Figures 14(a), 14(c) & 14(e)) and even reaches about 45% after 30% cold rolling. However, there is no evidence of the development of either twin boundaries (Σ3) or high order twin boundaries (Σ9, Σ27a & b). In DC material, the fraction of Σ1 boundaries increases to about 37% after 20% cold rolling (Fig. 14(d)) and then decreases dramatically to about 26% after 30% cold rolling (Fig. 14(f)). Further quantitative analyses show that the fraction of Σ1 boundaries drops to 12% while the fraction of twin boundaries (Σ3, Σ9, Σ27a & b) is kept constant in DC material after 40% cold rolling.

Fig. 15(a) & 15(b) display grain boundary maps in CC material after 30% and 40% cold rolling reductions, respectively. From 30% to 40% cold rolling, the LABs decrease by about 10% while the high-angle boundaries (HABs, $15^o \leq q$) increase about 10%. Therefore, it is reasonable to conclude that the HABs develope at the expense of the LABs. The same changes of grain boundaries can also be observed in DC material in which the LABs drops from 29.6% after 20% cold rolling (Fig. 16(a)) to 21.4% after 30% cold rolling (Fig. 16(b)) while the HABs increase from 63.5% to 74%.

The evolution of grain boundaries has been traced in both CC and DC materials during the early stages of cold rolling ($\leq$40%). In CC material, Σ1 boundaries are well developed before 30% cold rolling and thereafter HABs develop at the expense of Σ1 boundaries. Grain boundary evolution in DC material follows the same path as in CC material except that HABs start to increase after 20% cold rolling. There is not a remarkable change in twin boundaries (Σ3, Σ9, Σ27a & b) during the early stages of cold rolling. Therefore, mechanical twinning is not an acting mechanism in these early stages. Instead, grains are subdivided by the process of forming cell walls (Σ1 boundaries). These cell walls transform to HABs during further cold rolling as misorientation increases. It can be seen from Figure 15 and Figure 16 that the misorientation gradient along the TD becomes larger than that along the RD with increase in cold rolling reduction, which indicates an elongated grain structure.

3.2 Microstructures and Textures During Annealing

3.2.1 Recrystallization Kinetics

The status of recrystallization is determined by microstructures supported by microhardness, electrical resistivity and texture results. Fig. 17 shows microhardness vs. annealing time of AA 5052 CC material at 300 °C (Fig. 17(a)), 400 °C (Fig. 17(b)) and 500 °C (Fig. 17(c)). The higher the annealing temperature the earlier starting time for recrystallization. AA 5052 DC material (Fig. 18) displays the same progress of recrystallization as CC material. Fig. 19 and Fig. 20 give the change of electrical conductivity of AA 5052 CC and DC materials during the annealing process, respectively. With the increase of annealing time, electrical resistivity gradually decreases, which indicates that the density of dislocations decreases during recrystallization. The time for complete recrystallization of AA 5052 CC and DC samples under different cold rolling reductions are given in Fig. 21 (a) and (b), respectively. Solid lines indicate the starting time for recrystallization while the dash lines indicate complete recrystallization. The time for complete recrystallization decreases from 1000s to less than 100s for both materials. With increase in cold rolling reduction, the time required for incubation decreases. It appears that the time required for complete recrystallization is independent of cold rolling reduction.

3.2.2 Microstructure Evolution

At the same annealing condition, the recrystallized grain size decreases with increase of cold rolling reduction (Fig. 22 and 23). It is worth noting that there exists a band of elongated grain structure in the CC material at about half thickness layer as indicated by arrows (Fig.22). This banded structure forms the whole half thickness layer of CC material even at high cold rolling reduction. This banded grain structure, however, is not found in the DC material (Fig. 23). Fig. 24 shows the particle structure of CC (Fig. 24(a)) and DC (Fig. 24(b)) materials. The difference can easily be seen: constituent particles (Probably Al_6Mn) form many bands along the rolling direction in the CC material even after a high temperature annealing for a long time. On the contrary, the constituent particles are uniformly distributed in the sample of the DC material.

3.2.3 Texture Evolution

3.2.3.1 Effect of Annealing Time

Fig. 25 shows the texture evolution of the CC material during annealing at 400 °C for various times. Recrystallization starts between 250s and 550s. Complete recrystallization has been achieved by 550s' annealing and the Cube orientation {001}<100> is dominant. The intensity of the Cube orientation increases with the annealing time up to 1000s then remains stable, which suggests that intensity of the Cube orientation is independent of annealing time after a complete recrystallization has been achieved. It can also be seen that a weak Brass component {011}<211> is retained even after a long annealing time. The texture evolution of the DC material (Fig. 26) under the same annealing process follows the same procedure. The only difference is that the intensity of the retained Cube orientation in the DC material after cold rolling is higher than that in the CC material while the starting intensity of Brass component is higher in the CC material before annealing.

3.2.3.2 Effect of Cold Rolling Reduction

Fig. 27 through Fig. 29 shows the recrystallization texture of the CC material with different cold rolling reductions. The intensity of the Cube orientation increases from 3.1 at 70% cold rolling to 7.7 at 90% cold rolling. The R orientation {124}<211>, though low in intensity, is another major recrystallization texture component. The Copper orientation {112}<111> is retained in all samples. In the same way, the intensity of the Cube orientation increases to 11.9 of 90% cold rolling from 4.6 at 70% cold rolling for the DC material (Fig. 30, 31 and 32).

3.2.3.3 Effect of Annealing Temperature

Fig. 33 and Fig. 34 combined with Fig. 28 show the effect of annealing temperature on texture evolution of the CC material. While the typical deformation texture components Copper, Brass and S are retained at 300 °C annealing without recrystallization, recrystallization texture components Cube and R are dominant in samples annealed at 400 °C and 500 °C. It appears that increasing annealing temperature does not increase the

intensity of the Cube orientation as much as the R orientation. The annealing temperature has the same effect on the texture evolution in the DC material (Fig. 35, 31 and 36).

3.2.3.4 Volume Fraction of Texture Components

Volume fraction of various texture components have been calculated for both CC and DC materials. Results are listed in Table 4 through Table 9. Fig. 37 (a) and (b) display the dependence of the volume fraction of various texture components on the annealing time, respectively. The volume fraction of the Cube component remains constant after complete recrystallization for both materials. A striking result is that the volume fraction of the R component is higher than that of the Cube component and reaches about 15% after complete recrystallization. The random orientation increases after complete recrystallization at the expense of the deformation texture components. However, at least 10% of the Copper component is retained in both materials. The intensity of the R and Copper orientations is as low as about 2. However, the intensity does not drop around the ideal positions of the R and Copper orientations. Therefore, the volume fraction of R and Copper components is high.

Fig. 38 illustrates the dependence of volume fraction vs. annealing temperature. In general, volume fraction of the deformation texture components in the CC material decreases. The volume fraction of the Copper component drops from about 20% at 300 °C annealing to about 11% at 500 °C annealing for the CC material (Fig. 38(a)). However, the volume fraction of the Copper component in the DC material remains at about 10% at different annealing temperature (Fig. 38(b)). This implies that the sharp Copper orientation is weakened to a stable state where orientations near the ideal Copper orientation, with about the same intensity, are uniformly distributed. In both CC and DC materials, the volume fraction of Cube and random orientations is increased with the increasing annealing temperature.

The effects of cold rolling reduction on volume fraction of various texture components in CC and DC materials are depicted in Fig. 39(a) and 39(b), respectively. The notable point is that the volume fraction of the Cube component increases with the increasing cold rolling reduction.

4. Summary

A stronger Cube texture component is found in the AA 5052 DC hot band than in the AA 5052 CC hot band after complete recrystallization. With an increase in cold rolling reduction, both the *a* fiber and the *b* fiber develop at the expense of the Cube orientation. The *b* fiber is well developed beyond 60% and 70% cold rolling reductions for the CC and the DC materials, respectively. The Cube texture component is retained in the DC material even after 90% cold rolling reduction. However, no Cube component is found for the CC material beyond an 80% cold rolling reduction. The orientation intensity in the *b* fiber is not uniformly developed during cold rolling. The highest intensity on the *b* fiber is located close to the S orientation for both CC and DC material. In both CC and DC materials, cell structure develops with the indication of increasing LABs/MMBs during the early stages of cold rolling. However, LABs/MMBs decrease while HABs increase after 40% and 30% cold rolling for CC and DC materials, respectively. There is no evidence of the development of twin boundaries (Σ3, Σ9, Σ27a & b) in both CC and DC materials when cold rolling reductions are less than 40%.

A banded grain structure layer with elongated grains along the rolling direction is found in CC material. Constituent particles are formed in elongated bands along the rolling direction in the CC material, which cannot be eliminated by either further cold rolling or by annealing alone. The R and Cube orientations are the dominant recrystallization texture components in CC and DC material. The volume fraction of the Cube component can be increased by increasing cold rolling reduction and annealing temperature but not by increasing annealing time. A certain amount of the Copper component, with a volume fraction of about 10%, is retained in both CC and DC material even after complete recrystallization.

Table 1. Compositions of experimental materials, wt. %

Alloy	Si	Fe	Cu	Mn	Mg	Zn	Cr	Al
AA 5052 CC	0.13	0.35	—	0.03	2.40	0.02	0.18	Balance

AA 5052 DC	0.10	0.39	0.02	0.03	2.39	—	—	Balance

Table 2. Texture components of AA 5052 CC hot band during cold rolling[a]

Status	e	M_i [b]

Recrystallization texture components:		
(a) Cube component: $\{hkl\}<uvw>=\{001\}<100>$ [b]		
Hot band (as received)	—	—
Hot band (annealed at 1022 ^{o}F for 2hrs)	—	10.7%
10% cold rolling	0.11	8.3%
20% cold rolling	0.22	7.9%
30% cold rolling	0.36	7.0%
40% cold rolling	0.51	6.0%
50% cold rolling	0.69	5.9%
60% cold rolling	0.92	3.7%
70% cold rolling	1.20	4.4%
80% cold rolling	1.61	2.4%
90% cold rolling	2.30	—
(b) $Cube_{RD}$ component: $\{hkl\}<uvw>=\{012\}<100>$ [b]		
Hot band (as received)	—	—
Hot band (annealed at 1022 ^{o}F for 2hrs)	—	—
10% cold rolling	0.11	0.4%
20% cold rolling	0.22	0.4%
30% cold rolling	0.36	0.4%
40% cold rolling	0.51	0.4%
50% cold rolling	0.69	0.4%
60% cold rolling	0.92	0.4%
70% cold rolling	1.20	1.6%
80% cold rolling	1.61	0.4%
90% cold rolling	2.30	—
(c) $Cube_{ND}$ component: $\{hkl\}<uvw>=\{001\}<210>$ [b]		
Hot band (as received)	—	—
Hot band (annealed at 1022 ^{o}F for 2hrs)	—	0.5%
10% cold rolling	0.11	0.4%
20% cold rolling	0.22	0.5%
30% cold rolling	0.36	0.4%
40% cold rolling	0.51	0.5%
50% cold rolling	0.69	0.5%
60% cold rolling	0.92	0.3%
70% cold rolling	1.20	0.3%
80% cold rolling	1.61	—
90% cold rolling	2.30	—

Table 2. — Continued

Status	e	M_i [b]

(d) Goss component: $\{hkl\}<uvw>=\{011\}<100>$ [b]		
Hot band (as received)	—	2.8%
Hot band (annealed at 1022 ^{o}F for 2hrs)	—	—
10% cold rolling	0.11	4.9%
20% cold rolling	0.22	4.0%
30% cold rolling	0.36	4.9%
40% cold rolling	0.51	3.4%
50% cold rolling	0.69	2.9%
60% cold rolling	0.92	3.8%
70% cold rolling	1.20	3.7%
80% cold rolling	1.61	4.1%
90% cold rolling	2.30	3.8%

Rolling texture components:

(e) Copper/S component: $\{hkl\}<uvw>=\{123\}<111>$ [b]		
Hot band (as received)	—	14.0%
Hot band (annealed at 1022 ^{o}F for 2hrs)	—	—
10% cold rolling	0.11	3.8%
20% cold rolling	0.22	2.8%
30% cold rolling	0.36	4.0%
40% cold rolling	0.51	3.5%
50% cold rolling	0.69	4.0%
60% cold rolling	0.92	6.7%
70% cold rolling	1.20	8.3%
80% cold rolling	1.61	12.0%
90% cold rolling	2.30	13.7%

(f) Copper component: $\{hkl\}<uvw>=\{112\}<111>$ [b]		
Hot band (as received)	—	16.8%
Hot band (annealed at 1022 ^{o}F for 2hrs)	—	—
10% cold rolling	0.11	3.2%
20% cold rolling	0.22	0.3%
30% cold rolling	0.36	6.5%
40% cold rolling	0.51	2.7%
50% cold rolling	0.69	3.2%
60% cold rolling	0.92	13.2%
70% cold rolling	1.20	18.7%
80% cold rolling	1.61	19.6%
90% cold rolling	2.30	21.2%

Table 2.— Continued

Status	e	M_i [b]

(g) Brass/Goss component: $\{hkl\}<uvw>=\{011\}<411>$ [b]		
Hot band (as received)	—	—
Hot band (annealed at 1022 ^{o}F for 2hrs)	—	—
10% cold rolling	0.11	2.2%
20% cold rolling	0.22	1.7%
30% cold rolling	0.36	2.1%
40% cold rolling	0.51	1.6%
50% cold rolling	0.69	1.9%
60% cold rolling	0.92	—
70% cold rolling	1.20	—
80% cold rolling	1.61	—
90% cold rolling	2.30	—

(h) Brass component: $\{hkl\}<uvw>=\{011\}<211>$ [b]		
Hot band (as received)	—	19.6%
Hot band (annealed at 1022 ^{o}F for 2hrs)	—	—
10% cold rolling	0.11	1.7%
20% cold rolling	0.22	1.4%
30% cold rolling	0.36	2.0%
40% cold rolling	0.51	1.5%
50% cold rolling	0.69	1.7%
60% cold rolling	0.92	9.0%
70% cold rolling	1.20	10.7%
80% cold rolling	1.61	14.3%
90% cold rolling	2.30	17.2%

(i) Brass/S component: $\{hkl\}<uvw>=\{168\}<211>$ [b]		
Hot band (as received)	—	14.6%
Hot band (annealed at 1022 ^{o}F for 2hrs)	—	—
10% cold rolling	0.11	—
20% cold rolling	0.22	—
30% cold rolling	0.36	3.4%
40% cold rolling	0.51	3.2%
50% cold rolling	0.69	3.4%
60% cold rolling	0.92	5.9%
70% cold rolling	1.20	7.3%
80% cold rolling	1.61	10.6%
90% cold rolling	2.30	14.7%

Table 2.— Continued

Status	e	M_i [b]

(j) S component: $\{hkl\}<uvw>=\{123\}<634>$ [b]		
Hot band (as received)	—	15.4%
Hot band (annealed at 1022 ^{o}F for 2hrs)	—	—
10% cold rolling	0.11	3.3%
20% cold rolling	0.22	2.8%
30% cold rolling	0.36	3.9%
40% cold rolling	0.51	3.2%
50% cold rolling	0.69	3.9%
60% cold rolling	0.92	6.7%
70% cold rolling	1.20	8.4%
80% cold rolling	1.61	12.0%
90% cold rolling	2.30	13.9%
Fibers:		
(k) $\{100\}$ fibers: $\{hkl\}=\{100\}$		
Hot band (as received)	—	—
Hot band (annealed at 1022 ^{o}F for 2hrs)	—	14.6% [c]
10% cold rolling	0.11	21.7% [c]
20% cold rolling	0.22	23.1% [c]
30% cold rolling	0.36	19.5% [c]
40% cold rolling	0.51	26.4% [c]
50% cold rolling	0.69	20.1% [c]
60% cold rolling	0.92	13.1% [c]
70% cold rolling	1.20	14.1% [c]
80% cold rolling	1.61	4.0% [c]
90% cold rolling	2.30	—

[a] The texture components are quantitatively analyzed by using Gauss-type function. e denotes the strain, M_i the calculated volume fraction when half scatter width y_i is selected for the purpose of the best fitting of Gauss components.
[b] Approximated.
[c] The volume fraction is the sum of $Cube_{RD}$ and $Cube_{ND}$ fibers.

Table 3. Texture components of AA 5052 DC hot band during cold rolling[a]

Status	e	M_i [b]

Recrystallization texture components:		
(a) Cube component: $\{hkl\}<uvw>=\{001\}<100>$ [b]		
Hot band (as received)	—	3.9%
Hot band (annealed at 1022 ^{o}F for 2hrs)	—	35.0%
10% cold rolling	0.11	24.1%
20% cold rolling	0.22	19.4%
30% cold rolling	0.36	17.2%
40% cold rolling	0.51	17.2%
50% cold rolling	0.69	13.1%
60% cold rolling	0.92	11.5%
70% cold rolling	1.20	8.8%
80% cold rolling	1.61	3.8%
90% cold rolling	2.30	2.7%
(b) $Cube_{RD}$ component: $\{hkl\}<uvw>=\{013\}<100>$ [b]		
Hot band (as received)	—	—
Hot band (annealed at 1022 ^{o}F for 2hrs)	—	0.5%
10% cold rolling	0.11	0.4%
20% cold rolling	0.22	0.4%
30% cold rolling	0.36	0.5%
40% cold rolling	0.51	0.5%
50% cold rolling	0.69	0.6%
60% cold rolling	0.92	0.7%
70% cold rolling	1.20	0.6%
80% cold rolling	1.61	0.7%
90% cold rolling	2.30	0.6%
(c) $Cube_{ND}$ component: $\{hkl\}<uvw>=\{001\}<310>$ [b]		
Hot band (as received)	—	—
Hot band (annealed at 1022 ^{o}F for 2hrs)	—	0.7%
10% cold rolling	0.11	0.5%
20% cold rolling	0.22	0.4%
30% cold rolling	0.36	0.4%
40% cold rolling	0.51	0.4%
50% cold rolling	0.69	0.3%
60% cold rolling	0.92	0.3%
70% cold rolling	1.20	0.3%
80% cold rolling	1.61	—
90% cold rolling	2.30	—

Table 3.— Continued

Status	e	M_i [b]

(d) Goss component: $\{hkl\}<uvw>=\{011\}<100>$ [b]		
Hot band (as received)	—	3.9%
Hot band (annealed at 1022 ^{o}F for 2hrs)	—	—
10% cold rolling	0.11	—
20% cold rolling	0.22	—
30% cold rolling	0.36	—
40% cold rolling	0.51	—
50% cold rolling	0.69	2.6%
60% cold rolling	0.92	4.0%
70% cold rolling	1.20	3.2%
80% cold rolling	1.61	4.1%
90% cold rolling	2.30	4.0%

Rolling texture components:

(e) Copper/S component: $\{hkl\}<uvw>=\{123\}<111>$ [b]		
Hot band (as received)	—	12.6%
Hot band (annealed at 1022 ^{o}F for 2hrs)	—	—
10% cold rolling	0.11	—
20% cold rolling	0.22	0.3%
30% cold rolling	0.36	3.6%
40% cold rolling	0.51	3.5%
50% cold rolling	0.69	4.8%
60% cold rolling	0.92	5.7%
70% cold rolling	1.20	6.2%
80% cold rolling	1.61	9.1%
90% cold rolling	2.30	11.9%

(f) Copper component: $\{hkl\}<uvw>=\{112\}<111>$ [b]		
Hot band (as received)	—	18.3%
Hot band (annealed at 1022 ^{o}F for 2hrs)	—	—
10% cold rolling	0.11	—
20% cold rolling	0.22	2.8%
30% cold rolling	0.36	3.5%
40% cold rolling	0.51	3.1%
50% cold rolling	0.69	2.5%
60% cold rolling	0.92	4.8%
70% cold rolling	1.20	15.0%
80% cold rolling	1.61	16.3%
90% cold rolling	2.30	18.5%

Table 3.— Continued

Status	e	M_i [b]

(g) Brass/Goss component: $\{hkl\}<uvw>=\{011\}<411>$ [b]		
Hot band (as received)	—	—
Hot band (annealed at 1022 ^{o}F for 2hrs)	—	—
10% cold rolling	0.11	1.3%
20% cold rolling	0.22	—
30% cold rolling	0.36	—
40% cold rolling	0.51	—
50% cold rolling	0.69	—
60% cold rolling	0.92	—
70% cold rolling	1.20	—
80% cold rolling	1.61	—
90% cold rolling	2.30	—

(h) Brass component: $\{hkl\}<uvw>=\{011\}<211>$ [b]		
Hot band (as received)	—	15.8%
Hot band (annealed at 1022 ^{o}F for 2hrs)	—	—
10% cold rolling	0.11	—
20% cold rolling	0.22	—
30% cold rolling	0.36	1.7%
40% cold rolling	0.51	4.5%
50% cold rolling	0.69	6.1%
60% cold rolling	0.92	6.5%
70% cold rolling	1.20	7.2%
80% cold rolling	1.61	9.8%
90% cold rolling	2.30	12.2%

(i) Brass/S component: $\{hkl\}<uvw>=\{168\}<211>$ [b]		
Hot band (as received)	—	14.2%
Hot band (annealed at 1022 ^{o}F for 2hrs)	—	—
10% cold rolling	0.11	—
20% cold rolling	0.22	—
30% cold rolling	0.36	3.1%
40% cold rolling	0.51	3.2%
50% cold rolling	0.69	4.4%
60% cold rolling	0.92	5.0%
70% cold rolling	1.20	4.9%
80% cold rolling	1.61	8.0%
90% cold rolling	2.30	11.4%

Table 3.— Continued

Status	e	M_i [b]

(j) S component: $\{hkl\}<uvw>=\{123\}<634>$ [b]		
Hot band (as received)	—	11.5%
Hot band (annealed at 1022 ^{o}F for 2hrs)	—	—
10% cold rolling	0.11	—
20% cold rolling	0.22	0.4%
30% cold rolling	0.36	3.6%
40% cold rolling	0.51	3.5%
50% cold rolling	0.69	4.8%
60% cold rolling	0.92	5.7%
70% cold rolling	1.20	6.0%
80% cold rolling	1.61	8.9%
90% cold rolling	2.30	12.2%
Fibers:		
(k) $\{100\}$ fibers: $\{hkl\}=\{100\}$		
Hot band (as received)	—	5.9% [c]
Hot band (annealed at 1022 ^{o}F for 2hrs)	—	—
10% cold rolling	0.11	26.7% [c]
20% cold rolling	0.22	—
30% cold rolling	0.36	19.2% [c]
40% cold rolling	0.51	19.5% [c]
50% cold rolling	0.69	25.9% [c]
60% cold rolling	0.92	23.2% [c]
70% cold rolling	1.20	19.3% [c]
80% cold rolling	1.61	11.1% [c]
90% cold rolling	2.30	8.5% [c]

[a] The texture components are quantitatively analyzed by using Gauss-type function. e denotes the strain, M_i the calculated volume fraction when half scatter width y_i is selected for the purpose of the best fitting of Gauss components.
[b] Approximated.
[c] The volume fraction is the sum of $Cube_{RD}$ and $Cube_{ND}$ fibers.

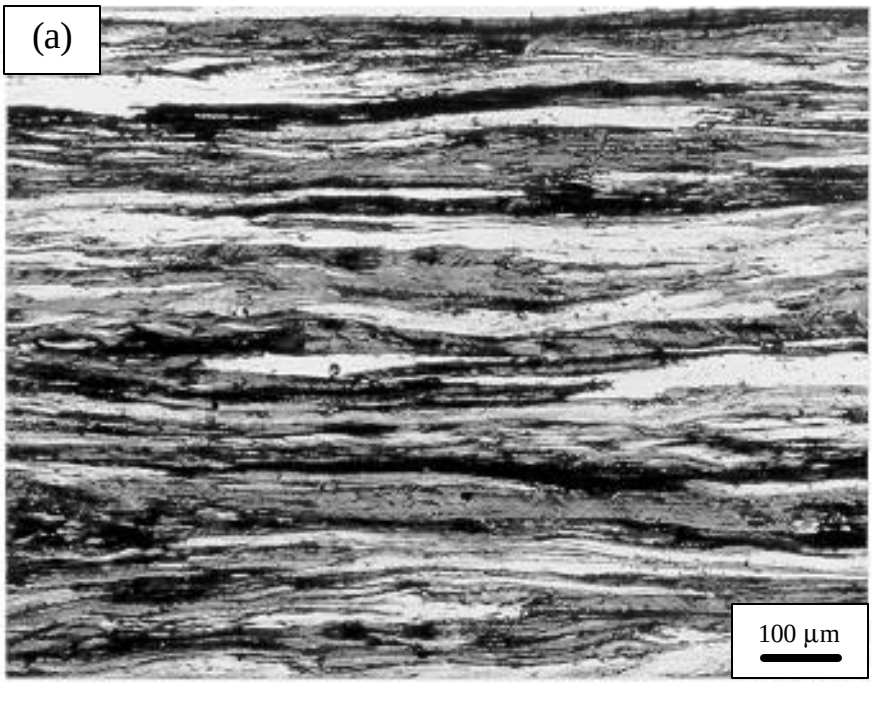

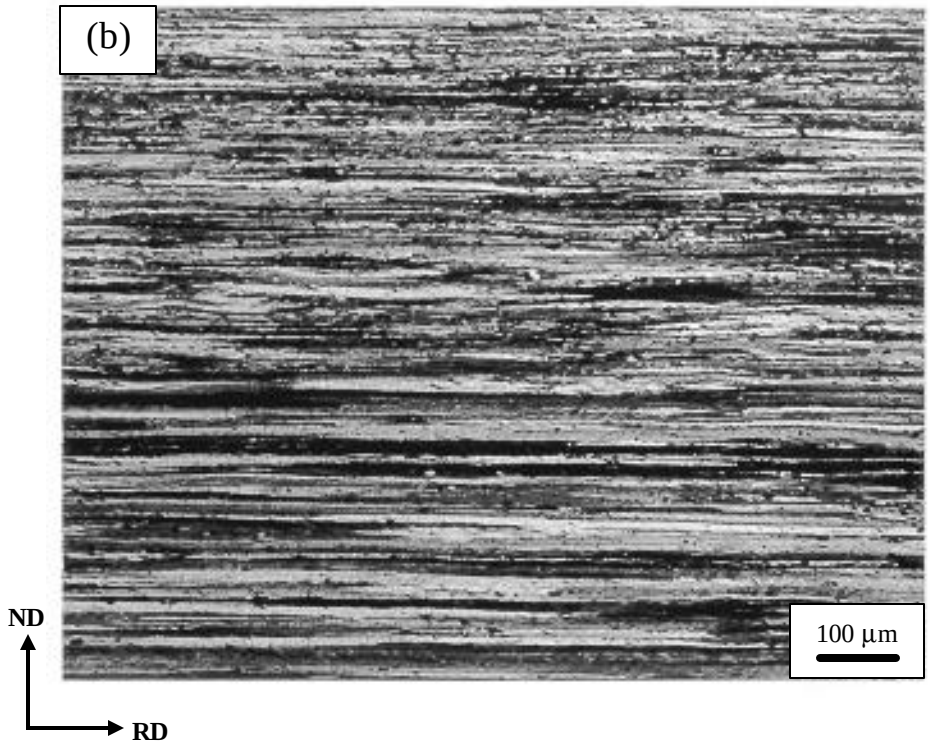

Fig. 1. Grain structure of hot bands (as received): (a) AA 5052 CC material; (b) AA 5052 DC material.

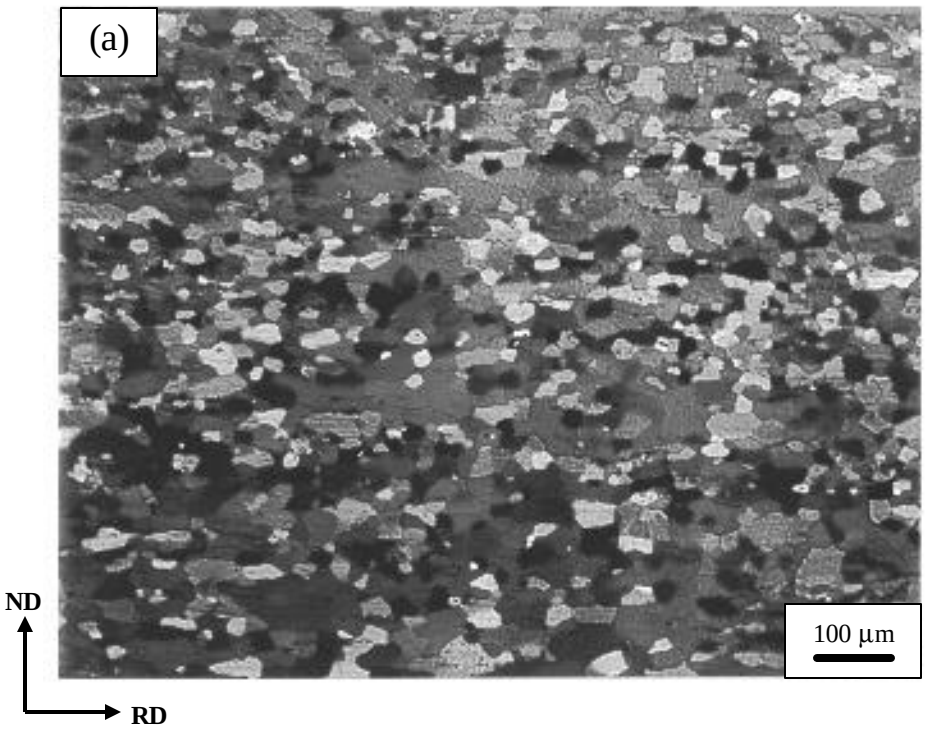

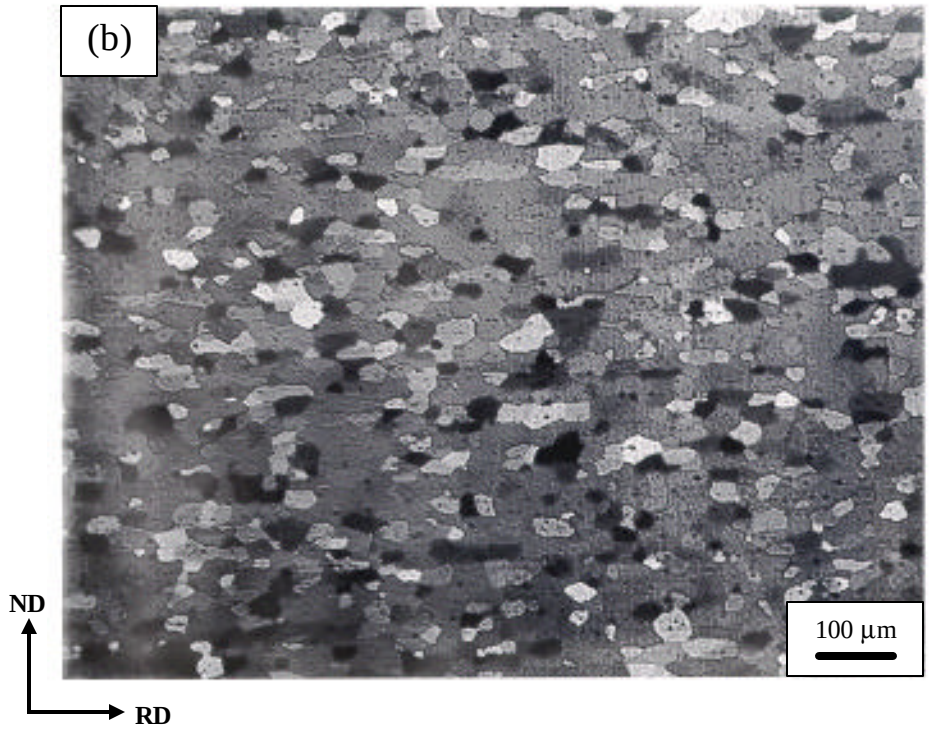

Fig. 2. Grain structure of hot bands after annealing at 1022 ^{o}F for 2 hrs.: (a) AA 5052 CC material; (b) AA 5052 DC material.

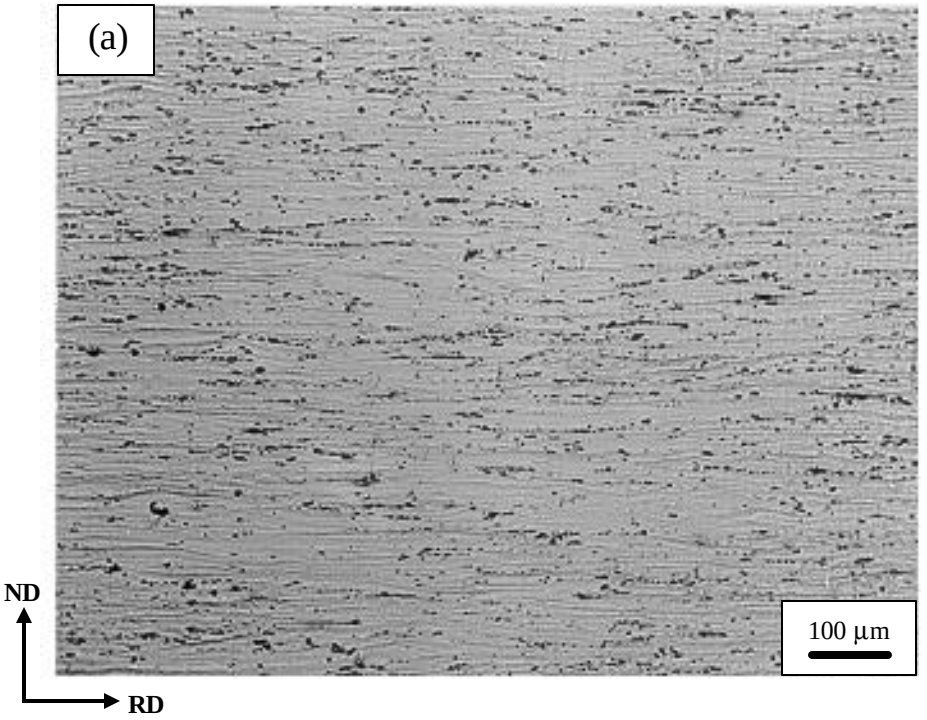

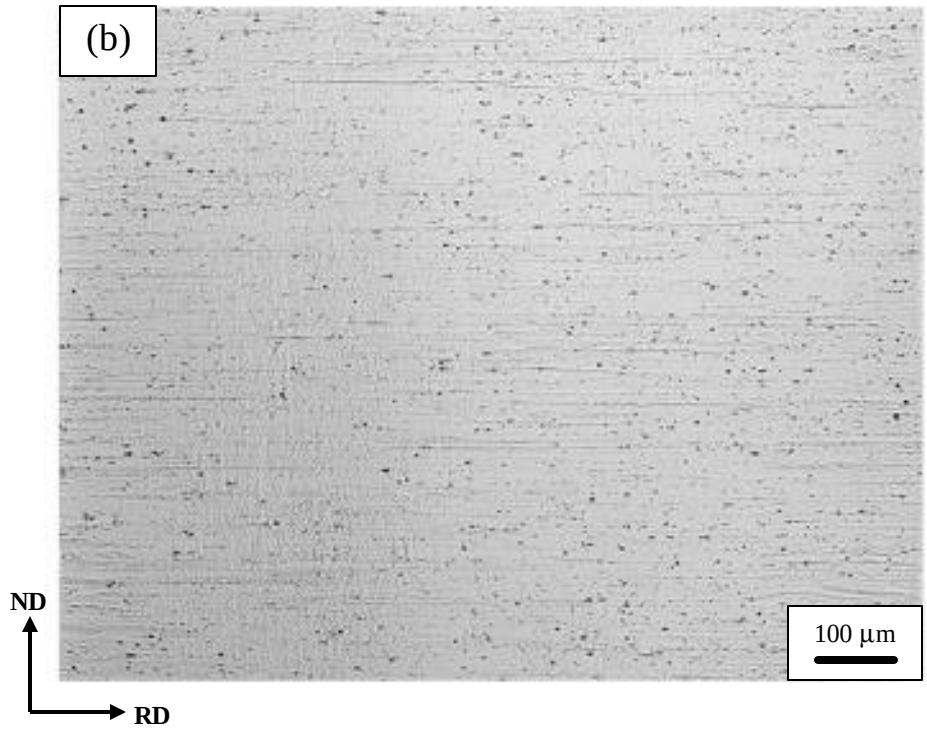

Fig. 3. Particle structure of hot bands (as received): (a) AA 5052 CC material; (b) AA 5052 DC material.

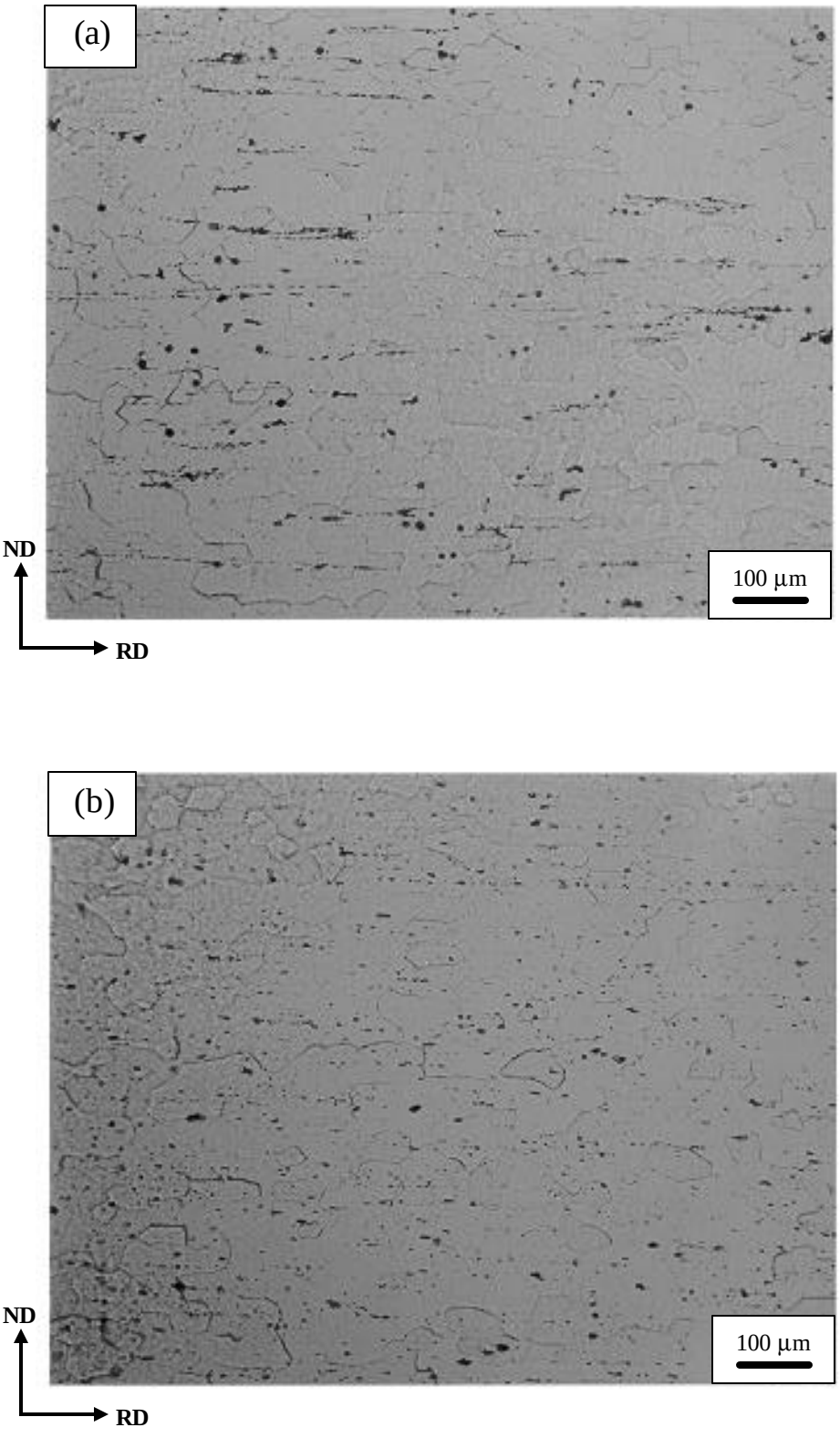

Fig. 4. Particle structure of hot bands after annealing at 1022 ^{o}F for 2 hrs.: (a) AA 5052 CC material; (b) AA 5052 DC material.

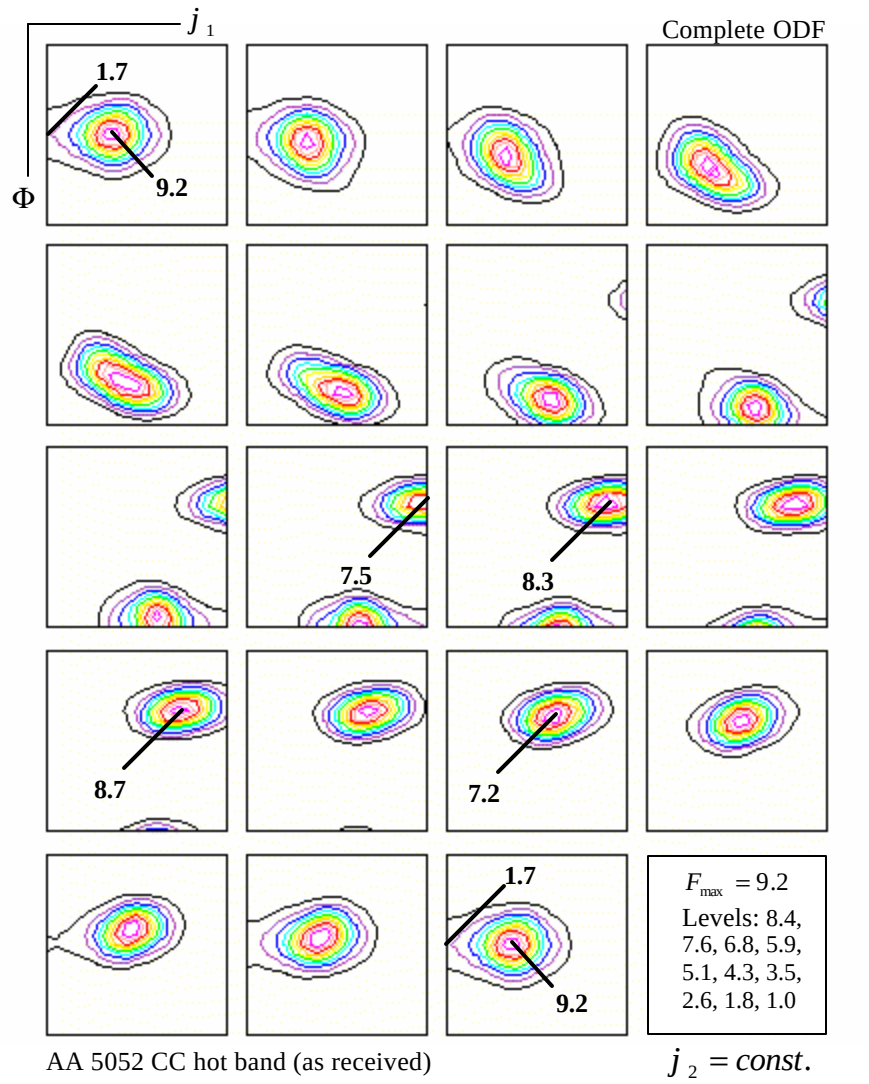

Fig. 5. (a) Complete ODFs of AA 5052 CC hot band (as received).

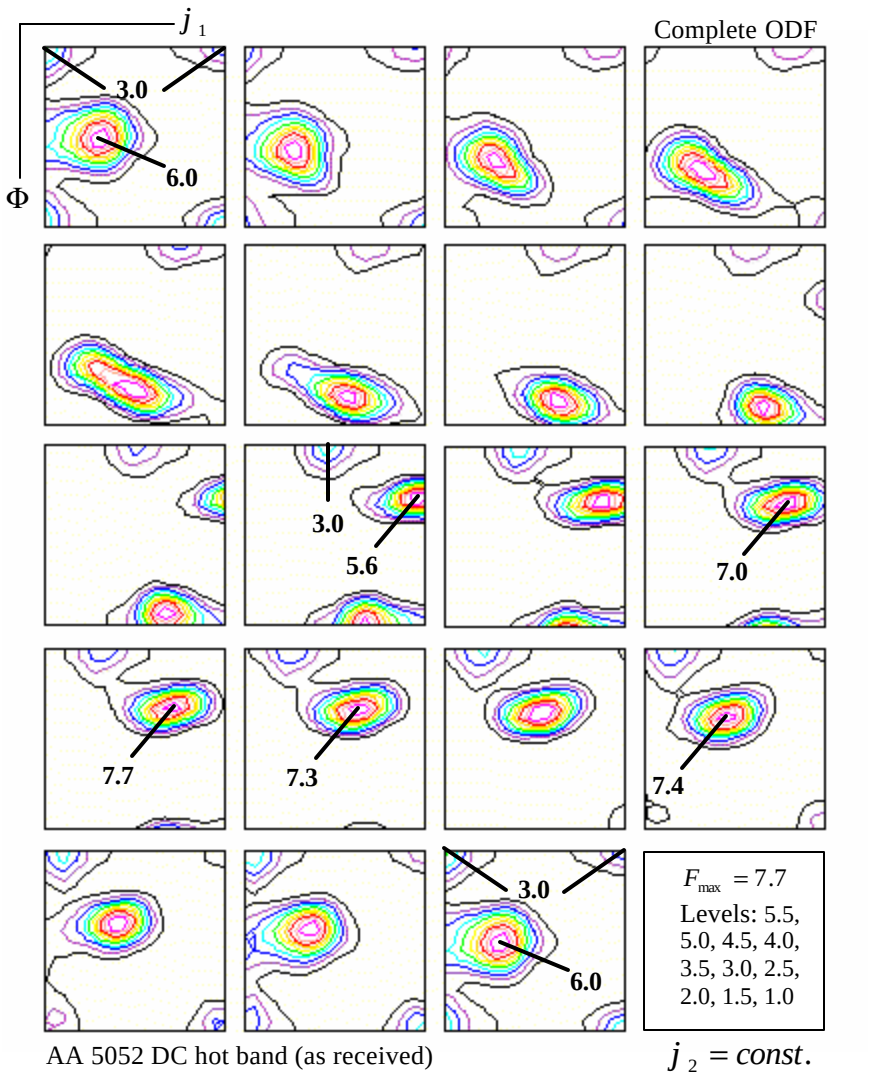

Fig. 5. (b) Complete ODFs of AA 5052 DC hot band (as received).

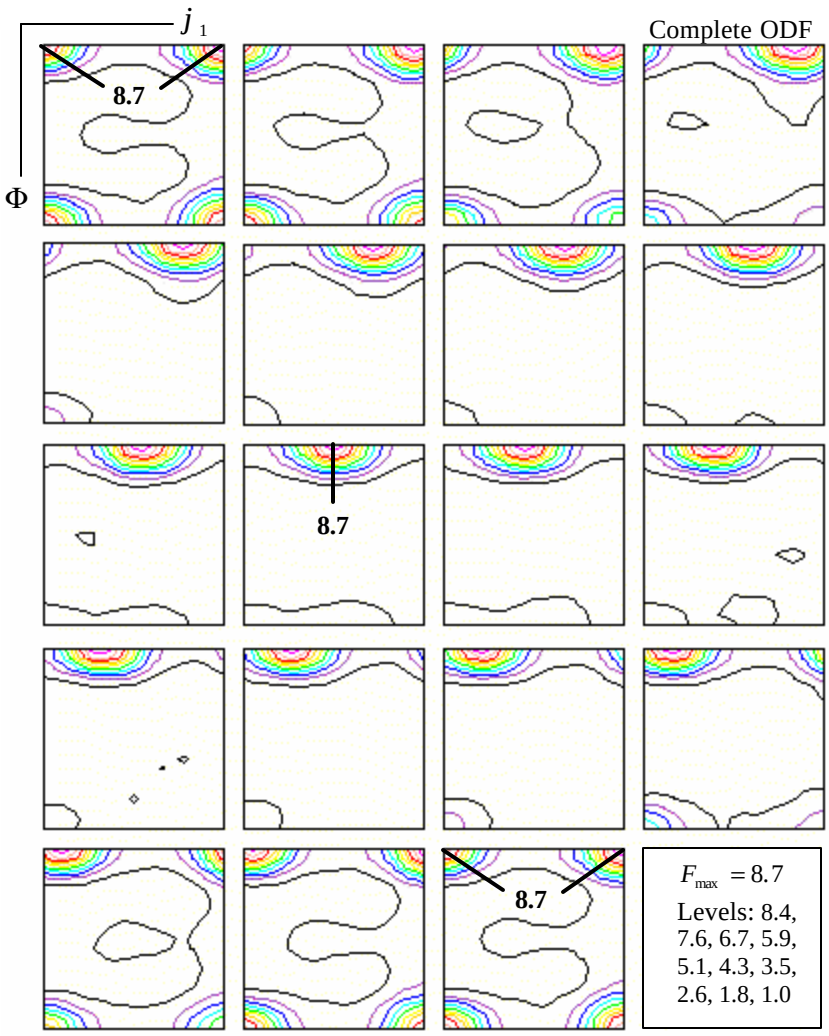

Fig. 6. (a) Complete ODFs of AA 5052 CC hot band after annealing at 1022 ^oF for 2 hrs.

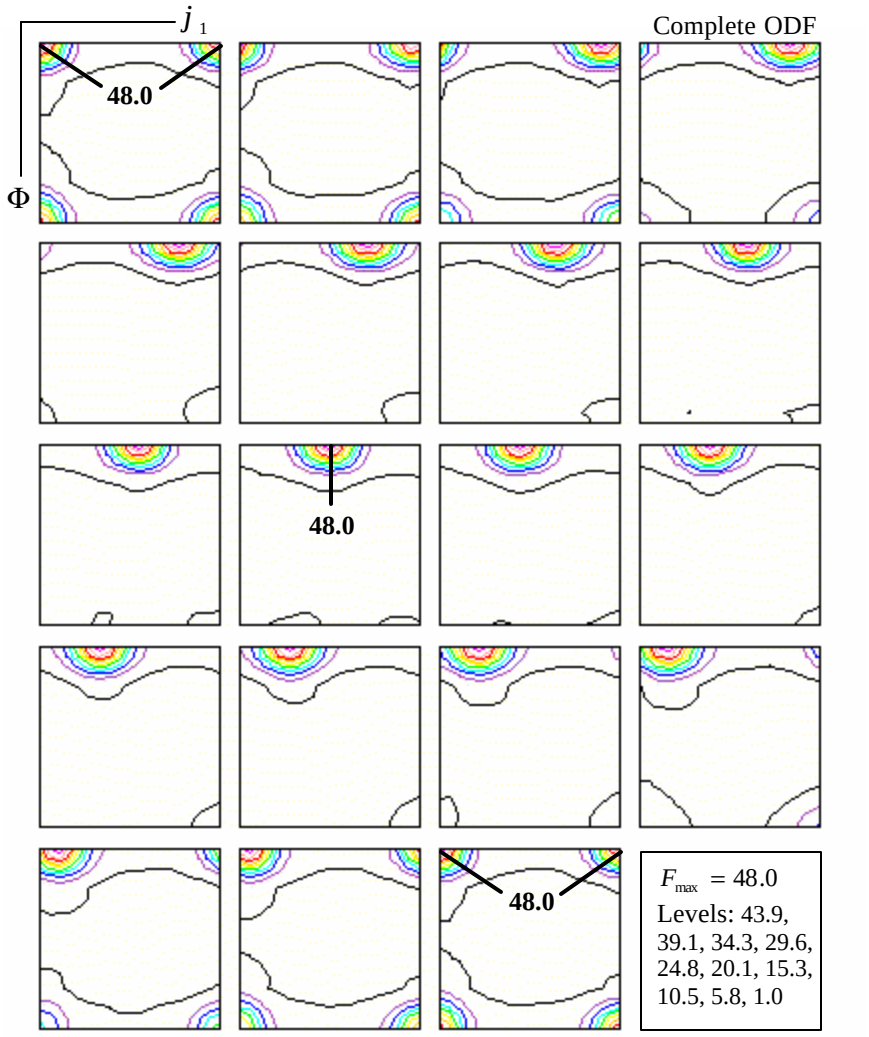

Fig. 6. (b) Complete ODFs of AA 5052 DC hot band after annealing at 1022 ^{o}F for 2 hrs.

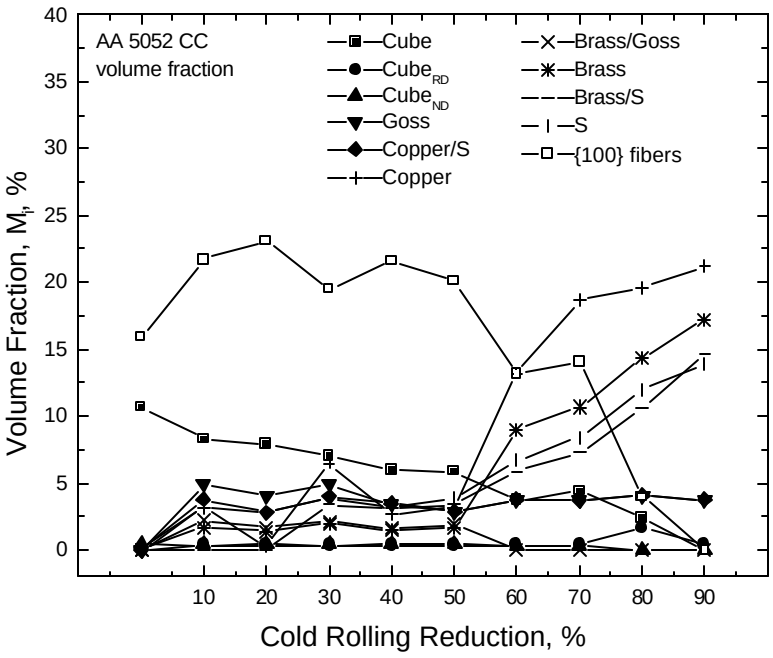

(a)

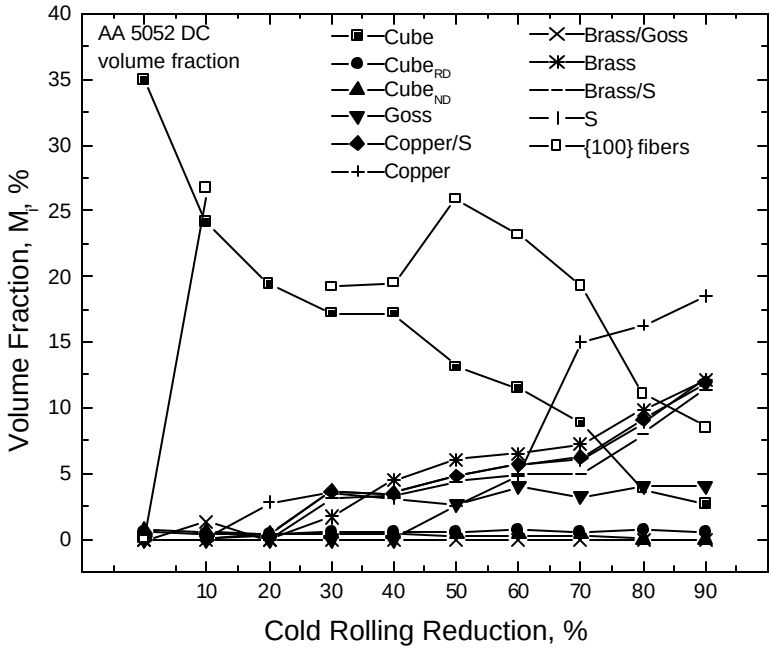

(b)

Fig. 7. Dependence of the volume fraction of different texture components in (a) AA 5052 CC materials and (b) AA 5052 DC materials on the degree of cold rolling reduction.

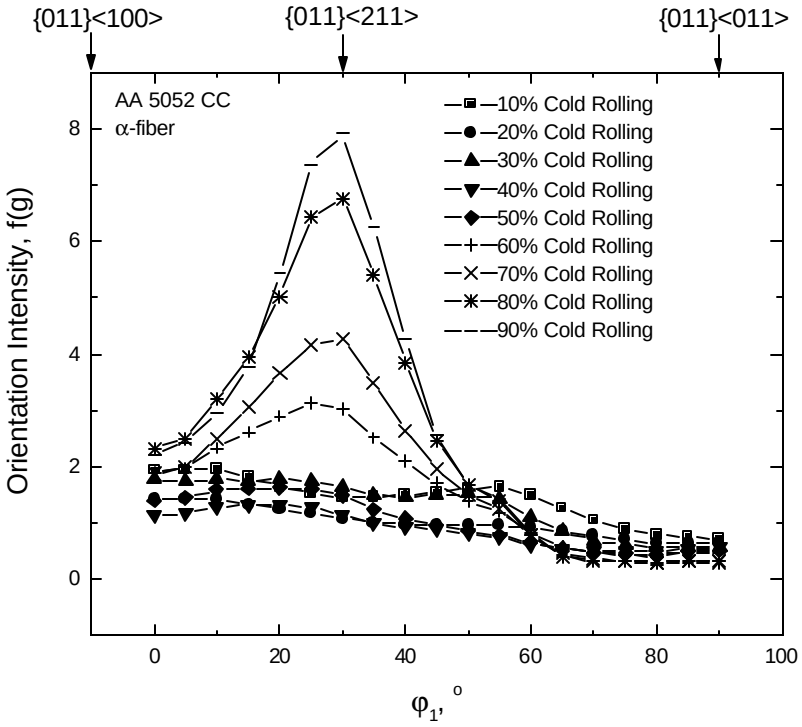

(a)

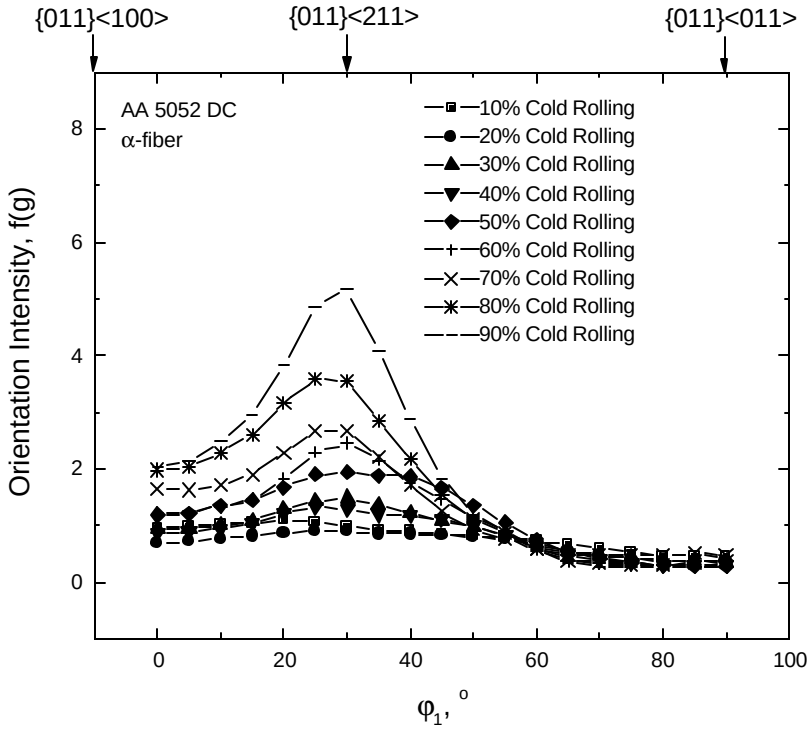

(b)

Fig. 8. Dependence of orientation intensity of (a) AA 5052 CC materials and (b) AA 5052 DC materials on the cold rolling reduction.

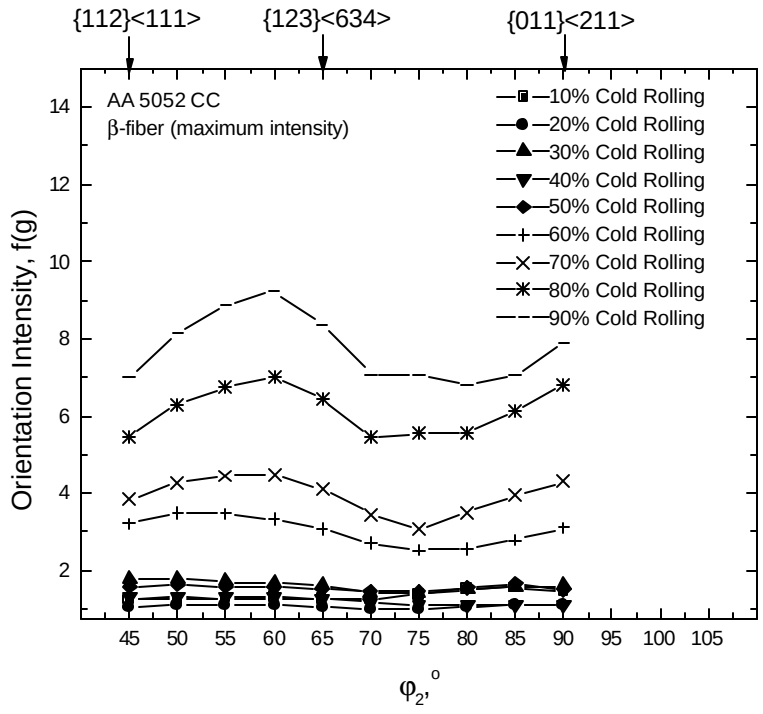

(a)

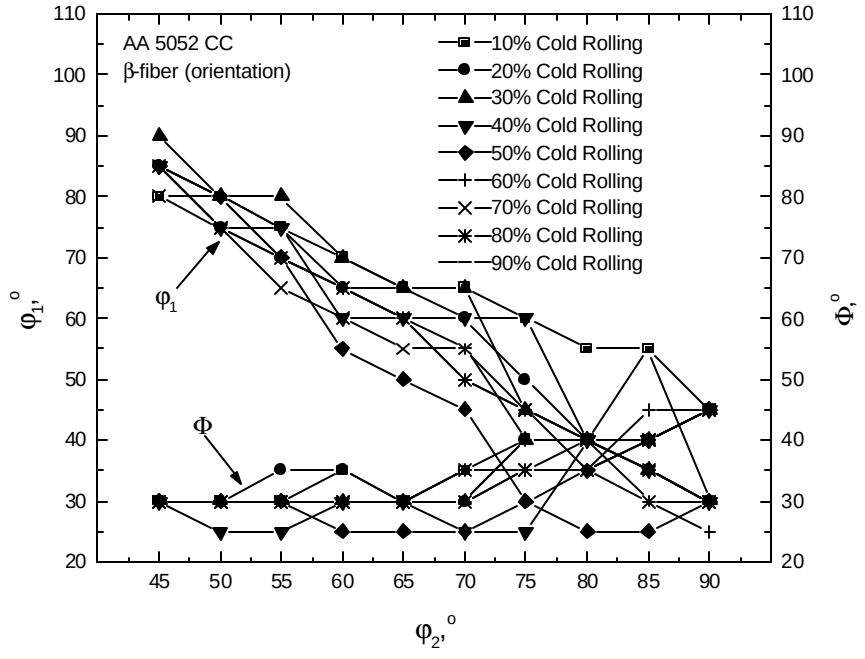

(b)

Fig. 9. Orientation intensity of orientations of AA 5052 CC materials along the b fiber (skeleton line) (a) and their exact positions in Euler space j_1, F as function of j_2.

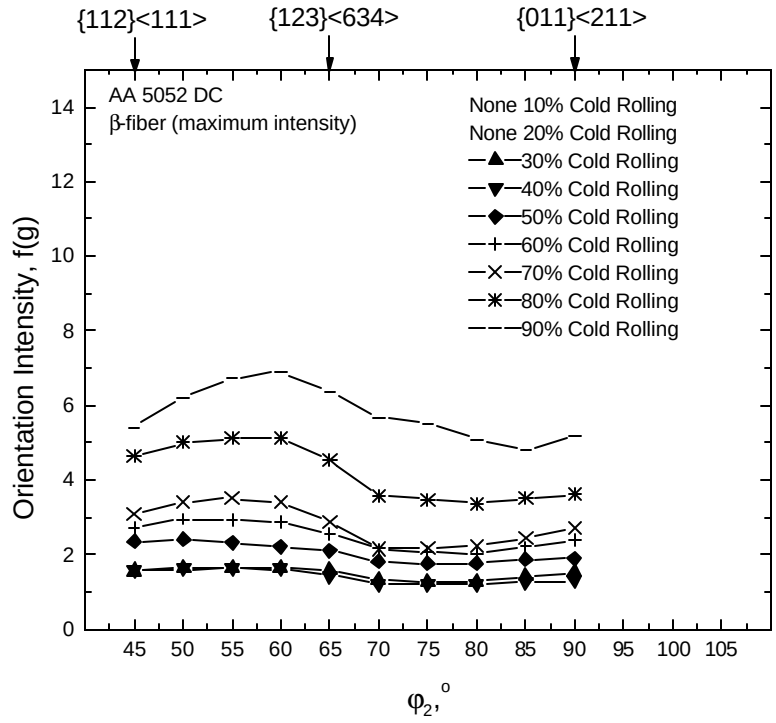

(a)

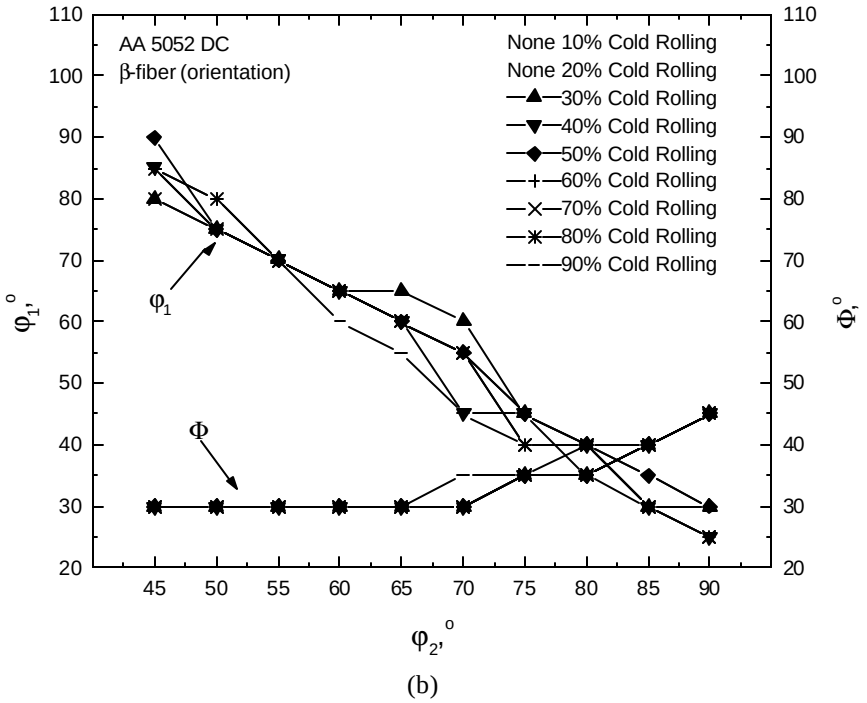

(b)

Fig. 10. Orientation intensity of orientations of AA 5052 DC materials along the b fiber (skeleton line) (a) and their exact positions in Euler space j_1, F as function of j_2.

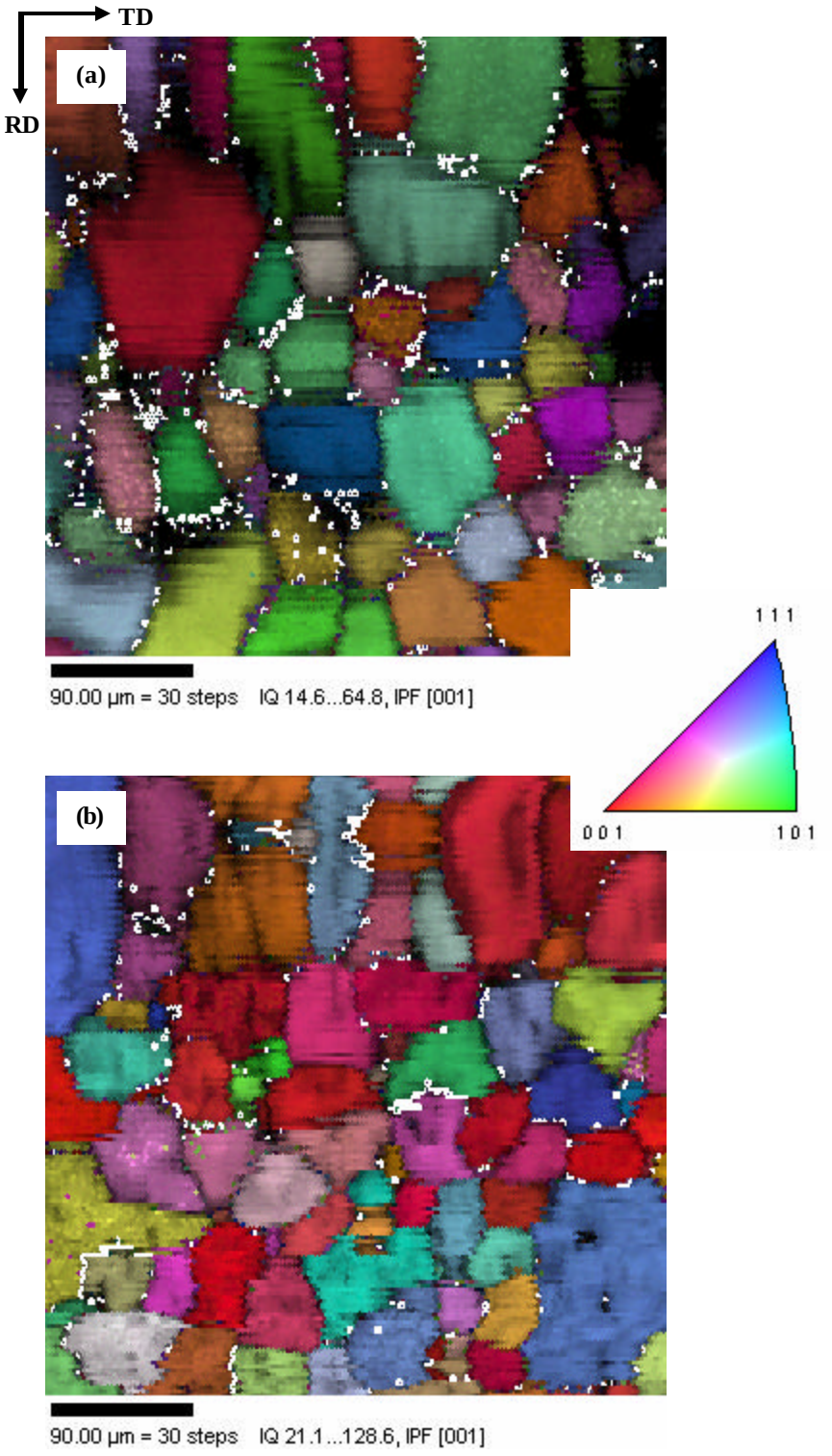

Fig. 11 Inverse pole figure (IPF) maps of completely recrystallized AA 5052 (a) CC and (b) DC hot bands. White segments indicate the twin (Σ3) and high order twin boundaries (Σ9, Σ27a&b).

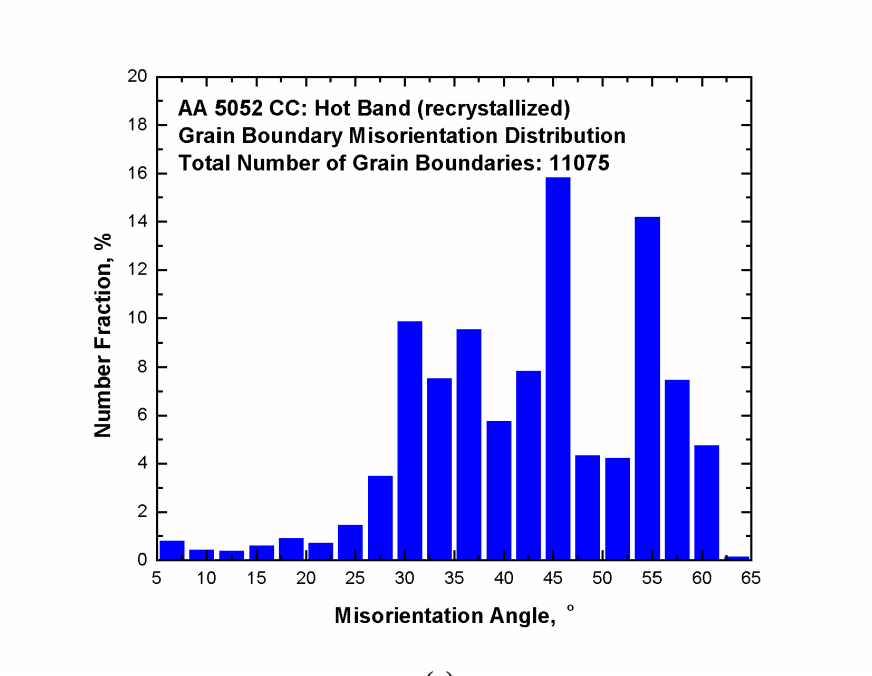

(a)

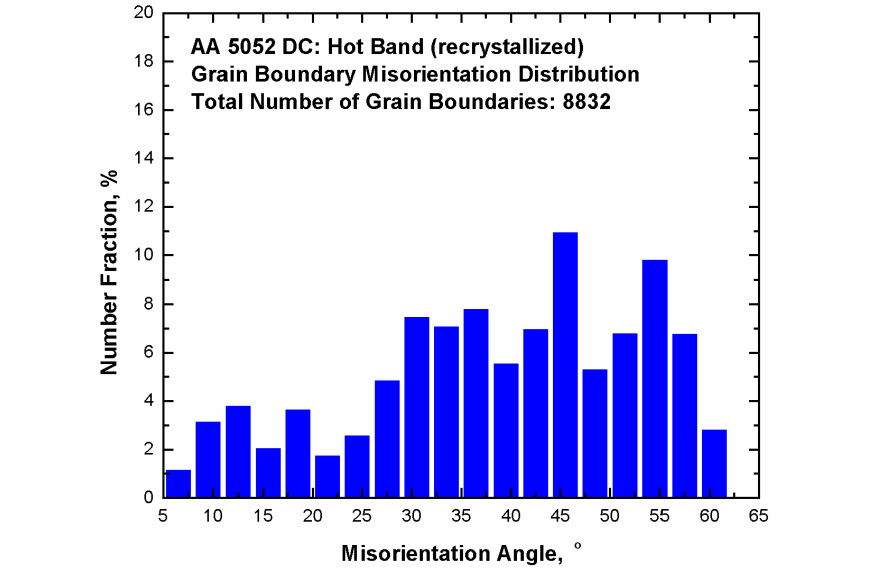

(b)

Fig. 12 Grain boundary misorientation distributions of completely recrystallized AA 5052 (a) CC and (b) DC hot bands.

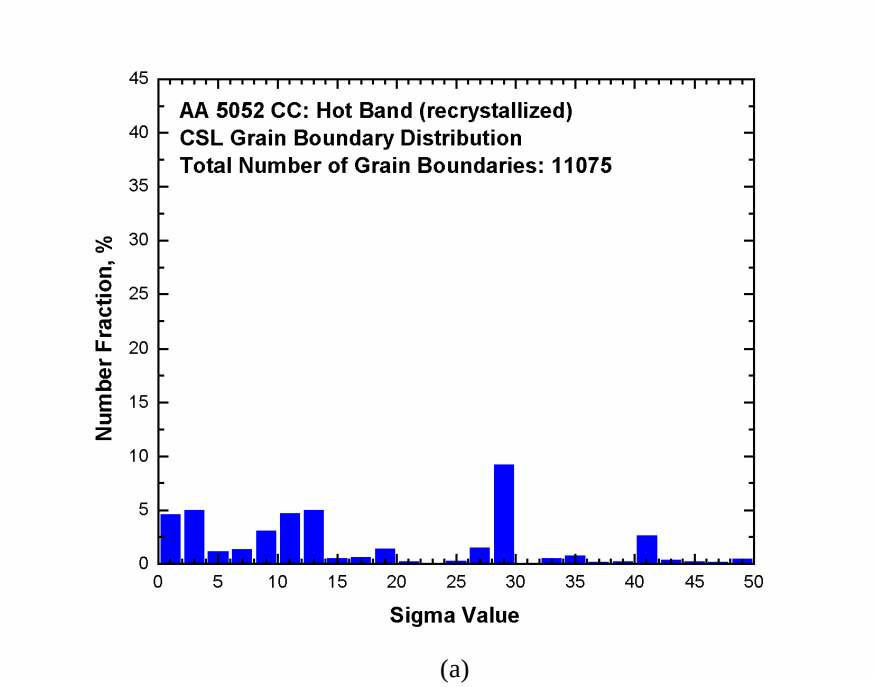

(a)

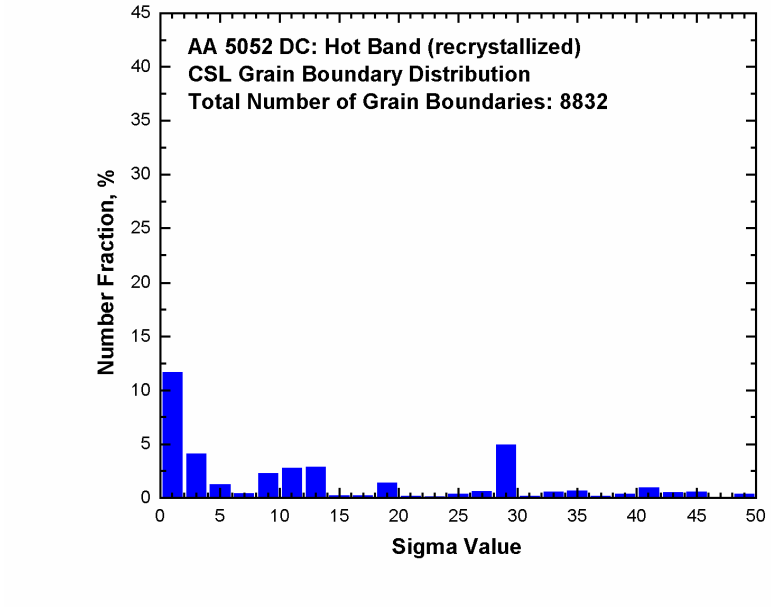

(b)

Fig. 13 CSL Grain boundary distributions of completely recrystallized AA 5052 (a) CC and (b) DC hot bands.

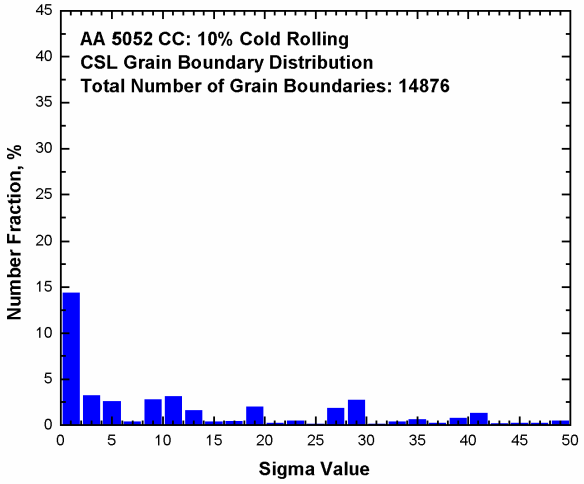

(a)

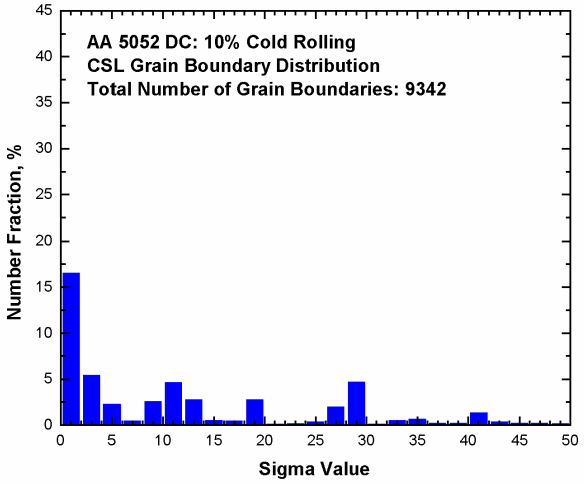

(b)

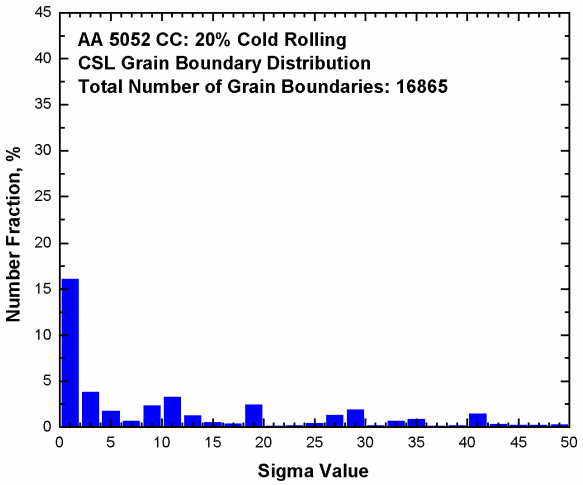

(c)

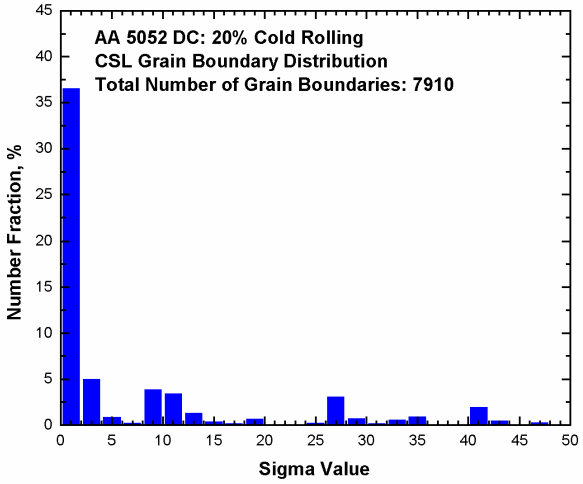

(d)

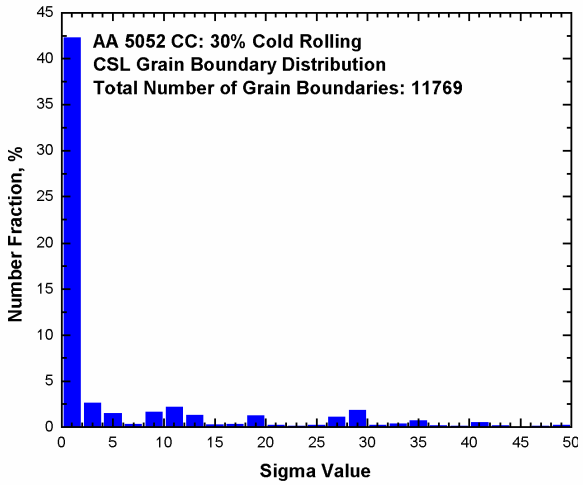

(e)

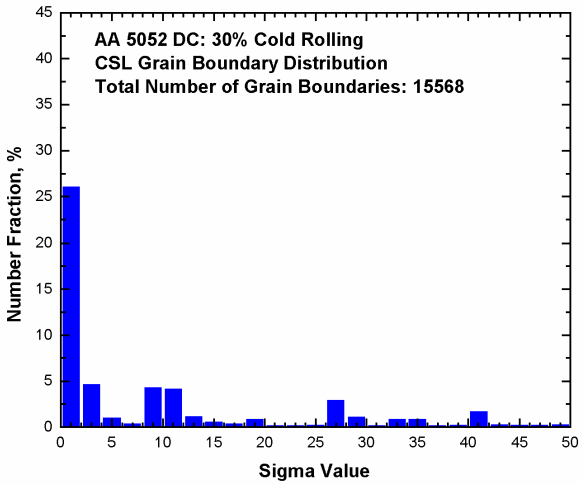

(f)

Fig. 14 CSL Grain boundary distributions after 10% cold rolling of AA 5052 (a) CC, (b) DC; 20% cold rolling of AA 5052 (c) CC, (d) DC; and 30% cold rolling of AA 5052 (e) CC, (f) DC materials.

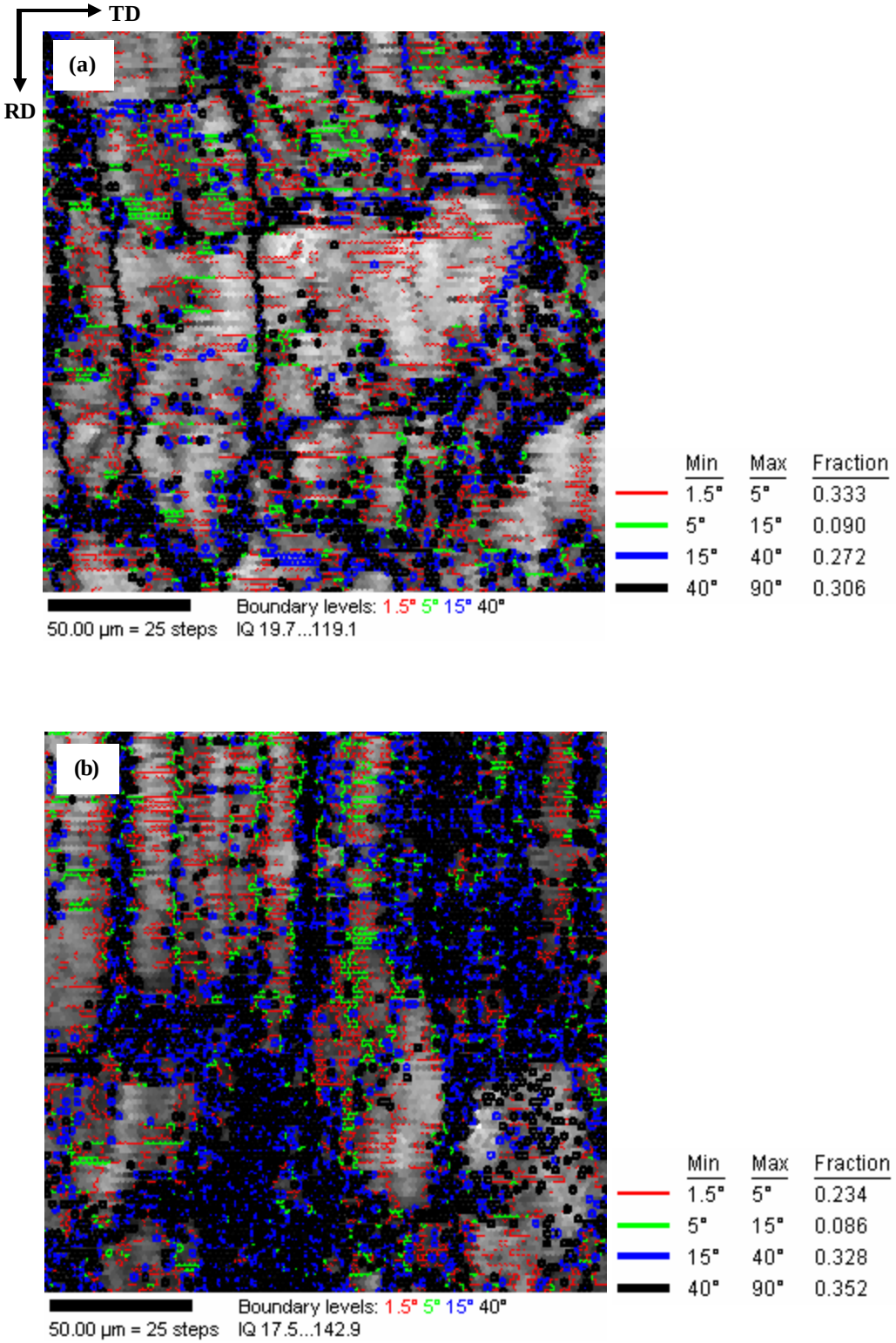

Fig. 15 Grain boundary maps of AA 5052 CC material after (a) 30% cold rolling and (b) 40% cold rolling.

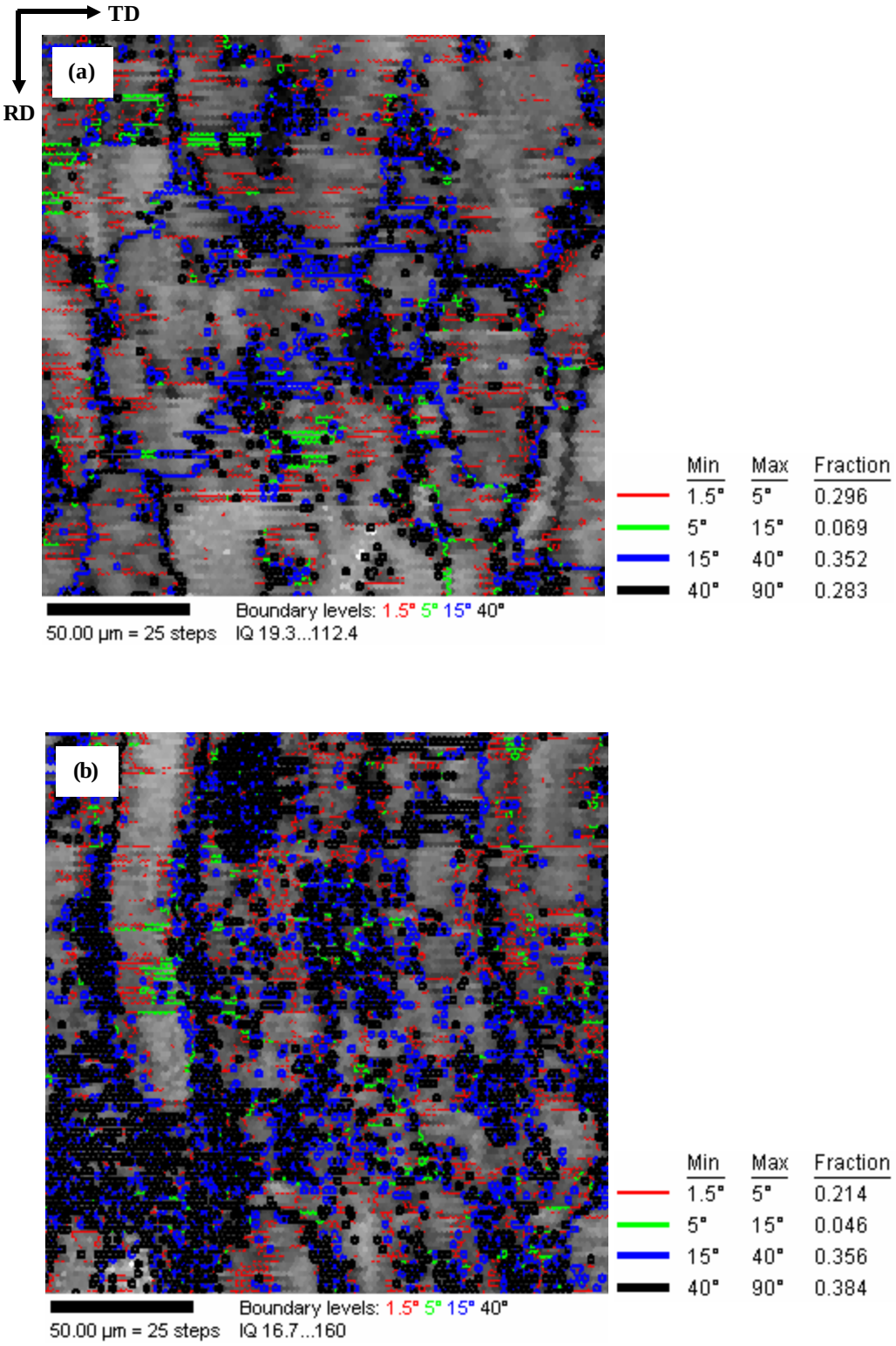

Fig. 16 Grain boundary maps of AA 5052 DC material after (a) 20% cold rolling and (b) 30% cold rolling.

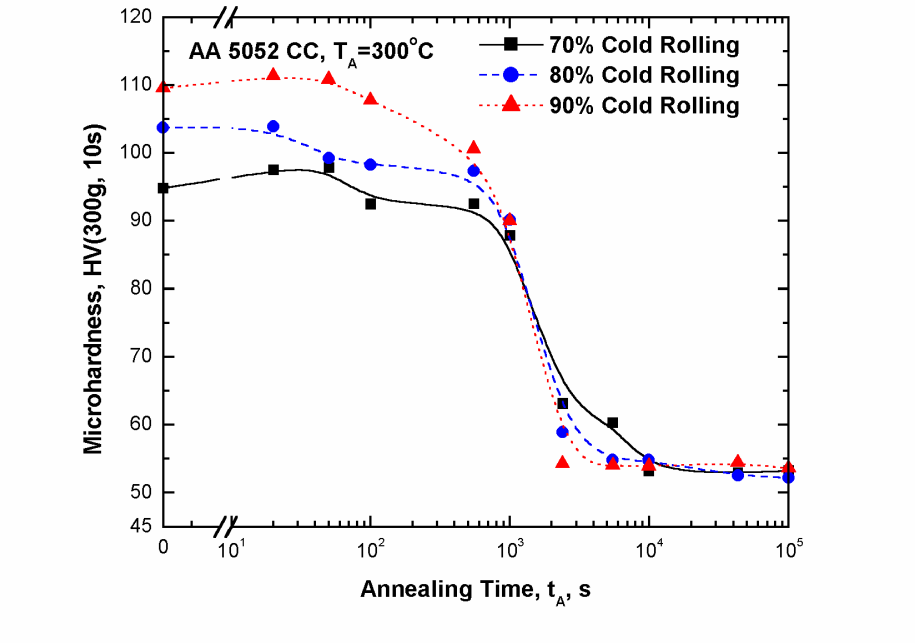
AA 5052 CC, T_A=300°C
70% Cold Rolling
80% Cold Rolling
90% Cold Rolling
Microhardness, HV(300g, 10s)
Annealing Time, t_A, s
120
110
100
90
80
70
60
50
45
0
10^1
10^2
10^3
10^4
10^5

(a)

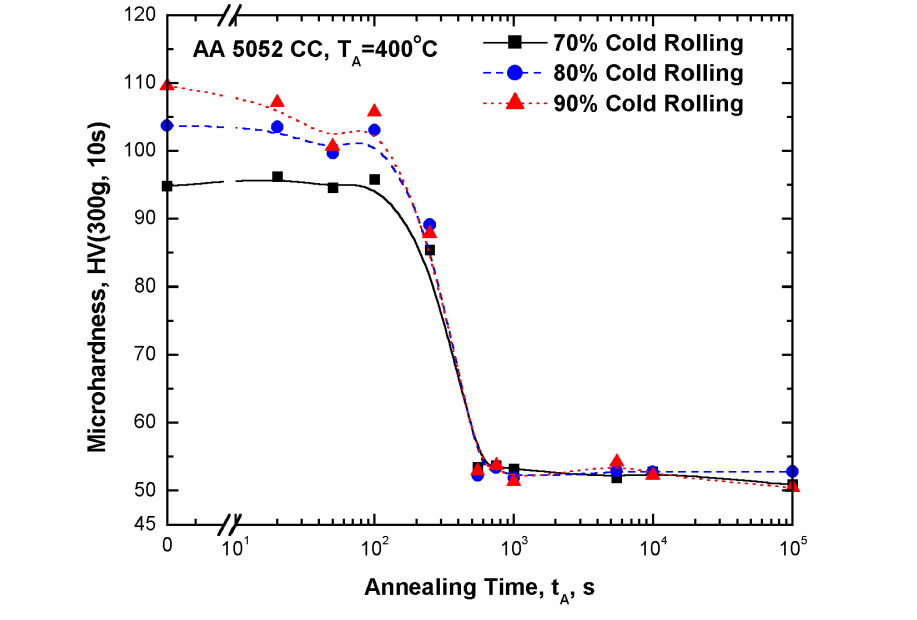
AA 5052 CC, T_A=400°C
70% Cold Rolling
80% Cold Rolling
90% Cold Rolling
Microhardness, HV(300g, 10s)
Annealing Time, t_A, s
120
110
100
90
80
70
60
50
45
0
10^1
10^2
10^3
10^4
10^5

(b)

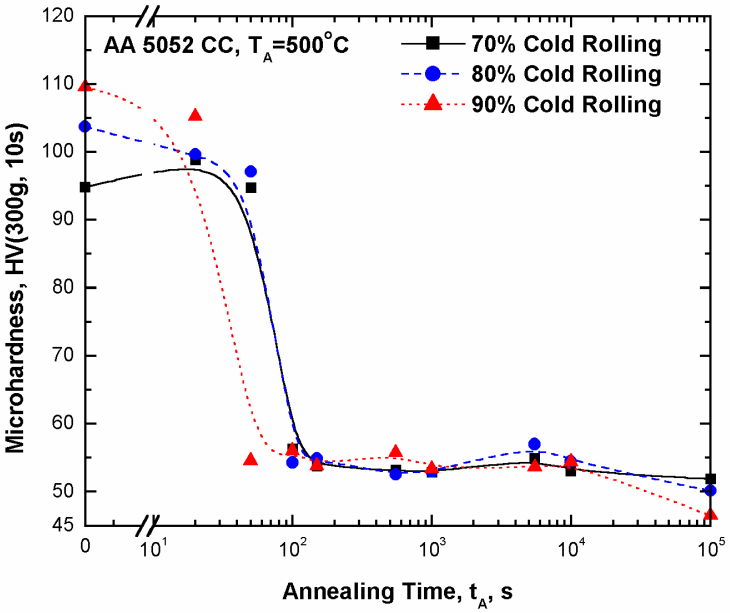

(c)

Fig. 17. Microhardness vs annealing time of AA 5052 CC material at (a) 300 ºC, (b) 400 ºC and (c) 500 ºC.

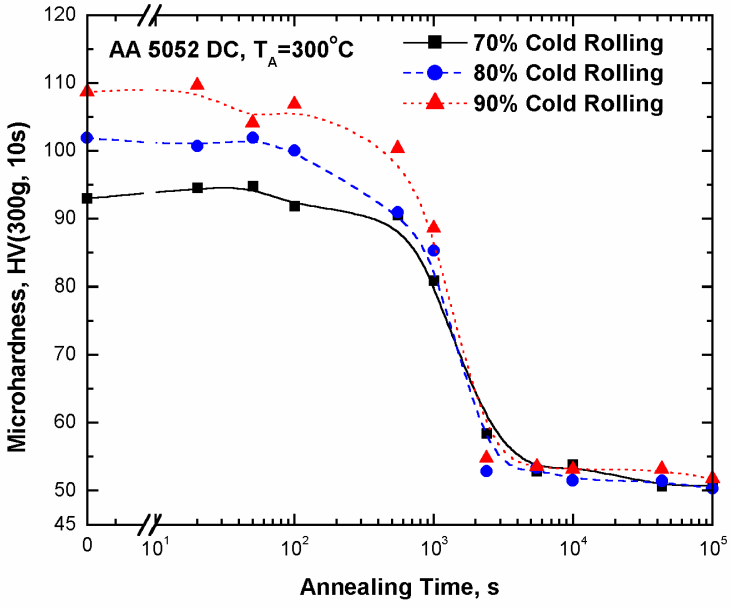
AA 5052 DC, T_A=300°C
70% Cold Rolling
80% Cold Rolling
90% Cold Rolling
Microhardness, HV(300g, 10s)
Annealing Time, s
120
110
100
90
80
70
60
50
45
0
10^1
10^2
10^3
10^4
10^5

(a)

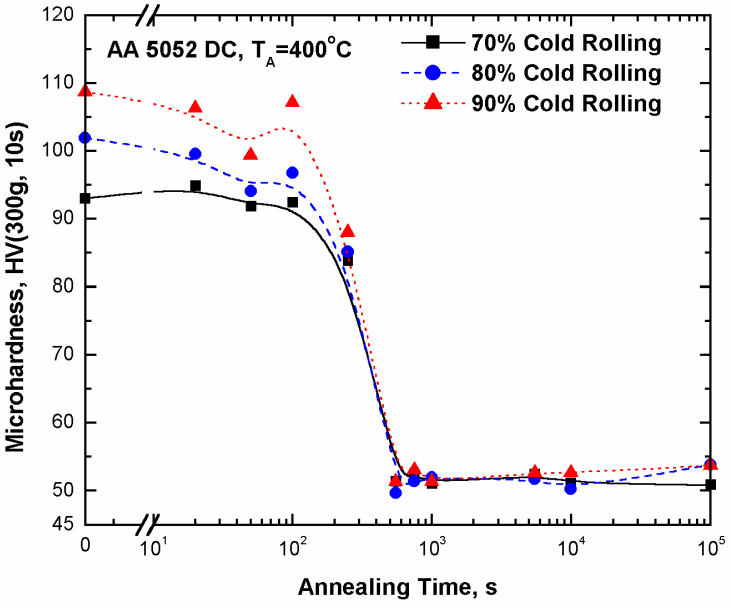
AA 5052 DC, T_A=400°C
70% Cold Rolling
80% Cold Rolling
90% Cold Rolling
Microhardness, HV(300g, 10s)
Annealing Time, s
120
110
100
90
80
70
60
50
45
0
10^1
10^2
10^3
10^4
10^5

(b)

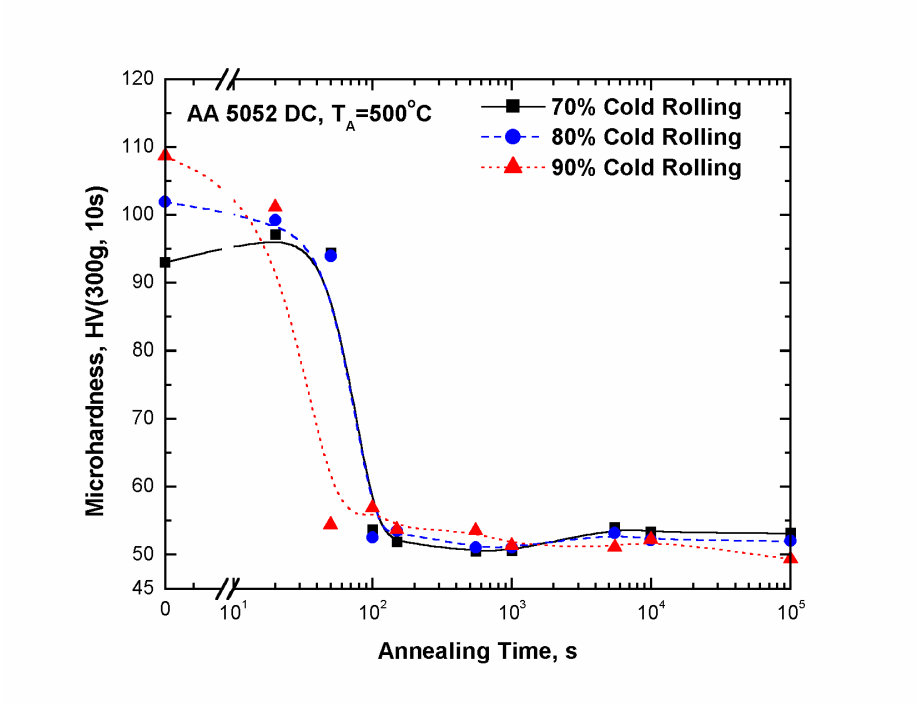

(c)

Fig. 18. Microhardness vs annealing time of AA 5052 DC material at (a) 300 ºC, (b) 400 ºC and (c) 500 ºC.

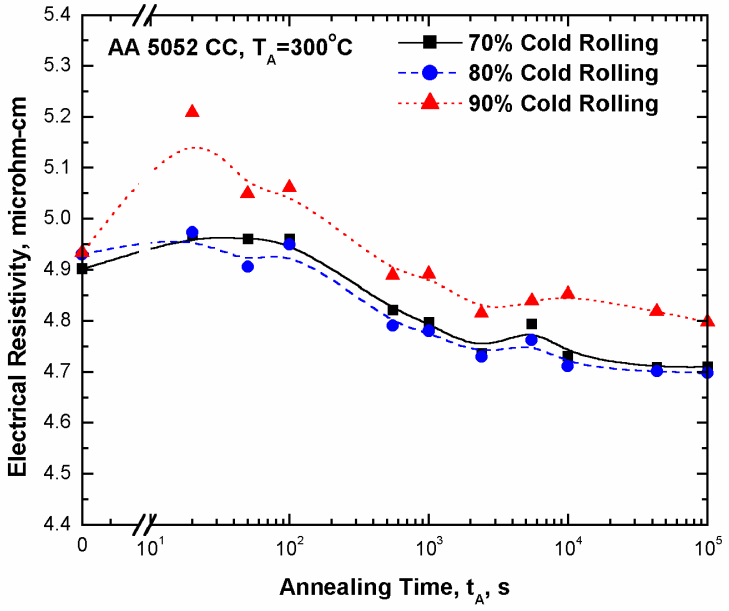
AA 5052 CC, T_A=300°C
70% Cold Rolling
80% Cold Rolling
90% Cold Rolling
Electrical Resistivity, microhm-cm
Annealing Time, t_A, s
5.4
5.3
5.2
5.1
5.0
4.9
4.8
4.7
4.6
4.5
4.4
0
10^1
10^2
10^3
10^4
10^5

(a)

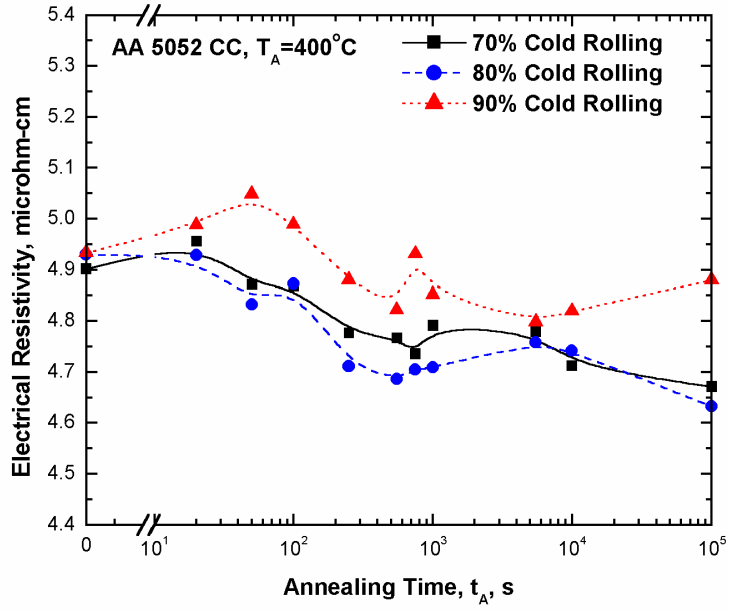
AA 5052 CC, T_A=400°C
70% Cold Rolling
80% Cold Rolling
90% Cold Rolling
Electrical Resistivity, microhm-cm
Annealing Time, t_A, s
5.4
5.3
5.2
5.1
5.0
4.9
4.8
4.7
4.6
4.5
4.4
0
10^1
10^2
10^3
10^4
10^5

(b)

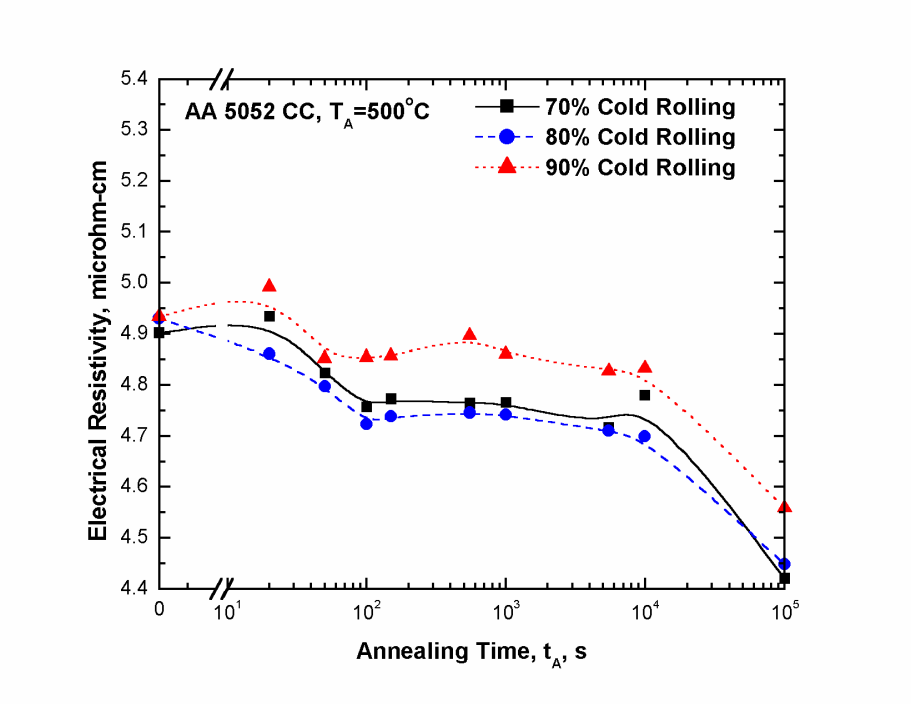

(c)

Fig. 19. Electrical resistivity vs annealing time of AA 5052 CC material at (a) 300 ºC, (b) 400 ºC and (c) 500 ºC.

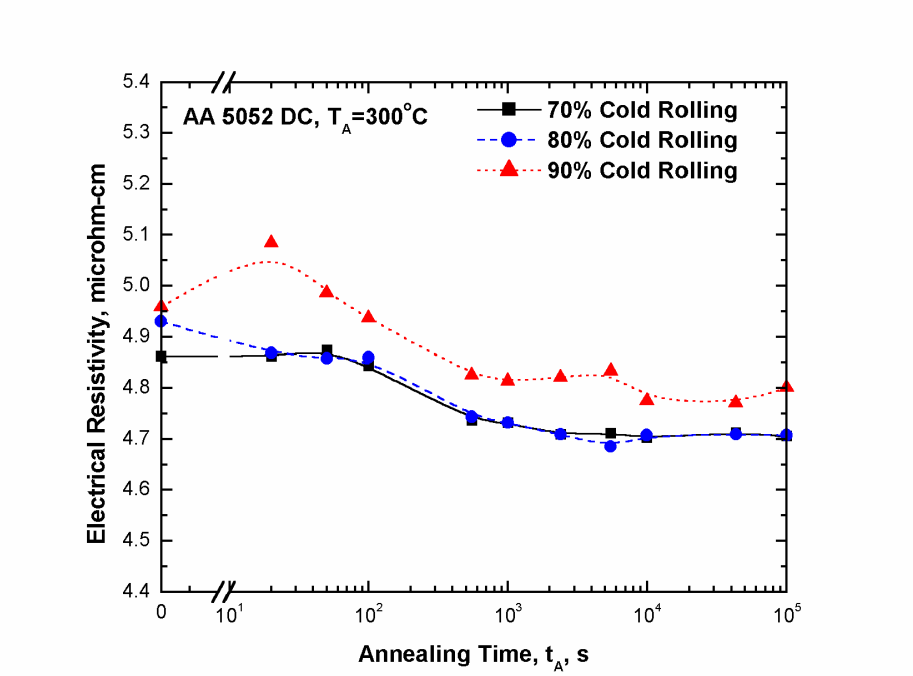
AA 5052 DC, T_A=300°C
70% Cold Rolling
80% Cold Rolling
90% Cold Rolling
Electrical Resistivity, microhm-cm
Annealing Time, t_A, s
5.4
5.3
5.2
5.1
5.0
4.9
4.8
4.7
4.6
4.5
4.4
0
10^1
10^2
10^3
10^4
10^5

(a)

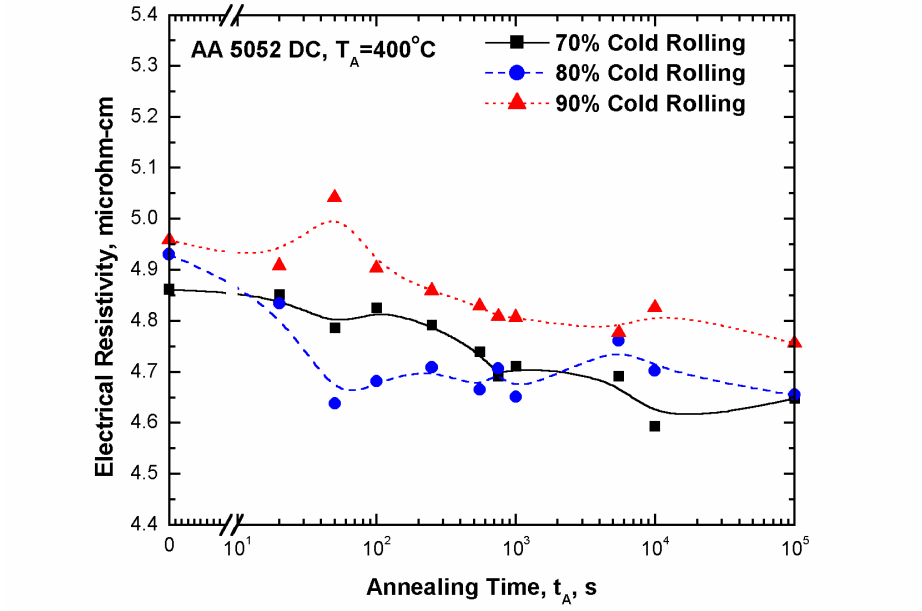
AA 5052 DC, T_A=400°C
70% Cold Rolling
80% Cold Rolling
90% Cold Rolling
Electrical Resistivity, microhm-cm
Annealing Time, t_A, s
5.4
5.3
5.2
5.1
5.0
4.9
4.8
4.7
4.6
4.5
4.4
0
10^1
10^2
10^3
10^4
10^5

(b)

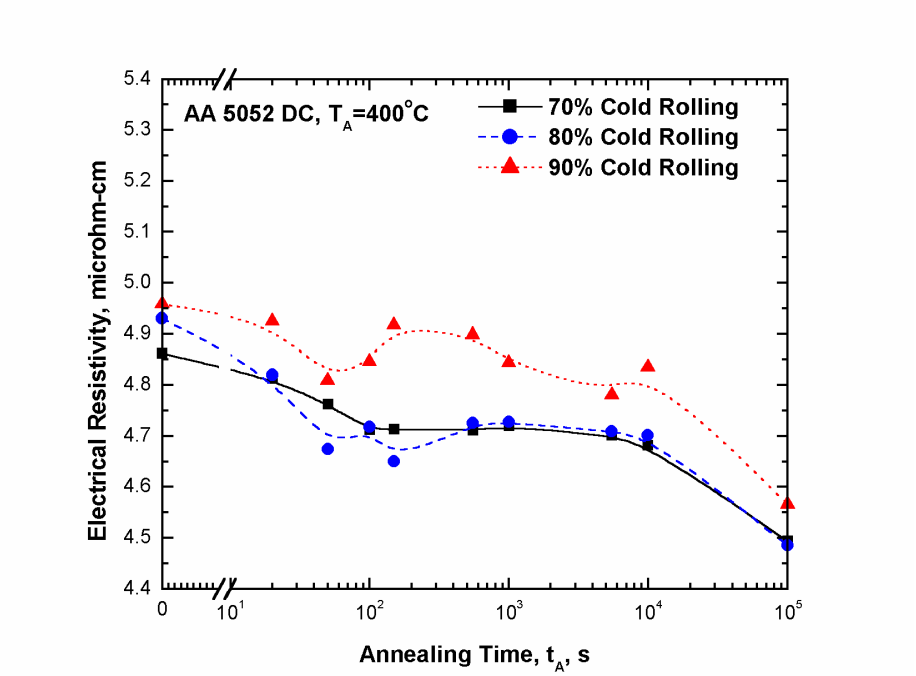

(c)

Fig. 20. Electrical resistivity vs annealing time of AA 5052 DC material at (a) 300 ºC, (b) 400 ºC and (c) 500 ºC.

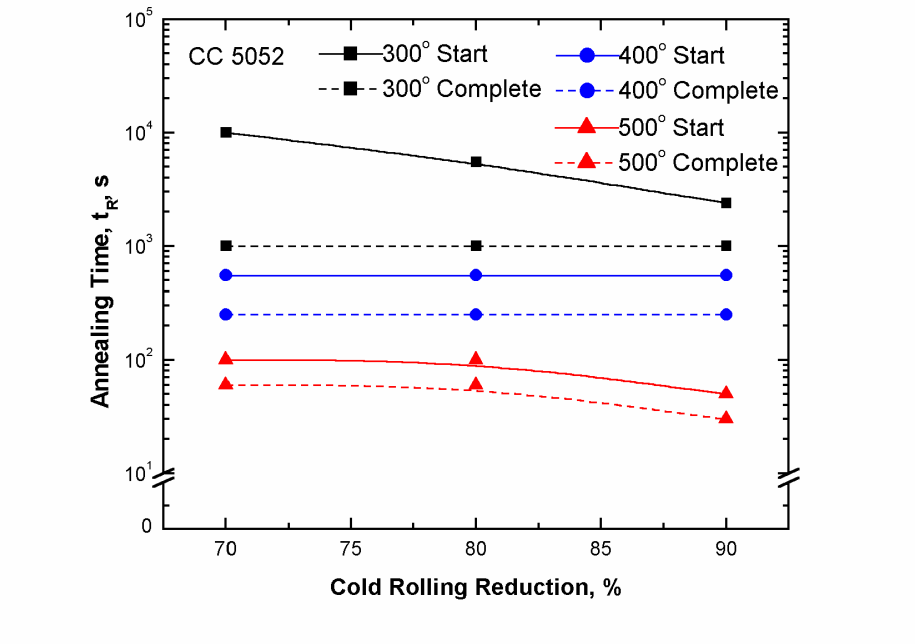

(a)

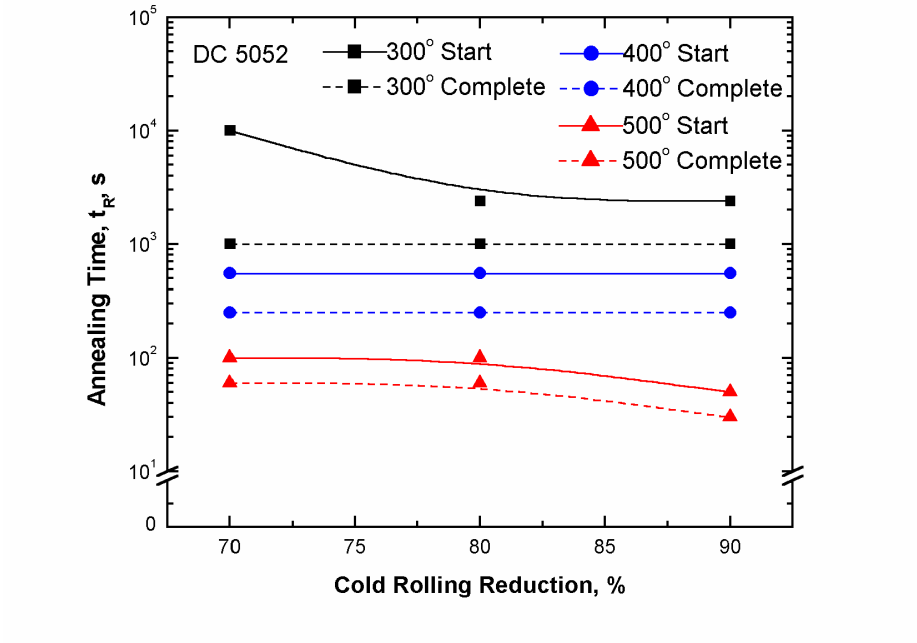

(b)

Fig. 21. Time for complete recrystallization t_R vs. cold rolling reduction of (a) AA 5052 CC and (b) AA 5052 DC materials.

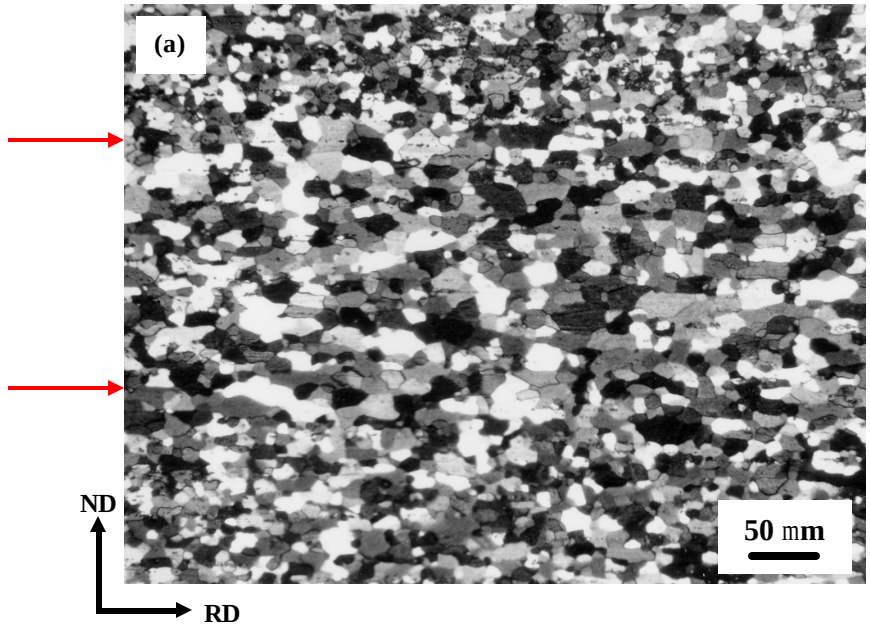
(a)
50 mm
ND
RD

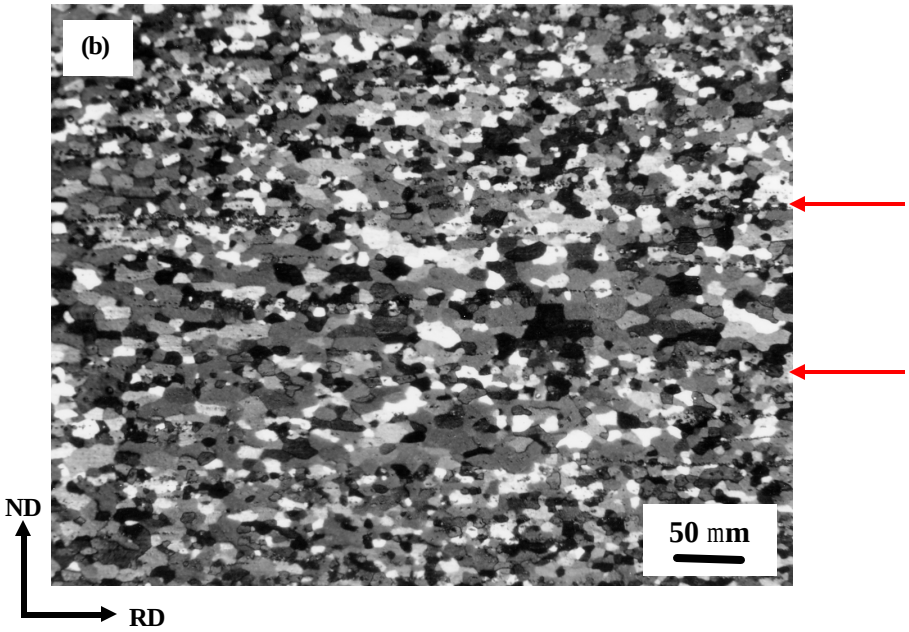
(b)
50 mm
ND
RD

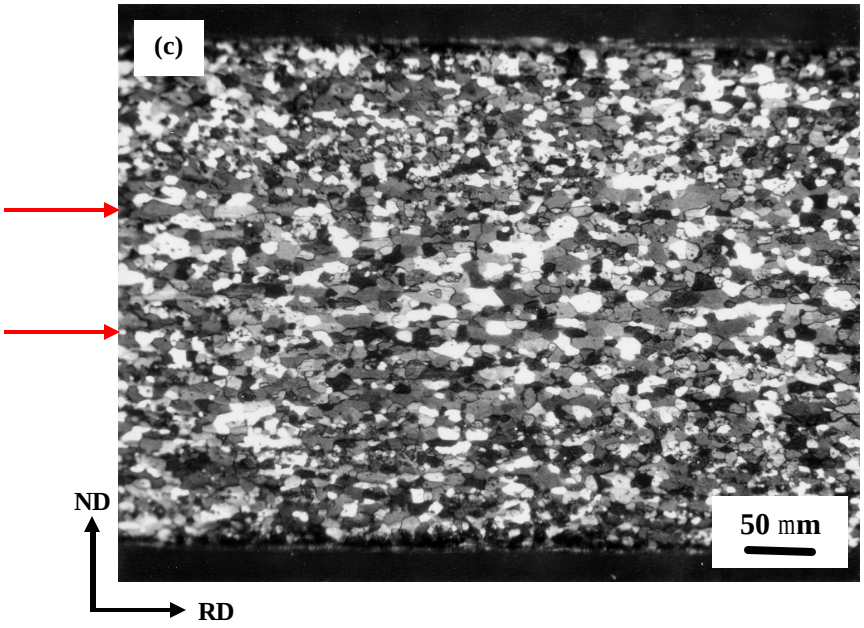

Fig. 22. Recrystallization grain structure of AA 5052 CC material after (a) 70 %, (b) 80% and (c) 90 cold rolling followed by annealing at 400 °C for 1000s.

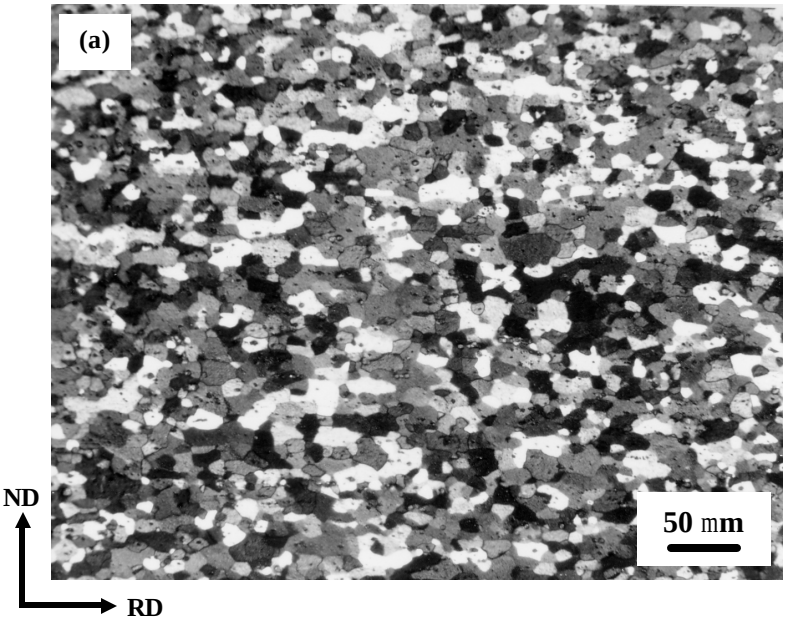
(a)
50 mm
ND
RD

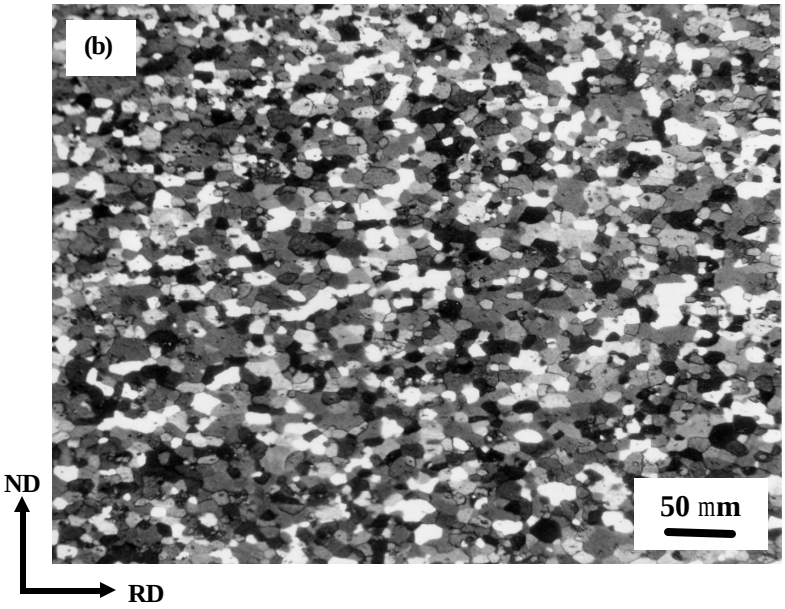
(b)
50 mm
ND
RD

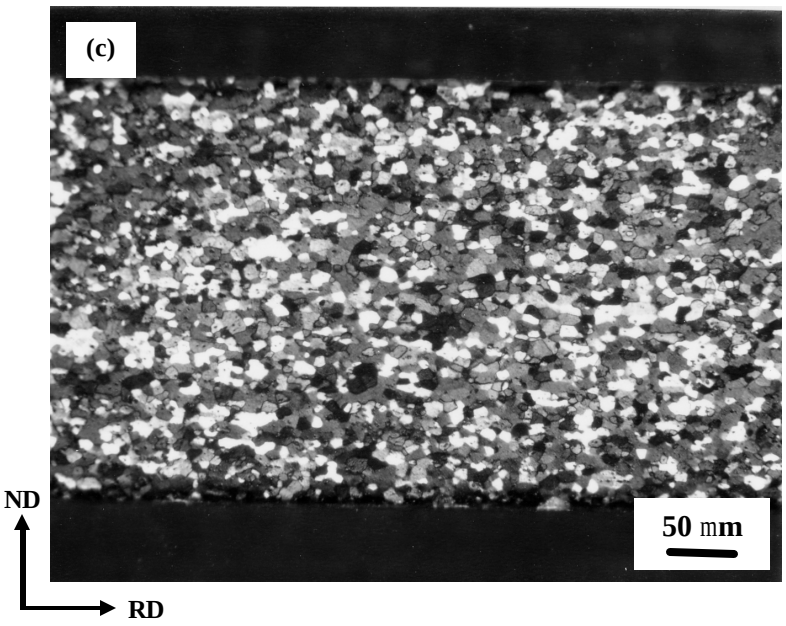

Fig. 23. Recrystallized grain structure of AA 5052 DC material after (a) 70 %, (b) 80% and (c) 90 cold rolling followed by annealing at 400 °C for 1000s.

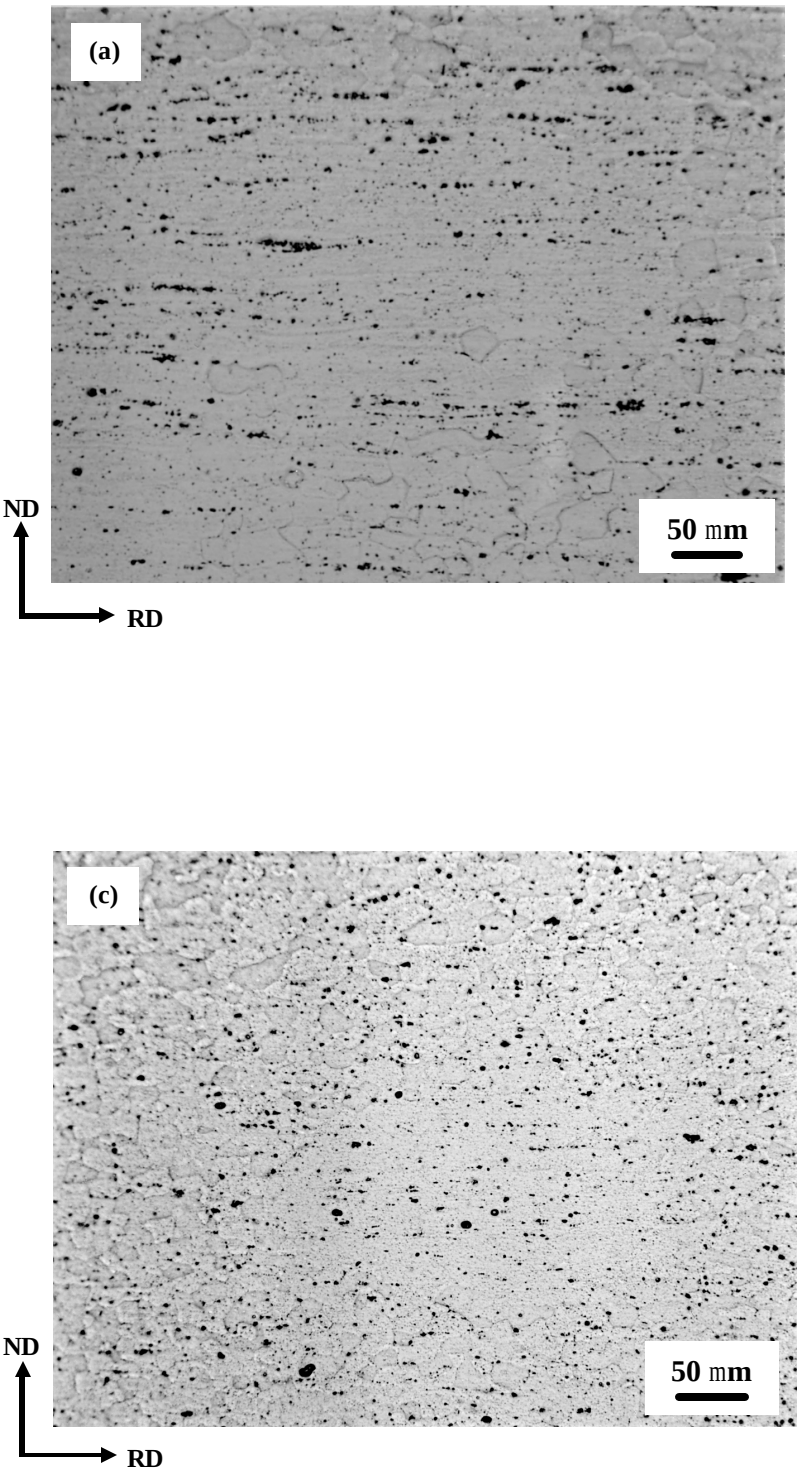

Fig. 24. Particle structure of (a) AA 5052 CC and (b) AA 5052 DC materials after annealing at 500 °C for 10^5s.

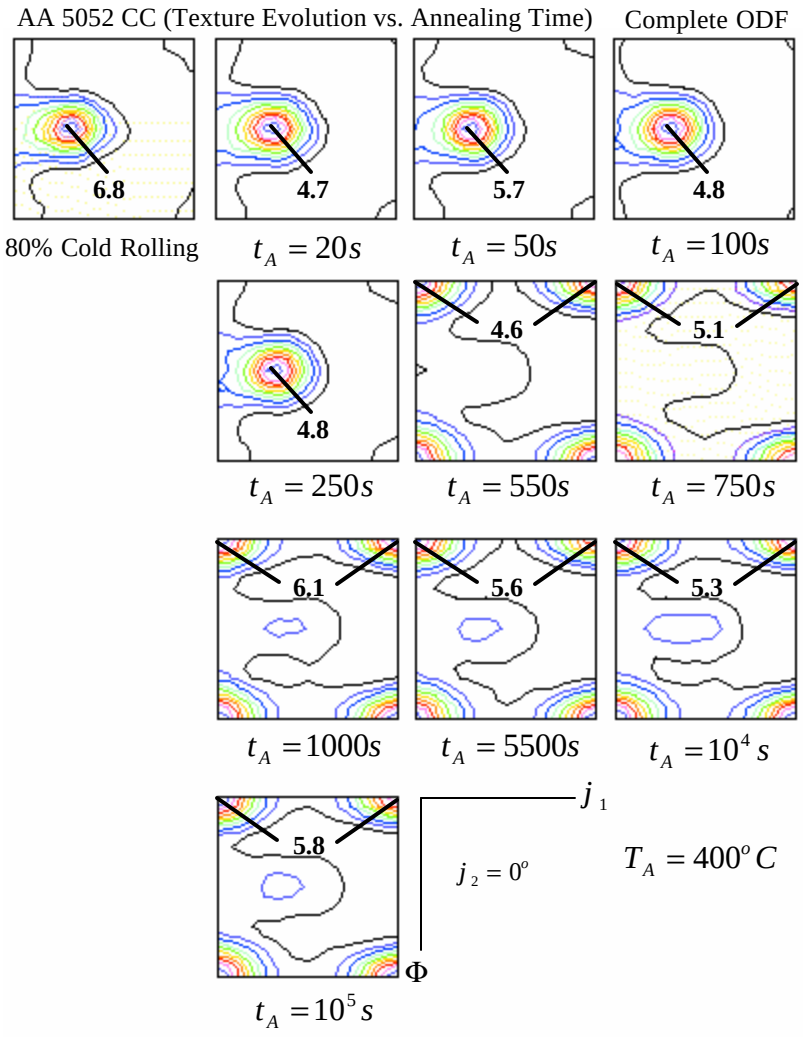

Fig. 25. ODFs (at section of $j_2 = 0^o$) of 80% cold rolled AA 5052 CC alloy during annealing at 400 °C for different time.

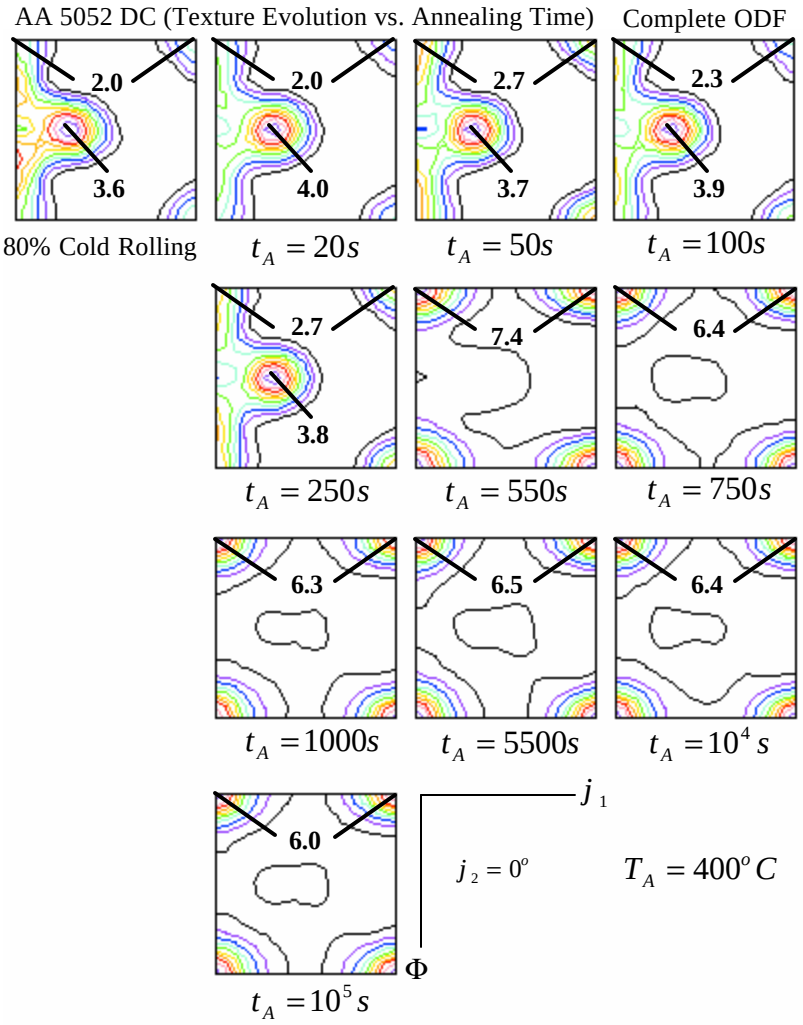

Fig. 26. ODFs (at section of $j_2 = 0^o$) of 80% cold rolled AA 5052 DC alloy during annealing at 400 °C for different time.

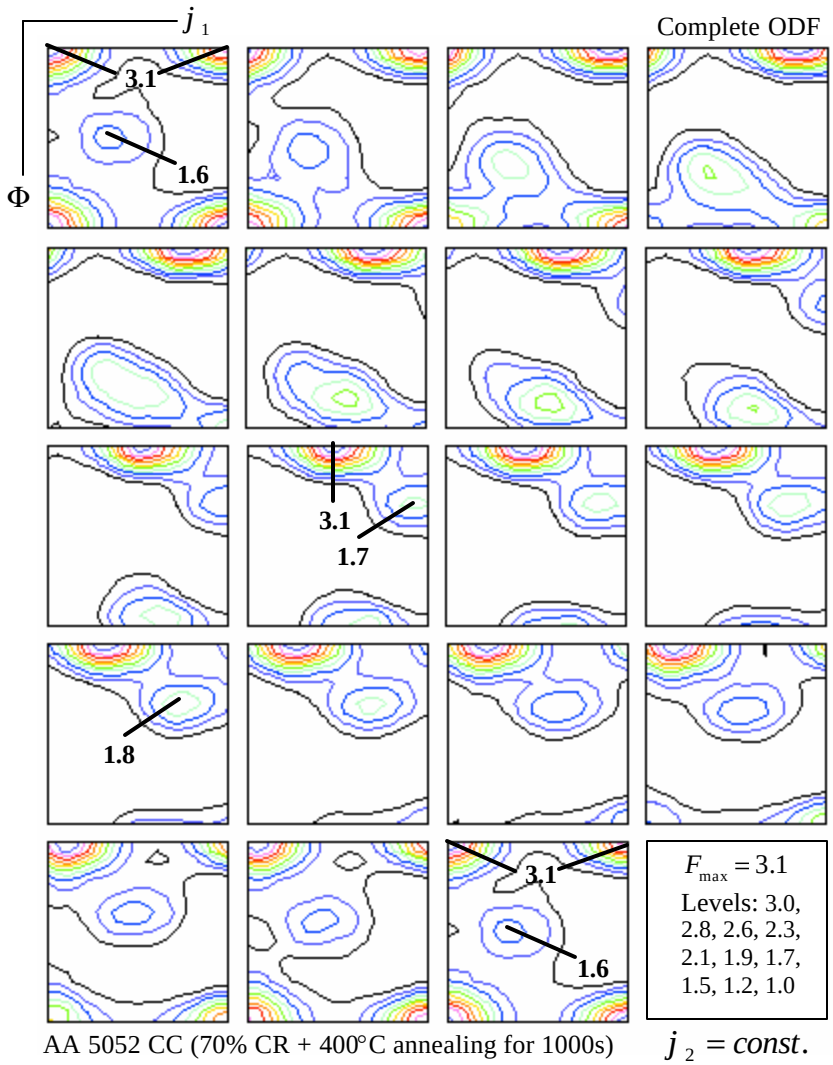

Fig. 27. Complete ODFs of AA 5052 CC after 70% cold rolling followed by annealing at 400 °C for 1000s.

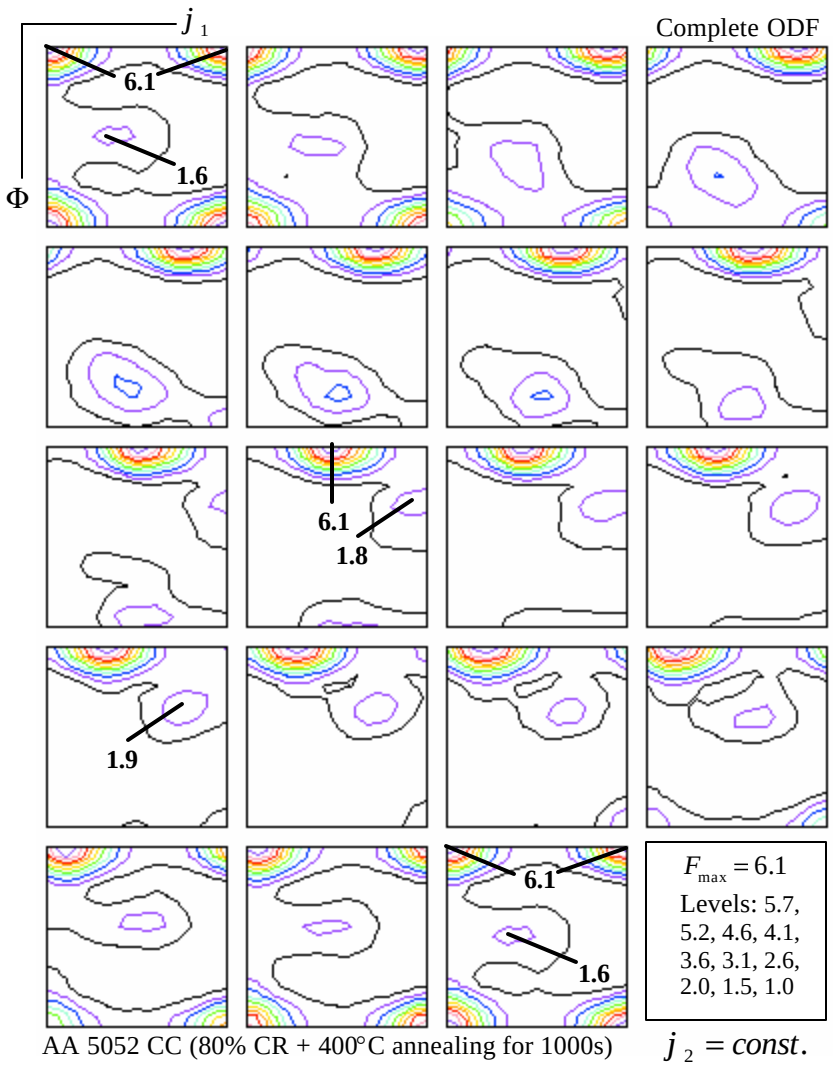

Fig. 28. Complete ODFs of AA 5052 CC after 80% cold rolling followed by annealing at 400 °C for 1000s.

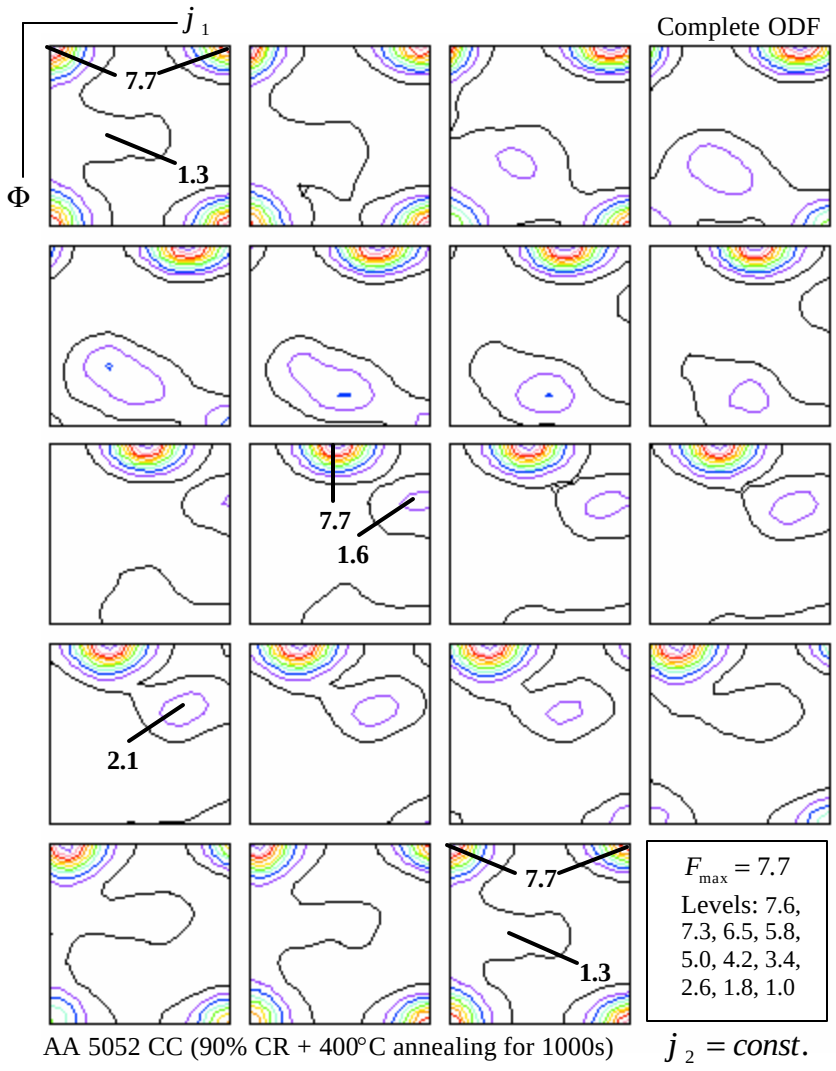

Fig. 29. Complete ODFs of AA 5052 CC after 90% cold rolling followed by annealing at 400 °C for 1000s.

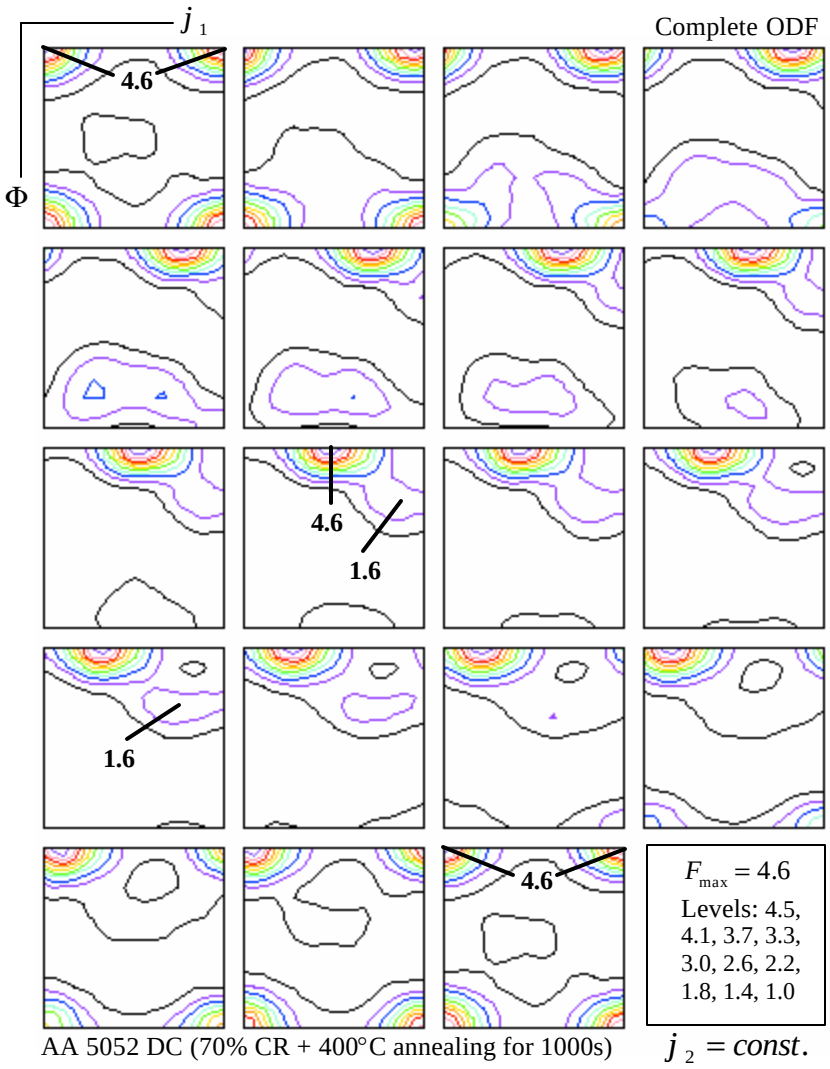

Fig. 30. Complete ODFs of AA 5052 DC after 70% cold rolling followed by annealing at 400 °C for 1000s.

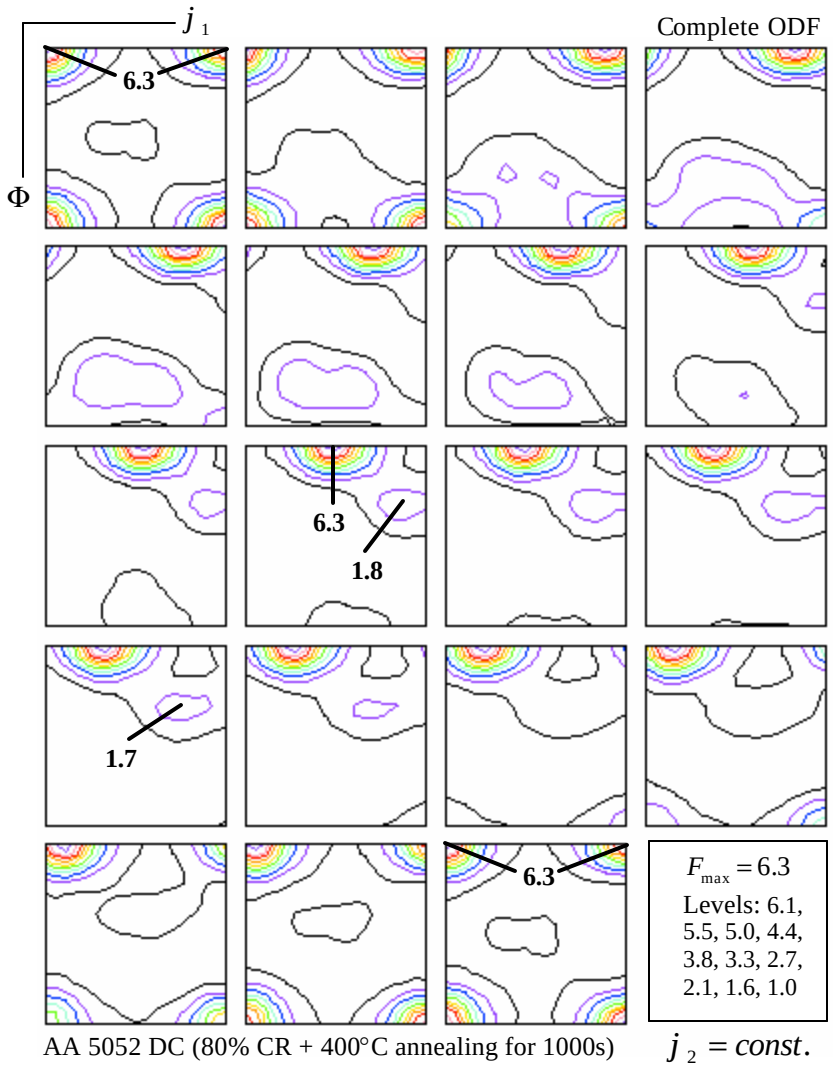

Fig. 31. Complete ODFs of AA 5052 DC after 80% cold rolling followed by annealing at 400 °C for 1000s.

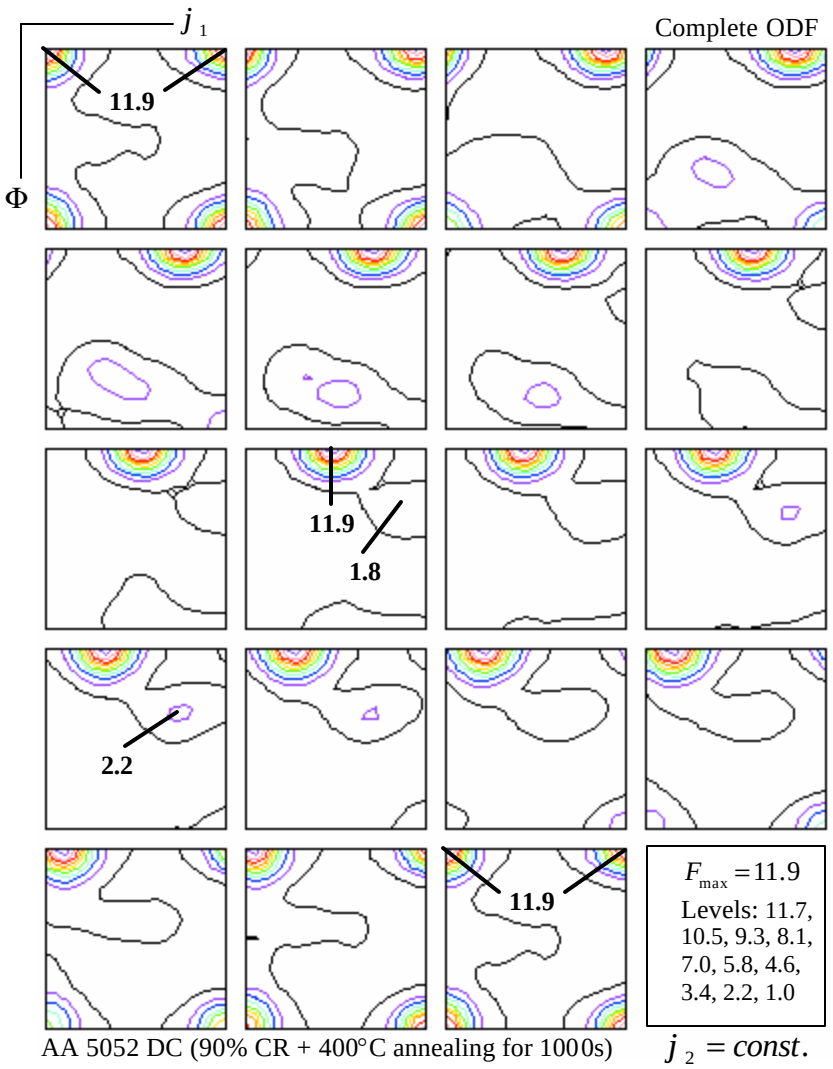

Fig. 32. Complete ODFs of AA 5052 DC after 90% cold rolling followed by annealing at 400 °C for 1000s.

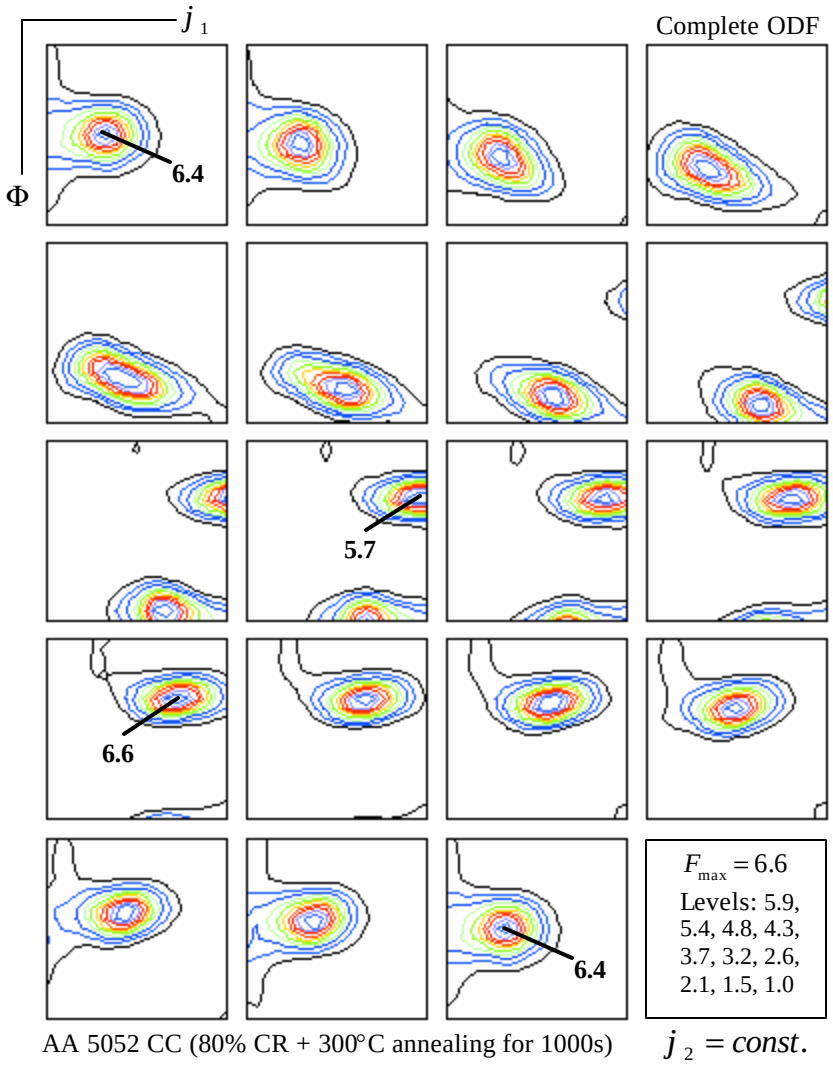

Fig. 33. Complete ODFs of AA 5052 CC after 80% cold rolling followed by annealing at 300 °C for 1000s.

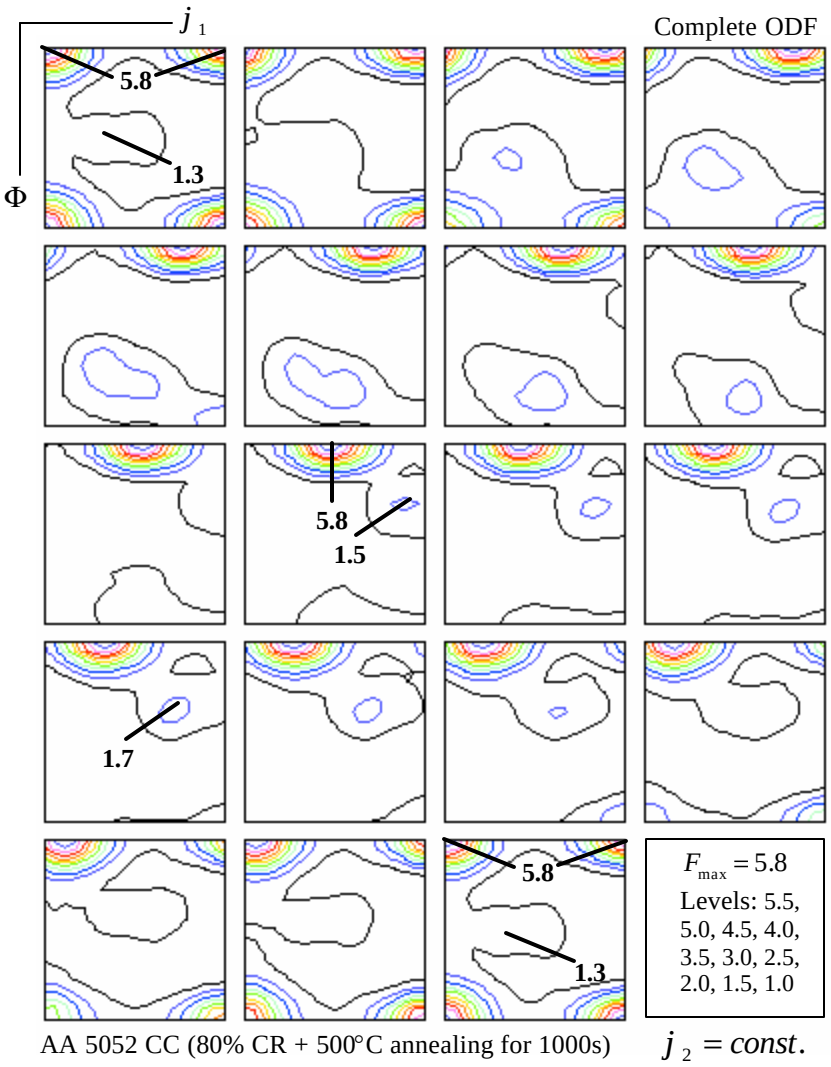

Fig. 34. Complete ODFs of AA 5052 CC after 80% cold rolling followed by annealing at 500 °C for 1000s.

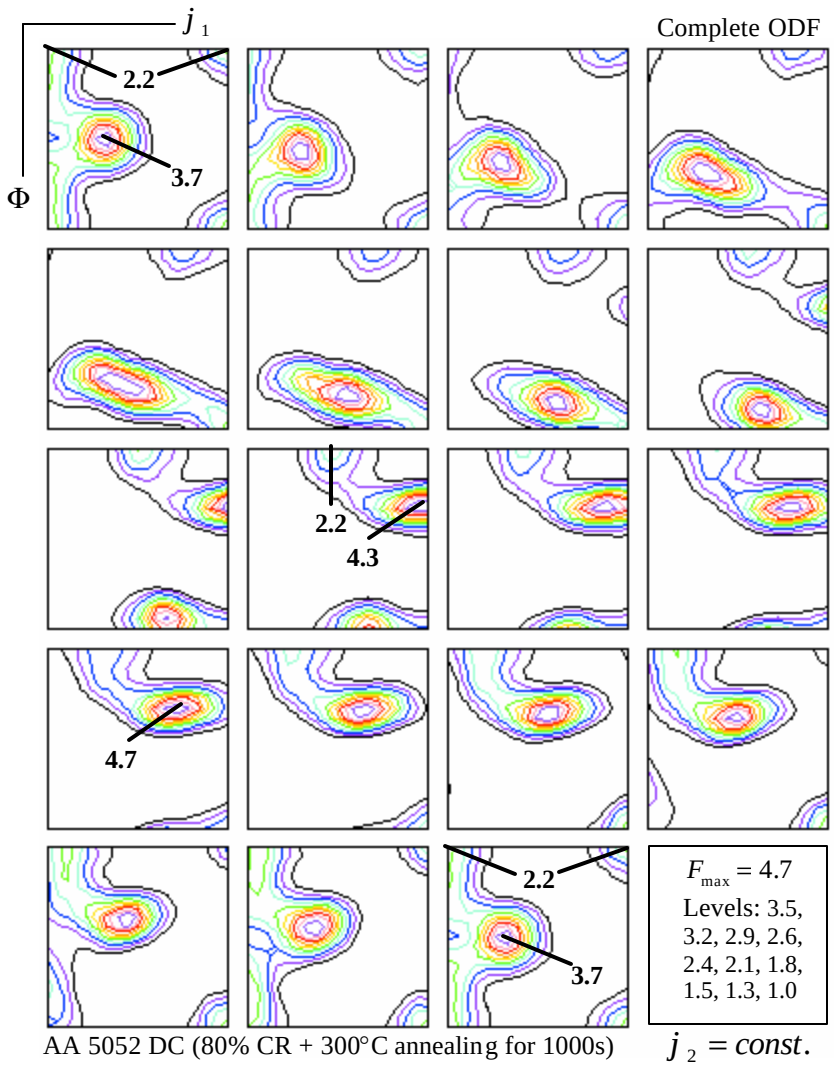

Fig. 35. Complete ODFs of AA 5052 DC after 80% cold rolling followed by annealing at 300 °C for 1000s.

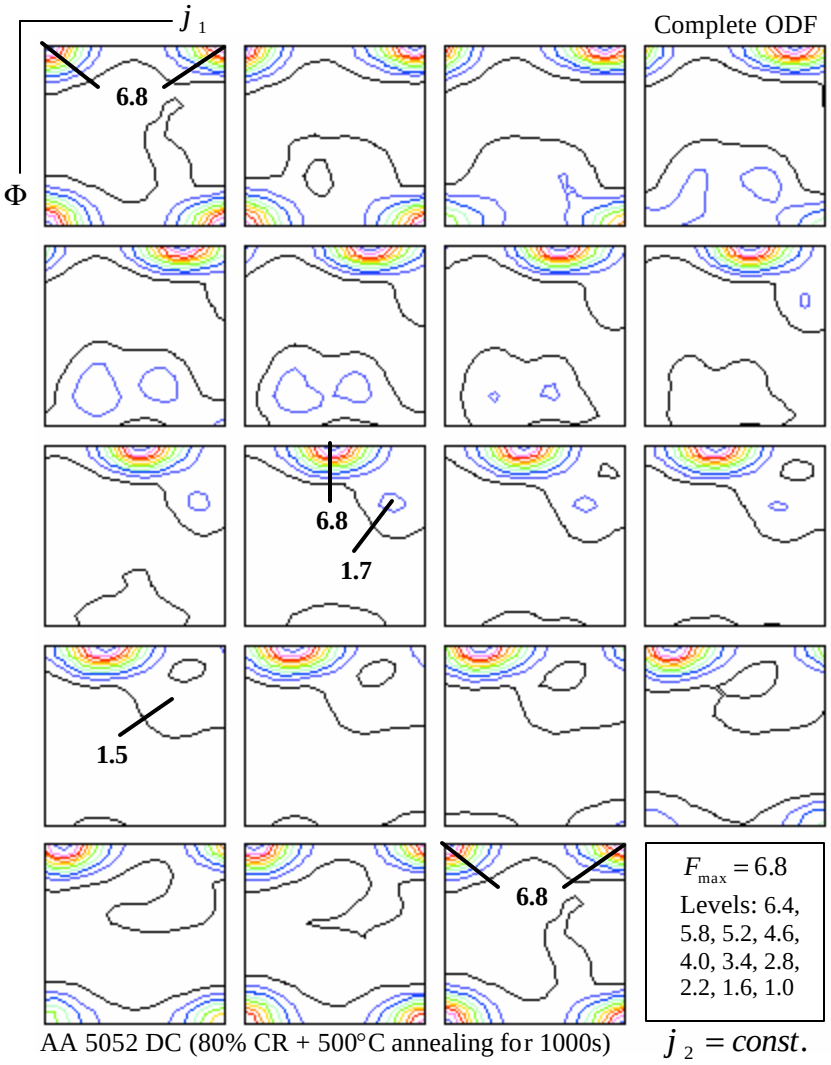

Fig. 36. Complete ODFs of AA 5052 DC after 80% cold rolling followed by annealing at 500 °C for 1000s.

Table 4. Texture components of AA 5052 CC during annealing[a] (M_i vs. t_A)

Status	Euler angles[b] (g_i) j_1	Φ	j_2	f_i [b]	y_i [b]	M_i [b]
Recrystallization texture components:						
(a) Cube component: $\{hkl\}<uvw>=\{001\}<100>$ [b]						
80% cold rolling (CR)	0°	0°	0°	1.3	10°	2.4%
80% CR + 400°C annealing for 20s	0°	0°	0°	1.2	15°	2.3%
80% CR + 400°C annealing for 50s	0°	0°	0°	1.3	15°	2.4%
80% CR + 400°C annealing for 100s	0°	0°	0°	1.1	15°	2.0%
80% CR + 400°C annealing for 250s	0°	0°	0°	1.3	15°	2.4%
80% CR + 400°C annealing for 550s	0°	0°	0°	4.6	15°	6.7%
80% CR + 400°C annealing for 750s	0°	0°	0°	5.1	15°	7.1%
80% CR + 400°C annealing for 1000s	0°	0°	0°	6.1	15°	8.3%
80% CR + 400°C annealing for 5500s	0°	0°	0°	5.6	15°	7.7%
80% CR + 400°C annealing for 10^4s	0°	0°	0°	5.3	15°	7.4%
80% CR + 400°C annealing for 10^5s	0°	0°	0°	5.8	15°	8.0%
(b) Goss component: $\{hkl\}<uvw>=\{011\}<100>$ [b]						
80% cold rolling (CR)	0°	45°	0°	2.3[c]	15°	4.1%
80% CR + 400°C annealing for 20s	90°	90°	45°	2.0[c]	10°	1.2%
80% CR + 400°C annealing for 50s	90°	90°	45°	2.0[c]	10°	1.2%
80% CR + 400°C annealing for 100s	90°	90°	45°	1.8[c]	10°	1.1%
80% CR + 400°C annealing for 250s	90°	90°	45°	1.8[c]	10°	1.0%
80% CR + 400°C annealing for 550s	—	—	—	—	—	—
80% CR + 400°C annealing for 750s	—	—	—	—	—	—
80% CR + 400°C annealing for 1000s	—	—	—	—	—	—
80% CR + 400°C annealing for 5500s	—	—	—	—	—	—
80% CR + 400°C annealing for 10^4s	—	—	—	—	—	—
80% CR + 400°C annealing for 10^5s	—	—	—	—	—	—
(c) R component: $\{hkl\}<uvw>=\{124\}<211>$ [b]						
80% cold rolling (CR)	—	—	—	—	—	—
80% CR + 400°C annealing for 20s	—	—	—	—	—	—
80% CR + 400°C annealing for 50s	—	—	—	—	—	—
80% CR + 400°C annealing for 100s	—	—	—	—	—	—
80% CR + 400°C annealing for 250s	—	—	—	—	—	—
80% CR + 400°C annealing for 550s	65°	30°	60°	1.7	15°	12.8%
80% CR + 400°C annealing for 750s	65°	35°	60°	1.7	15°	12.5%
80% CR + 400°C annealing for 1000s	70°	30°	60°	1.9	15°	12.3%
80% CR + 400°C annealing for 5500s	65°	35°	60°	1.9	15°	13.4%
80% CR + 400°C annealing for 10^4s	70°	30°	60°	1.9	15°	12.4%
80% CR + 400°C annealing for 10^5s	65°	35°	60°	1.8	15°	13.1%

Table 4. — Continued

Status	Euler angles[b] (g_i)			f_i [b]	y_i [b]	M_i [b]
	j_1	Φ	j_2			
Rolling texture components:						
(d) Copper/S component: $\{hkl\}<uvw>=\{123\}<111>$ [b]						
80% cold rolling (CR)	65°	30°	60°	7.0	10°	12.0%
80% CR + 400°C annealing for 20s	65°	30°	60°	5.6	10°	10.1%
80% CR + 400°C annealing for 50s	65°	30°	60°	6.1	10°	11.0%
80% CR + 400°C annealing for 100s	60°	30°	60°	5.9	10°	10.5%
80% CR + 400°C annealing for 250s	65°	30°	60°	5.5	10°	9.9%
80% CR + 400°C annealing for 550s	—	—	—	—	—	—
80% CR + 400°C annealing for 750s	—	—	—	—	—	—
80% CR + 400°C annealing for 1000s	—	—	—	—	—	—
80% CR + 400°C annealing for 5500s	—	—	—	—	—	—
80% CR + 400°C annealing for 10^4s	—	—	—	—	—	—
80% CR + 400°C annealing for 10^5s	—	—	—	—	—	—
(e) Copper component: $\{hkl\}<uvw>=\{112\}<111>$ [b]						
80% cold rolling (CR)	85°	30°	45°	5.5	15°	19.6%
80% CR + 400°C annealing for 20s	85°	30°	45°	4.9	15°	17.6%
80% CR + 400°C annealing for 50s	85°	30°	45°	5.0	15°	18.2%
80% CR + 400°C annealing for 100s	85°	30°	45°	5.2	15°	18.0%
80% CR + 400°C annealing for 250s	85°	30°	45°	4.5	15°	17.2%
80% CR + 400°C annealing for 550s	85°	30°	45°	1.6	15°	9.6%
80% CR + 400°C annealing for 750s	80°	30°	45°	1.5	15°	11.2%
80% CR + 400°C annealing for 1000s	85°	30°	45°	1.8	15°	9.9%
80% CR + 400°C annealing for 5500s	80°	30°	45°	1.8	15°	12.1%
80% CR + 400°C annealing for 10^4s	85°	30°	45°	1.7	15°	10.0%
80% CR + 400°C annealing for 10^5s	80°	30°	45°	1.7	15°	11.9%
(f) Brass component: $\{hkl\}<uvw>=\{011\}<211>$ [b]						
80% cold rolling (CR)	30°	45°	0°	6.8	15°	14.3%
80% CR + 400°C annealing for 20s	30°	45°	0°	4.7	15°	11.9%
80% CR + 400°C annealing for 50s	30°	45°	0°	5.7	15°	13.6%
80% CR + 400°C annealing for 100s	30°	45°	0°	4.8	15°	12.4%
80% CR + 400°C annealing for 250s	30°	45°	0°	4.8	15°	12.1%
80% CR + 400°C annealing for 550s	30°	45°	0°	1.3	15°	5.3%
80% CR + 400°C annealing for 750s	30°	45°	0°	1.3	15°	5.2%
80% CR + 400°C annealing for 1000s	30°	45°	0°	1.5	15°	5.5%
80% CR + 400°C annealing for 5500s	30°	45°	0°	1.5	15°	5.8%
80% CR + 400°C annealing for 10^4s	30°	45°	0°	1.7	15°	5.8%
80% CR + 400°C annealing for 10^5s	30°	45°	0°	1.7	15°	5.8%

Table 4. — Continued

Status	Euler angles[b] (g_i) j_1	Φ	j_2	f_i [b]	y_i [b]	M_i [b]
(g) Brass/S component: $\{hkl\}<uvw>=\{168\}<211>$ [b]						
80% cold rolling (CR)	40°	35°	80°	5.6	10°	10.6%
80% CR + 400°C annealing for 20s	45°	35°	75°	4.6	10°	9.9%
80% CR + 400°C annealing for 50s	45°	35°	75°	5.6	10°	11.5%
80% CR + 400°C annealing for 100s	45°	35°	75°	5.0	10°	10.5%
80% CR + 400°C annealing for 250s	45°	35°	75°	4.6	10°	10.0%
80% CR + 400°C annealing for 550s	50°	35°	75°	1.6	10°	4.0%
80% CR + 400°C annealing for 750s	50°	35°	75°	1.5	10°	3.9%
80% CR + 400°C annealing for 1000s	50°	40°	80°	1.6	10°	3.7%
80% CR + 400°C annealing for 5500s	50°	35°	75°	1.6	10°	4.3%
80% CR + 400°C annealing for 10^4s	45°	40°	80°	1.7	10°	3.8%
80% CR + 400°C annealing for 10^5s	40°	40°	80°	1.7	10°	3.8%
(h) S component: $\{hkl\}<uvw>=\{123\}<634>$ [b]						
80% cold rolling (CR)	60°	30°	65°	6.5	10°	12.0%
80% CR + 400°C annealing for 20s	55°	30°	65°	5.3	10°	10.3%
80% CR + 400°C annealing for 50s	55°	30°	65°	5.8	10°	11.4%
80% CR + 400°C annealing for 100s	60°	30°	65°	5.6	10°	10.6%
80% CR + 400°C annealing for 250s	65°	30°	60°	5.3	10°	10.1%
80% CR + 400°C annealing for 550s	—	—	—	—	—	—
80% CR + 400°C annealing for 750s	—	—	—	—	—	—
80% CR + 400°C annealing for 1000s	—	—	—	—	—	—
80% CR + 400°C annealing for 5500s	—	—	—	—	—	—
80% CR + 400°C annealing for 10^4s	—	—	—	—	—	—
80% CR + 400°C annealing for 10^5s	—	—	—	—	—	—

[a] The texture components are quantitatively analyzed by using Gauss-type function. e denotes the strain. j_1, Φ, j_2 the Euler angles of the central position of the Gauss component, f_i the maximum orientation density in the complete (true) ODF, M_i the calculated volume fraction when half scatter width y_i is selected for the purpose of the best fitting of Gauss components.

[b] Approximated.

[c] No absolute maximum.

Table 5. Texture components of AA 5052 CC during annealing[a] (M_i vs. T_A)

Status	Euler angles[b] (g_i) j_1	Φ	j_2	f_i [b]	y_i [b]	M_i [b]
Recrystallization texture components:						
(a) Cube component: $\{hkl\}<uvw>=\{001\}<100>$ [b]						
80% CR + 300°C annealing for 1000s	0°	0°	0°	2.0	10°	2.0%
80% CR + 400°C annealing for 1000s	0°	0°	0°	6.1	15°	8.3%
80% CR + 500°C annealing for 1000s	0°	0°	0°	5.8	15°	8.0%
(b) Goss component: $\{hkl\}<uvw>=\{011\}<100>$ [b]						
80% CR + 300°C annealing for 1000s	90°	90°	45°	2.2[c]	10°	1.3%
80% CR + 400°C annealing for 1000s	—	—	—	—	—	—
80% CR + 500°C annealing for 1000s	—	—	—	—	—	—
(c) R component: $\{hkl\}<uvw>=\{124\}<211>$ [b]						
80% CR + 300°C annealing for 1000s	—	—	—	—	—	—
80% CR + 400°C annealing for 1000s	70°	30°	60°	1.9	15°	12.3%
80% CR + 500°C annealing for 1000s	70°	35°	55°	1.6	15°	12.1%
Rolling texture components:						
(d) Copper/S component: $\{hkl\}<uvw>=\{123\}<111>$ [b]						
80% CR + 300°C annealing for 1000s	65°	30°	60°	6.6	10°	11.3%
80% CR + 400°C annealing for 1000s	—	—	—	—	—	—
80% CR + 500°C annealing for 1000s	—	—	—	—	—	—
(e) Copper component: $\{hkl\}<uvw>=\{112\}<111>$ [b]						
80% CR + 300°C annealing for 1000s	85°	30°	45°	5.7	15°	19.1%
80% CR + 400°C annealing for 1000s	85°	30°	45°	1.8	15°	9.9%
80% CR + 500°C annealing for 1000s	80°	30°	45°	1.5	15°	11.1%
(f) Brass component: $\{hkl\}<uvw>=\{011\}<211>$ [b]						
80% CR + 300°C annealing for 1000s	30°	45°	0°	6.4	15°	14.3%
80% CR + 400°C annealing for 1000s	30°	45°	0°	1.5	15°	5.5%
80% CR + 500°C annealing for 1000s	30°	45°	0°	1.3	15°	4.9%
(g) Brass/S component: $\{hkl\}<uvw>=\{168\}<211>$ [b]						
80% CR + 300°C annealing for 1000s	40°	35°	80°	5.7	15°	10.7%
80% CR + 400°C annealing for 1000s	50°	40°	80°	1.6	10°	3.7%
80% CR + 500°C annealing for 1000s	55°	35°	75°	1.5	10°	3.8%

Table 5. — Continued

Status	Euler angles[b] (g_i) j_1	Φ	j_2	f_i [b]	y_i [b]	M_i [b]
(h) S component: $\{hkl\}<uvw>=\{123\}<634>$ [b]						
80% CR + 300°C annealing for 1000s	60°	30°	65°	6.2	10°	11.5%
80% CR + 400°C annealing for 1000s	—	—	—	—	—	—
80% CR + 500°C annealing for 1000s	—	—	—	—	—	—

[a] The texture components are quantitatively analyzed by using Gauss-type function. e denotes the strain. j_1, Φ, j_2 the Euler angles of the central position of the Gauss component, f_i the maximum orientation density in the complete (true) ODF, M_i the calculated volume fraction when half scatter width y_i is selected for the purpose of the best fitting of Gauss components.

[b] Approximated.

[c] No absolute maximum.

Table 6. Texture components of AA 5052 CC during annealing[a] (M_i vs. CRR)

Status	Euler angles[b] (g_i) j_1	Φ	j_2	f_i [b]	y_i [b]	M_i [b]
Recrystallization texture components:						
(a) Cube component: $\{hkl\}<uvw>=\{001\}<100>$ [b]						
70% CR + 400°C annealing for 1000s	0°	0°	0°	3.1	15°	5.0%
80% CR + 400°C annealing for 1000s	0°	0°	0°	6.1	15°	8.3%
90% CR + 400°C annealing for 1000s	0°	0°	0°	7.7	15°	9.4%
(b) Goss component: $\{hkl\}<uvw>=\{011\}<100>$ [b]						
70% CR + 400°C annealing for 1000s	—	—	—	—	—	—
80% CR + 400°C annealing for 1000s	—	—	—	—	—	—
90% CR + 400°C annealing for 1000s	—	—	—	—	—	—
(c) R component: $\{hkl\}<uvw>=\{124\}<211>$ [b]						
70% CR + 400°C annealing for 1000s	65°	35°	60°	1.8	15°	13.0%
80% CR + 400°C annealing for 1000s	70°	30°	60°	1.9	15°	12.3%
90% CR + 400°C annealing for 1000s	65°	35°	60°	2.1	15°	13.9%
Rolling texture components:						
(d) Copper/S component: $\{hkl\}<uvw>=\{123\}<111>$ [b]						
70% CR + 400°C annealing for 1000s	—	—	—	—	—	—
80% CR + 400°C annealing for 1000s	—	—	—	—	—	—
90% CR + 400°C annealing for 1000s	—	—	—	—	—	—
(e) Copper component: $\{hkl\}<uvw>=\{112\}<111>$ [b]						
70% CR + 400°C annealing for 1000s	80°	30°	45°	1.7	15°	11.7%
80% CR + 400°C annealing for 1000s	85°	30°	45°	1.8	15°	9.9%
90% CR + 400°C annealing for 1000s	85°	30°	45°	1.8	15°	10.2%
(f) Brass component: $\{hkl\}<uvw>=\{011\}<211>$ [b]						
70% CR + 400°C annealing for 1000s	30°	45°	0°	1.5	15°	5.8%
80% CR + 400°C annealing for 1000s	30°	45°	0°	1.5	15°	5.5%
90% CR + 400°C annealing for 1000s	25°	45°	0°	1.3	15°	1.5%
(g) Brass/S component: $\{hkl\}<uvw>=\{168\}<211>$ [b]						
70% CR + 400°C annealing for 1000s	45°	35°	75°	1.6	10°	4.2%
80% CR + 400°C annealing for 1000s	50°	40°	80°	1.6	10°	3.7%
90% CR + 400°C annealing for 1000s	50°	35°	75°	1.7	10°	4.2%

Table 6. — Continued

Status	Euler angles[b] (g_i)			f_i [b]	y_i [b]	M_i [b]
	j_1	Φ	j_2			
(h) S component: $\{hkl\}<uvw>=\{123\}<634>$ [b]						
70% CR + 400°C annealing for 1000s	—	—	—	—	—	—
80% CR + 400°C annealing for 1000s	—	—	—	—	—	—
90% CR + 400°C annealing for 1000s	—	—	—	—	—	—

[a] The texture components are quantitatively analyzed by using Gauss-type function. e denotes the strain. j_1, Φ, j_2 the Euler angles of the central position of the Gauss component, f_i the maximum orientation density in the complete (true) ODF, M_i the calculated volume fraction when half scatter width y_i is selected for the purpose of the best fitting of Gauss components.

[b] Approximated.

[c] No absolute maximum.

Table 7. Texture components of AA 5052 DC during annealing[a] (M_i vs. t_A)

Status	Euler angles[b] (g_i) j_1	Φ	j_2	f_i [b]	y_i [b]	M_i [b]
Recrystallization texture components:						
(a) Cube component: $\{hkl\}<uvw>=\{001\}<100>$ [b]						
80% cold rolling (CR)	0°	0°	0°	2.0	15°	3.8%
80% CR + 400°C annealing for 20s	0°	0°	0°	2.0	15°	3.6%
80% CR + 400°C annealing for 50s	0°	0°	0°	2.7	15°	4.6%
80% CR + 400°C annealing for 100s	0°	0°	0°	2.3	15°	4.1%
80% CR + 400°C annealing for 250s	0°	0°	0°	2.7	15°	4.3%
80% CR + 400°C annealing for 550s	0°	0°	0°	7.4	15°	9.0%
80% CR + 400°C annealing for 750s	0°	0°	0°	6.4	15°	8.1%
80% CR + 400°C annealing for 1000s	0°	0°	0°	6.1	15°	8.1%
80% CR + 400°C annealing for 5500s	0°	0°	0°	6.4	15°	8.2%
80% CR + 400°C annealing for 10^4s	0°	0°	0°	6.4	15°	8.0%
80% CR + 400°C annealing for 10^5s	0°	0°	0°	5.9	15°	7.7%
(b) Goss component: $\{hkl\}<uvw>=\{011\}<100>$ [b]						
80% cold rolling (CR)	0°	45°	0°	2.0[c]	15°	4.1%
80% CR + 400°C annealing for 20s	90°	90°	45°	1.8[c]	10°	1.1%
80% CR + 400°C annealing for 50s	90°	90°	45°	1.6[c]	10°	1.0%
80% CR + 400°C annealing for 100s	90°	90°	45°	1.9[c]	10°	1.1%
80% CR + 400°C annealing for 250s	90°	90°	45°	1.6[c]	10°	1.0%
80% CR + 400°C annealing for 550s	—	—	—	—	—	—
80% CR + 400°C annealing for 750s	—	—	—	—	—	—
80% CR + 400°C annealing for 1000s	—	—	—	—	—	—
80% CR + 400°C annealing for 5500s	—	—	—	—	—	—
80% CR + 400°C annealing for 10^4s	—	—	—	—	—	—
80% CR + 400°C annealing for 10^5s	—	—	—	—	—	—
(c) R component: $\{hkl\}<uvw>=\{124\}<211>$ [b]						
80% cold rolling (CR)	—	—	—	—	—	—
80% CR + 400°C annealing for 20s	—	—	—	—	—	—
80% CR + 400°C annealing for 50s	—	—	—	—	—	—
80% CR + 400°C annealing for 100s	—	—	—	—	—	—
80% CR + 400°C annealing for 250s	—	—	—	—	—	—
80% CR + 400°C annealing for 550s	70°	30°	55°	2.0	15°	14.1%
80% CR + 400°C annealing for 750s	70°	30°	55°	1.8	15°	13.3%
80% CR + 400°C annealing for 1000s	70°	30°	55°	1.8	15°	10.8%
80% CR + 400°C annealing for 5500s	75°	30°	55°	2.3	15°	13.6%
80% CR + 400°C annealing for 10^4s	75°	30°	55°	1.8	15°	11.6%
80% CR + 400°C annealing for 10^5s	70°	30°	55°	1.8	15°	13.4%

Table 7. — Continued

Status	Euler angles[b] (g_i)			f_i [b]	y_i [b]	M_i [b]
	j_1	Φ	j_2			
Rolling texture components:						
(d) Copper/S component: $\{hkl\}<uvw>=\{123\}<111>$ [b]						
80% cold rolling (CR)	65°	30°	60°	5.1	10°	9.1%
80% CR + 400°C annealing for 20s	65°	30°	60°	5.1	10°	9.3%
80% CR + 400°C annealing for 50s	65°	30°	60°	4.8	10°	8.9%
80% CR + 400°C annealing for 100s	65°	30°	60°	4.9	10°	8.9%
80% CR + 400°C annealing for 250s	65°	30°	60°	4.6	10°	8.6%
80% CR + 400°C annealing for 550s	—	—	—	—	—	—
80% CR + 400°C annealing for 750s	—	—	—	—	—	—
80% CR + 400°C annealing for 1000s	—	—	—	—	—	—
80% CR + 400°C annealing for 5500s	—	—	—	—	—	—
80% CR + 400°C annealing for 10^4s	—	—	—	—	—	—
80% CR + 400°C annealing for 10^5s	—	—	—	—	—	—
(e) Copper component: $\{hkl\}<uvw>=\{112\}<111>$ [b]						
80% cold rolling (CR)	85°	30°	45°	4.6	15°	16.3%
80% CR + 400°C annealing for 20s	85°	30°	45°	4.4	15°	16.2%
80% CR + 400°C annealing for 50s	85°	30°	45°	4.4	15°	16.1%
80% CR + 400°C annealing for 100s	85°	30°	45°	4.6	15°	16.0%
80% CR + 400°C annealing for 250s	85°	30°	45°	4.1	15°	15.4%
80% CR + 400°C annealing for 550s	80°	30°	45°	2.0	15°	13.3%
80% CR + 400°C annealing for 750s	80°	30°	45°	1.8	15°	12.5%
80% CR + 400°C annealing for 1000s	80°	30°	45°	1.8	15°	12.5%
80% CR + 400°C annealing for 5500s	80°	30°	45°	2.0	15°	14.6%
80% CR + 400°C annealing for 10^4s	80°	30°	45°	1.8	15°	12.5%
80% CR + 400°C annealing for 10^5s	80°	30°	45°	1.8	15°	12.7%
(f) Brass component: $\{hkl\}<uvw>=\{011\}<211>$ [b]						
80% cold rolling (CR)	25°	45°	0°	3.6	15°	9.8%
80% CR + 400°C annealing for 20s	30°	45°	0°	3.5	15°	10.3%
80% CR + 400°C annealing for 50s	30°	45°	0°	3.7	15°	9.5%
80% CR + 400°C annealing for 100s	30°	45°	0°	3.3	15°	10.0%
80% CR + 400°C annealing for 250s	30°	45°	0°	3.8	15°	9.7%
80% CR + 400°C annealing for 550s	30°	45°	0°	1.3	10°	1.6%
80% CR + 400°C annealing for 750s	35°	45°	0°	1.2	10°	1.5%
80% CR + 400°C annealing for 1000s	30°	45°	0°	1.1	10°	1.3%
80% CR + 400°C annealing for 5500s	30°	45°	0°	1.1	10°	1.4%
80% CR + 400°C annealing for 10^4s	25°	45°	0°	1.2	10°	1.4%
80% CR + 400°C annealing for 10^5s	30°	45°	0°	1.1	10°	1.4%

Table 7. — Continued

Status	Euler angles[b] (g_i) j_1	Φ	j_2	f_i [b]	y_i [b]	M_i [b]
(g) Brass/S component: $\{hkl\}<uvw>=\{168\}<211>$ [b]						
80% cold rolling (CR)	40°	35°	75°	3.5	10°	8.0%
80% CR + 400°C annealing for 20s	45°	35°	75°	4.1	10°	8.9%
80% CR + 400°C annealing for 50s	45°	35°	75°	3.8	10°	8.3%
80% CR + 400°C annealing for 100s	45°	35°	75°	4.1	10°	8.6%
80% CR + 400°C annealing for 250s	45°	35°	75°	3.9	10°	8.3%
80% CR + 400°C annealing for 550s	50°	40°	75°	1.5	10°	3.6%
80% CR + 400°C annealing for 750s	50°	35°	75°	1.5	10°	3.9%
80% CR + 400°C annealing for 1000s	50°	35°	75°	1.4	10°	3.6%
80% CR + 400°C annealing for 5500s	55°	35°	75°	1.5	10°	4.2%
80% CR + 400°C annealing for 10^4s	50°	35°	80°	1.4	10°	3.7%
80% CR + 400°C annealing for 10^5s	50°	35°	75°	1.4	10°	3.8%
(h) S component: $\{hkl\}<uvw>=\{123\}<634>$ [b]						
80% cold rolling (CR)	60°	30°	65°	4.6	10°	8.9%
80% CR + 400°C annealing for 20s	60°	30°	65°	4.7	10°	9.3%
80% CR + 400°C annealing for 50s	60°	30°	65°	4.5	10°	8.8%
80% CR + 400°C annealing for 100s	60°	30°	65°	4.5	10°	9.0%
80% CR + 400°C annealing for 250s	60°	30°	65°	4.2	10°	8.7%
80% CR + 400°C annealing for 550s	—	—	—	—	—	—
80% CR + 400°C annealing for 750s	—	—	—	—	—	—
80% CR + 400°C annealing for 1000s	—	—	—	—	—	—
80% CR + 400°C annealing for 5500s	—	—	—	—	—	—
80% CR + 400°C annealing for 10^4s	—	—	—	—	—	—
80% CR + 400°C annealing for 10^5s	—	—	—	—	—	—

[a] The texture components are quantitatively analyzed by using Gauss-type function. e denotes the strain. j_1, Φ, j_2 the Euler angles of the central position of the Gauss component, f_i the maximum orientation density in the complete (true) ODF, M_i the calculated volume fraction when half scatter width y_i is selected for the purpose of the best fitting of Gauss components.

[b] Approximated.

[c] No absolute maximum.

Table 8. Texture components of AA 5052 DC during annealing[a] (M_i vs. T_A)

Status	Euler angles[b] (g_i) j_1	Φ	j_2	f_i [b]	y_i [b]	M_i [b]
Recrystallization texture components:						
(a) Cube component: $\{hkl\}<uvw>=\{001\}<100>$ [b]						
80% CR + 300°C annealing for 1000s	0°	0°	0°	2.2	15°	3.9%
80% CR + 400°C annealing for 1000s	0°	0°	0°	6.1	15°	8.1%
80% CR + 500°C annealing for 1000s	0°	0°	0°	6.8	15°	8.6%
(b) Goss component: $\{hkl\}<uvw>=\{011\}<100>$ [b]						
80% CR + 300°C annealing for 1000s	90°	90°	45°	1.7[c]	10°	1.0%
80% CR + 400°C annealing for 1000s	—	—	—	—	—	—
80% CR + 500°C annealing for 1000s	—	—	—	—	—	—
(c) R component: $\{hkl\}<uvw>=\{124\}<211>$ [b]						
80% CR + 300°C annealing for 1000s	—	—	—	—	—	—
80% CR + 400°C annealing for 1000s	70°	30°	55°	1.8	15°	10.8%
80% CR + 500°C annealing for 1000s	65°	30°	55°	1.6	15°	12.2%
Rolling texture components:						
(d) Copper/S component: $\{hkl\}<uvw>=\{123\}<111>$ [b]						
80% CR + 300°C annealing for 1000s	65°	30°	60°	4.7	10°	8.9%
80% CR + 400°C annealing for 1000s	—	—	—	—	—	—
80% CR + 500°C annealing for 1000s	—	—	—	—	—	—
(e) Copper component: $\{hkl\}<uvw>=\{112\}<111>$ [b]						
80% CR + 300°C annealing for 1000s	90°	30°	45°	4.3	15°	11.3%
80% CR + 400°C annealing for 1000s	80°	30°	45°	1.8	15°	12.5%
80% CR + 500°C annealing for 1000s	80°	30°	45°	1.6	15°	11.7%
(f) Brass component: $\{hkl\}<uvw>=\{011\}<211>$ [b]						
80% CR + 300°C annealing for 1000s	30°	45°	0°	3.7	15°	10.0%
80% CR + 400°C annealing for 1000s	30°	45°	0°	1.1	10°	1.3%
80% CR + 500°C annealing for 1000s	—	—	—	—	—	—
(g) Brass/S component: $\{hkl\}<uvw>=\{168\}<211>$ [b]						
80% CR + 300°C annealing for 1000s	45°	35°	75°	4.1	10°	8.7%
80% CR + 400°C annealing for 1000s	50°	35°	75°	1.4	10°	3.6%
80% CR + 500°C annealing for 1000s	50°	35°	75°	1.2	10°	3.3%

Table 8.— Continued

Status	Euler angles[b] (g_i) j_1	Φ	j_2	f_i [b]	y_i [b]	M_i [b]
(h) S component: $\{hkl\}<uvw>=\{123\}<634>$ [b]						
80% CR + 300°C annealing for 1000s	60°	30°	65°	4.4	10°	8.9%
80% CR + 400°C annealing for 1000s	—	—	—	—	—	—
80% CR + 500°C annealing for 1000s	—	—	—	—	—	—

[a] The texture components are quantitatively analyzed by using Gauss-type function. e denotes the strain. j_1, Φ, j_2 the Euler angles of the central position of the Gauss component, f_i the maximum orientation density in the complete (true) ODF, M_i the calculated volume fraction when half scatter width y_i is selected for the purpose of the best fitting of Gauss components.

[b] Approximated.

[c] No absolute maximum.

Table 9. Texture components of AA 5052 DC during annealing[a] (M_i vs. CRR)

Status	Euler angles[b] (g_i) j_1	Φ	j_2	f_i [b]	y_i [b]	M_i [b]
Recrystallization texture components:						
(a) Cube component: $\{hkl\}<uvw>=\{001\}<100>$ [b]						
70% CR + 400°C annealing for 1000s	0°	0°	0°	4.6	15°	3.9%
80% CR + 400°C annealing for 1000s	0°	0°	0°	6.1	15°	8.1%
90% CR + 400°C annealing for 1000s	0°	0°	0°	11.9	15°	12.5%
(b) Goss component: $\{hkl\}<uvw>=\{011\}<100>$ [b]						
70% CR + 400°C annealing for 1000s	—	—	—	—	—	—
80% CR + 400°C annealing for 1000s	—	—	—	—	—	—
90% CR + 400°C annealing for 1000s	90°	90°	45°	1.2[c]	10°	0.7%
(c) R component: $\{hkl\}<uvw>=\{124\}<211>$ [b]						
70% CR + 400°C annealing for 1000s	65°	30°	55°	1.6	15°	12.5%
80% CR + 400°C annealing for 1000s	70°	30°	55°	1.8	15°	10.8%
90% CR + 400°C annealing for 1000s	70°	30°	55°	2.1	15°	13.6%
Rolling texture components:						
(d) Copper/S component: $\{hkl\}<uvw>=\{123\}<111>$ [b]						
70% CR + 400°C annealing for 1000s	—	—	—	—	—	—
80% CR + 400°C annealing for 1000s	—	—	—	—	—	—
90% CR + 400°C annealing for 1000s	—	—	—	—	—	—
(e) Copper component: $\{hkl\}<uvw>=\{112\}<111>$ [b]						
70% CR + 400°C annealing for 1000s	80°	30°	45°	1.6	15°	11.6%
80% CR + 400°C annealing for 1000s	80°	30°	45°	1.8	15°	12.5%
90% CR + 400°C annealing for 1000s	80°	30°	45°	1.8	15°	12.4%
(f) Brass component: $\{hkl\}<uvw>=\{011\}<211>$ [b]						
70% CR + 400°C annealing for 1000s	30°	45°	0°	1.1	10°	1.4%
80% CR + 400°C annealing for 1000s	30°	45°	0°	1.1	10°	1.3%
90% CR + 400°C annealing for 1000s	30°	45°	0°	1.2	10°	1.4%
(g) Brass/S component: $\{hkl\}<uvw>=\{168\}<211>$ [b]						
70% CR + 400°C annealing for 1000s	50°	35°	75°	1.3	10°	3.5%
80% CR + 400°C annealing for 1000s	50°	35°	75°	1.4	10°	3.6%
90% CR + 400°C annealing for 1000s	40°	35°	80°	1.4	10°	3.4%

Table 9.— Continued

Status	Euler angles[b] (g_i) j_1	Φ	j_2	f_i [b]	y_i [b]	M_i [b]
(h) S component: $\{hkl\}<uvw>=\{123\}<634>$ [b]						
70% CR + 400°C annealing for 1000s	—	—	—	—	—	—
80% CR + 400°C annealing for 1000s	—	—	—	—	—	—
90% CR + 400°C annealing for 1000s	—	—	—	—	—	—

[a] The texture components are quantitatively analyzed by using Gauss-type function. e denotes the strain. j_1, Φ, j_2 the Euler angles of the central position of the Gauss component, f_i the maximum orientation density in the complete (true) ODF, M_i the calculated volume fraction when half scatter width y_i is selected for the purpose of the best fitting of Gauss components.

[b] Approximated.

[c] No absolute maximum.

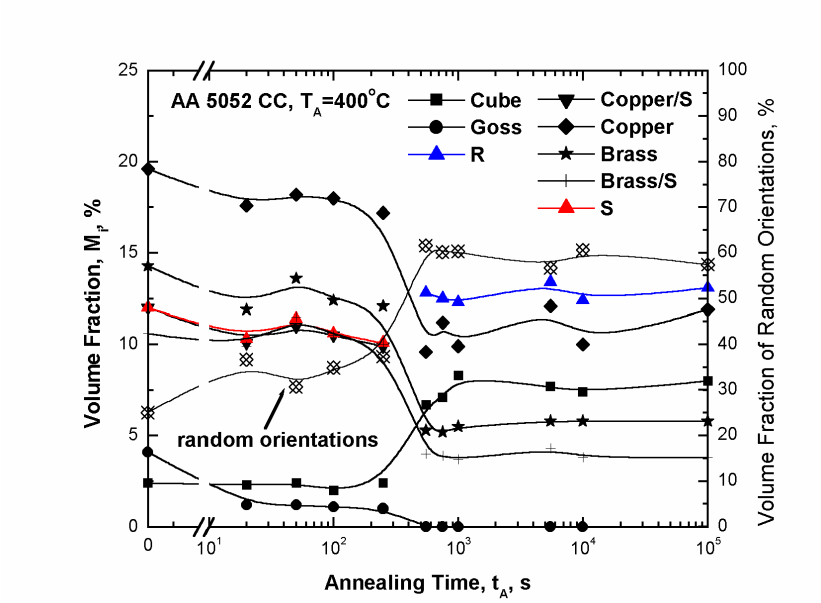

(a)

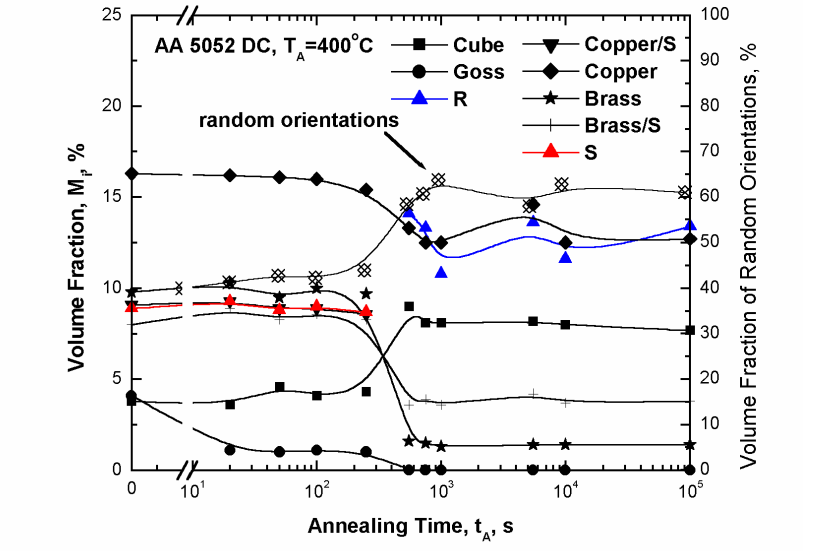

(b)

Fig. 37. Dependence of the volume fraction of texture components in (a) AA 5052 CC and (b) AA 5052 DC materials on annealing time during annealing at 400 °C.

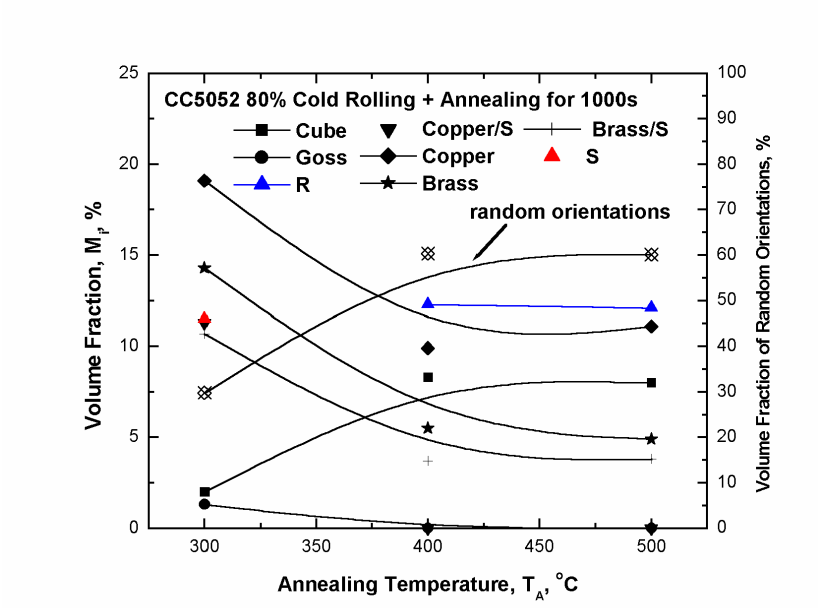

(a)

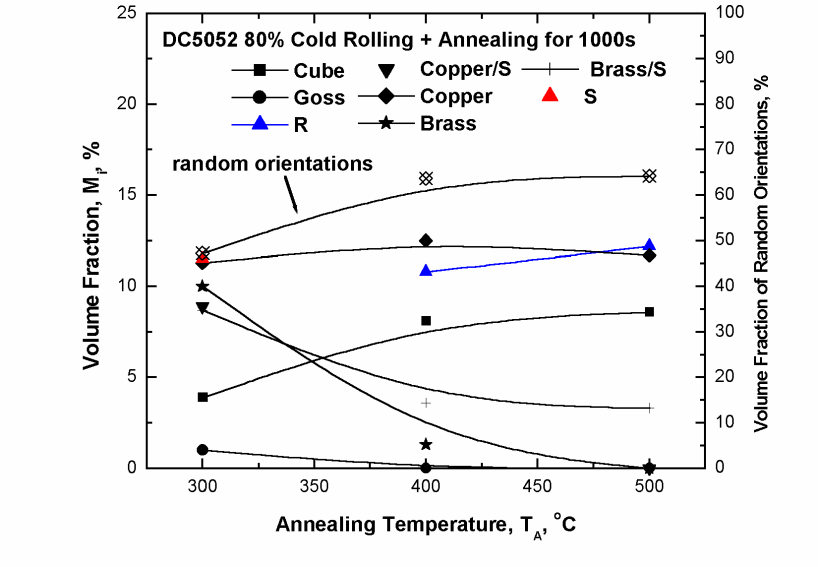

(b)

Fig. 38. Dependence of the volume fraction of texture components in (a) AA 5052 CC and (b) AA 5052 DC materials on annealing temperature for annealing 1000s.

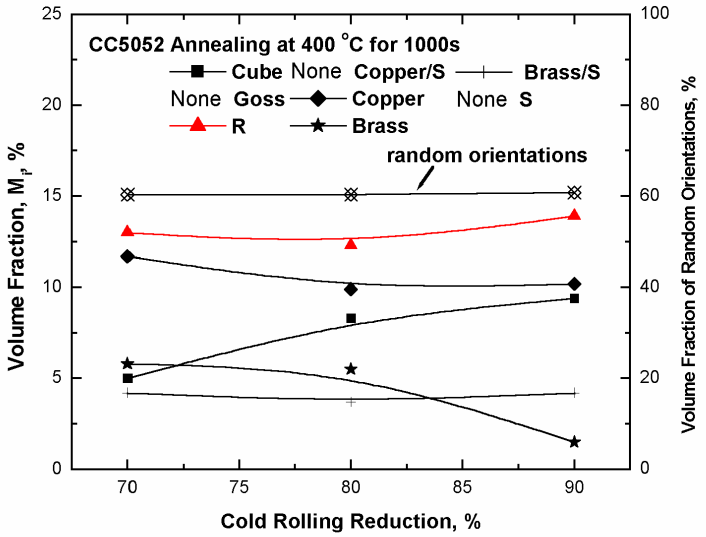

(a)

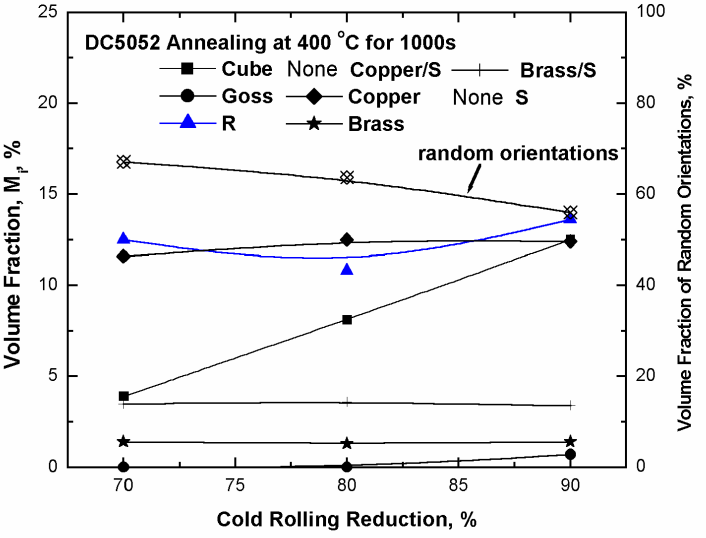

(b)

Fig. 39. Dependence of the volume fraction of texture components in (a) AA 5052 CC and (b) AA 5052 DC materials on cold rolling reduction during annealing at 400°C for 1000s.